1.0

2.8
3.2

2.5

2.2

1.1

2.0

1.8

1.25 1.4 1.6

MICROCOPY RESOLUTION TEST CHART
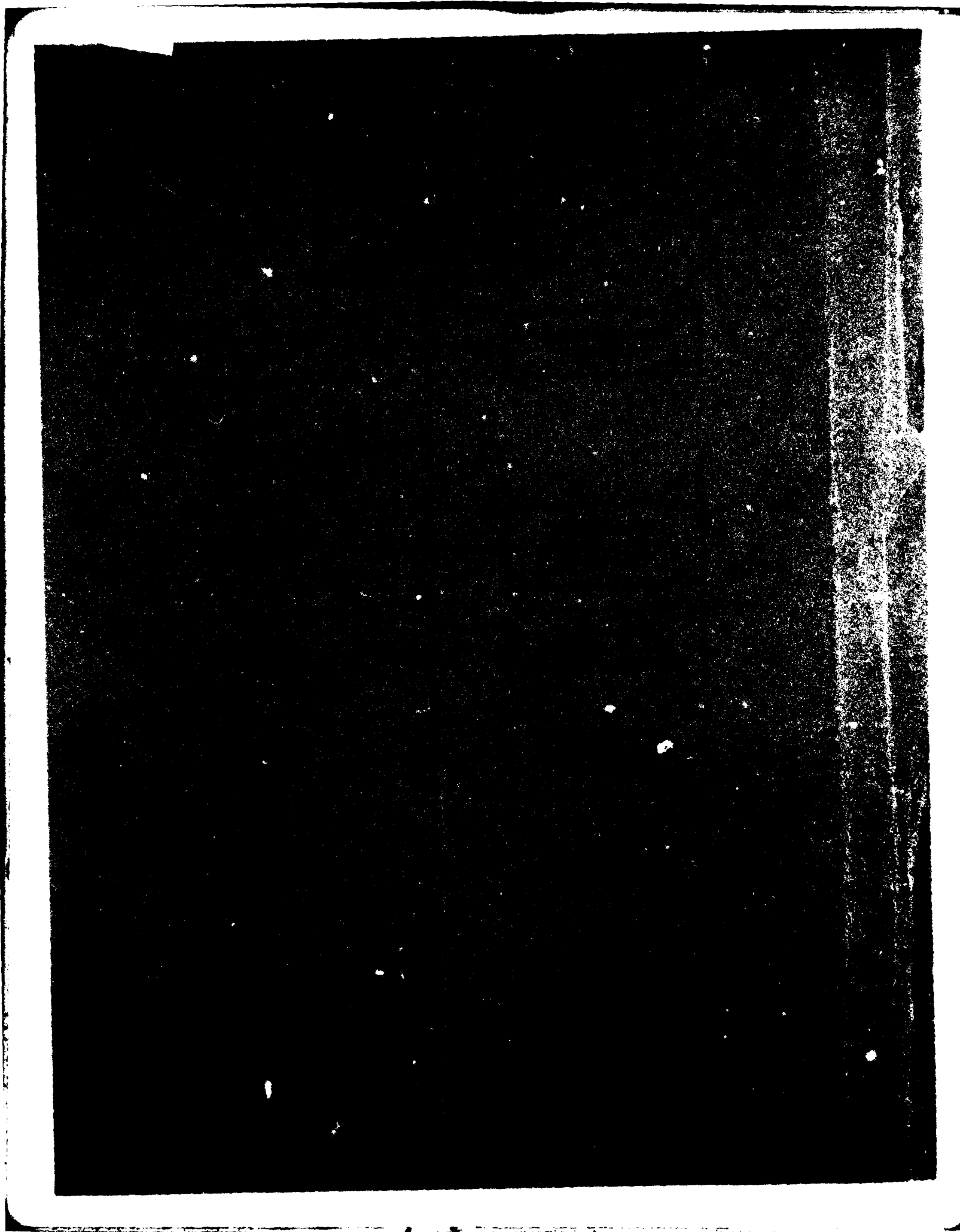
REPORT DOCUMENTATION PAGE		READ INSTRUCTIONS BEFORE COMPLETING FORM
1. REPORT NUMBER DTNSRDC-82/025	2. GOVT ACCESSION NO. AD-A116 339	3. RECIPIENT'S CATALOG NUMBER
4. TITLE (and Subtitle) COMPARISON OF FORCE AND MOTION PREDICTIONS USING STRIP THEORY AND A THREE-DIMENSIONAL METHOD FOR HULLS AT ZERO SPEED IN WAVES		5 TYPE OF REPORT & PERIOD COVERED Final
		6 PERFORMING ORG. REPORT NUMBER
7. AUTHOR(s) H. T. Wang M. S. Chang		8 CONTRACT OR GRANT NUMBER(s)
9. PERFORMING ORGANIZATION NAME AND ADDRESS David W. Taylor Naval Ship Research and Development Center Bethesda, Maryland 20084		10. PROGRAM ELEMENT, PROJECT, TASK AREA & WORK UNIT NUMBERS (See reverse side)
11. CONTROLLING OFFICE NAME AND ADDRESS Naval Sea Systems Command Hull R&T Office Washington, D.C. 20362		12. REPORT DATE June 1982
		13. NUMBER OF PAGES 81
14. MONITORING AGENCY NAME & ADDRESS(if different from Controlling Office)		15. SECURITY CLASS. (of this report) UNCLASSIFIED
		15a. DECLASSIFICATION DOWNGRADING SCHEDULE

16. DISTRIBUTION STATEMENT (of this Report)

APPROVED FOR PUBLIC RELEASE: DISTRIBUTION UNLIMITED

17. DISTRIBUTION STATEMENT (of the abstract entered in Block 20, if different from Report)

18. SUPPLEMENTARY NOTES

19. KEY WORDS (Continue on reverse side if necessary and identify by block number)

Ship Motion   Wave Force
Added Mass and Damping   Potential Flow
Strip Theory
Three-Dimensional Calculation

20. ABSTRACT (Continue on reverse side if necessary and identify by block number)

A comparison is presented of ship added mass, damping, exciting force, and motion coefficients calculated by Program SMP which uses strip theory and Program MOTIONSO which uses a three-dimensional singularity method. The comparison is made for four ship hulls at zero speed in waves. A summary is given of similarities and differences between the two methods.

(Continued on reverse side)

DD FORM 1473 EDITION OF 1 NOV 65 IS OBSOLETE
1 JAN 73
S/N 0102-LF-014-6601

(Block 10)

Program Element SR02301
Task Area SR0730101
Work Unit 1542-105

(Block 20 continued)

For the vertical modes of motion: surge, heave, and pitch, the comparison between the two methods generally shows the expected trend of poor agreement at lower frequencies and better agreement at higher frequencies. For the lateral modes of motion: sway, roll, and yaw, the agreement is more dependent upon the shape of the hull and the density and distribution of points used by MOTIONSO to represent the hull. Comparison of calculated and measured motions for one ship hull shows that the agreement is fair.

Accession For

NTIS
DTIC
Unann
Justification

By
Distribution/
Availability
A
Dist

TABLE OF CONTENTS

LIST OF FIGURES

LIST OF TABLES

iv

ABSTRACT

A comparison is presented of ship added mass, damping, exciting force, and motion coefficients calculated by Program SMP which uses strip theory and Program MOTIONSO which uses a three-dimensional singularity method. The comparison is made for four ship hulls at zero speed in waves. A summary is given of similarities and differences between the two methods.

For the vertical modes of motion: surge, heave, and pitch, the comparison between the two methods generally shows the expected trend of poor agreement at lower frequencies and better agreement at higher frequencies. For the lateral modes of motion: sway, roll, and yaw, the agreement is more dependent upon the shape of the hull and the density and distribution of points used by MOTIONSO to represent the hull. Comparison of calculated and measured motions for one ship hull shows that the agreement is fair.

ADMINISTRATIVE INFORMATION

INTRODUCTION

For a number of years, the "DTNSRDC Ship-Motion and Sea-Load Computer Program,"[1]* hereafter referred to as SMP, has been extensively used at the Center to predict the forces and motions for a ship advancing in waves in six degrees of freedom. The program uses a strip theory approach, which reduces the actual three-dimensional problem to a series of two-dimensional problems, to calculate the added mass, damping, and wave-exciting forces. Since these forces are calculated by using the potential flow theory, they are hereafter referred to as potential forces. The program then performs additional calculations to obtain the hydrostatic displacement and restoring forces, the lift force on the hull and appendages, and viscous roll damping due to the hull and appendages. The program next uses a frequency-domain approach to calculate the motions resulting from the above forces for a discrete set

---

*A complete listing of references is given on page 75.

1

of wave frequencies. In the present report, all of the above calculations outside of the prediction of the potential forces are referred to as the motion prediction part of SMP.

In a more recent development, Chang[2] has formulated a three-dimensional singularity method for calculating the potential forces on a ship hull. The method has been developed into two computer programs: MOTIONSO for zero ship speed and MOTION25 for nonzero forward ship speed. The programs have been developed to the point that it is of interest to evaluate them by comparing their predictions with those given by SMP and with experimental results.

The present report compares the potential forces predicted by SMP and MOTIONSO for four surface ship hulls at zero forward speed: the DE-1006 destroyer, the FRIESLAND frigate, the S7-175 container ship, and the CVA-59 carrier. The motions, using the potential forces predicted by SMP and MOTIONSO, obtained by the motion prediction part of SMP, are also compared. For one ship, the CVA-59, the predicted motions are also compared with the experimental results obtained at low speed. For the remaining hulls, no experimental results are shown since they were not available for zero or sufficiently low speeds. In a later report, the forces and motions predicted by MOTION25 and SMP will be compared with each other and with more extensive experimental results for the above four ships at forward speed.

The report first gives a brief description of the theory underlying SMP and MOTIONSO. In the case of SMP, separate descriptions are given of the potential force and motion calculations. The geometrical characteristics of the four chosen ship hulls are given next. The reasons for choosing the particular ships are discussed. The detailed geometrical representation used by each program to model each of the four ships is given in tabular form. For two ships, the FRIESLAND and the CVA-59, MOTIONSO was run for the entire range of frequencies with two different panel representations. For the S7-175, MOTIONSO was also run for two frequencies for a representation with four additional panels to model the large bulbous bow.

The predicted potential forces and motions are compared and discussed in three ways. First, the results predicted by MOTIONSO for 78- and 104-panel representations of FRIESLAND, 71- and 103-panel representations of CVA-59, and 78- and 82-panel representations of S7-175 are compared. It is noted that the different panel representations give reasonably consistent results in most cases, with the exception of the forces and motions involving sway and yaw, for which there are significant

2

differences in the cases of CVA-59 and S7-175. Secondly, the results predicted by both programs are compared with each other. In the vertical plane, composed of surge, heave, and pitch motions, MOTIONSO generally predicts added mass forces which are higher than corresponding results predicted by SMP. The reverse is true for the damping forces. The agreement generally improves with increasing frequency. In head seas, there is good agreement between the exciting forces and motions predicted by both programs. In the lateral plane, both programs predict approximately the same values for most of the forces and motions involving only sway and/or roll. With one exception, there is generally poor agreement in all the forces and motions involving yaw. The exception occurs for CVA-59, for which the MOTIONSO results with the more dense panel representation, are in generally good agreement with corresponding results predicted by SMP. Finally, for CVA-59, the predicted motions are compared with experimental values. The computed results are in fair agreement with the experimental results.

DESCRIPTION OF PROGRAMS

The SMP is a major computer program, which is widely used at the Center to compute the forces and motions of surface ships advancing at constant speed with arbitrary heading into regular as well as irregular waves. Figure 1 shows the coordinate system and sign conventions for ship motions and wave direction currently used in SMP. A user's manual describing input and output of an earlier version of SMP, referred to as HANSEL, is given as Reference 1. User's manuals for successive modifications of SMP have been issued as unpublished drafts. The theoretical basis for the program is given in References 3 and 4.

Both MOTIONSO and MOTION25 are more recently developed computer programs which calculate the potential forces on surface ships at zero and nonzero forward speed, respectively. The theoretical basis for these programs is given in Reference 2.

The present section gives a description of the essential aspects of the theory as contained in References 2 through 4. Since the principal interest in the present report is the case of zero speed, the description is also restricted to this case. The focus is on the principal differences between the potential force calculation methods of these two programs at zero speed. As mentioned previously, a later report will compare SMP and MOTION25 for cases with forward speed.

3

Separate descriptions are given of the potential force and motion calculation methods contained in SMP. As mentioned previously, the potential forces calculated by both SMP and MOTIONSO were input into the motion prediction part of SMP to calculate the resultant motions.

POTENTIAL FORCE CALCULATIONS: SMP

The SMP uses strip theory to calculate the added mass, damping, and exciting forces on the ship hull. That is, the method assumes that the length of the waves generated by the ship's oscillations are sufficiently short compared to ship length so that interaction between cross sections normal to the longitudinal axis of the ship may be neglected. Since wavelength is inversely proportional to the square of wave frequency, the above assumption tends to limit the applicability of the theory to high frequencies. The above assumption reduces the actual three-dimensional problem to a series of simpler two-dimensional problems. The overall forces are then obtained by summing over all the sections.

For a given section, SMP calculates the two-dimensional added mass and damping forces by using the Frank close-fit source-distribution method.[5] The program contains *two* options for describing the shape of a section. In the first option, the shape of the section is mathematically represented by a Lewis form which has the same beam, draft, and area of the given section. This option reduces the number of input variables, but is not as accurate as the second option, in which the actual shape is described by a series of offset points. For this reason, the second option was used to represent the shape of the section.

In calculating the motions, the Frank method assumes the motion of the fluid to be irrotational and the ship motion to be small enough so that nonlinear terms may be neglected. Under these assumptions, the method attempts to find the potential for a section in the vertical y-z plane undergoing forced harmonic motion, $A^{(m)} \cos \omega t$, where $m = 1,2,3$, and 4 denote surge,* sway, heave, and roll, respectively; see Figure 1. The potential $\Phi^{(m)}$ is given by the following expression:

---

*In References 3 and 4, the solution is indicated only for $m = 2,3,4$. In a later development, DTNSRDC has implemented into SMP a solution for surge. In the case of surge, the normal to the cross section has a component in the longitudinal X-direction, based on the change of half breadth of the ship with X.

4

$$\phi^{(m)}(y,z,t) = R_e[\phi^{(m)}(y,z)e^{-i\omega t}] \qquad \text{for } m = 1,2,3,4 \qquad (1)$$

and satisfies the following conditions:

(a) The two-dimensional Laplace equation

$$\nabla^2 \phi^{(m)} = \phi_{yy}^{(m)} + \phi_{zz}^{(m)} = 0 \qquad (2)$$

in the fluid domain

(b) The free surface condition

$$\phi_z^{(m)} - \frac{\omega^2}{g} \phi^{(m)} = 0 \qquad (3)$$

on the undisturbed free surface $z = 0$, where g is the gravitational constant.

(c) The bottom condition

$$\lim_{z \to -\infty} \left| \nabla \phi^{(m)} \right| = 0 \qquad (4)$$

(d) The kinematic boundary condition

$$\underset{\sim}{n} \cdot \nabla \phi^{(m)} = v_n^{(m)} \qquad (5)$$

on the mean position of the section contour S_B, where $v_n^{(m)}$ is the velocity component of the mth forced oscillation along $\underset{\sim}{n}$, the outward normal to the section contour.

(e) The radiation condition is that the disturbance far from the section takes the form of progressive outgoing gravity waves.

The solution to the above boundary-value problem is formally expressed in the form of a line integral over the cross section contour as

5

$$\phi^{(m)}(p,t) = R_e \int_{S_B} Q^{(m)}(q) \, G(p,q) \, e^{-i\omega t} \, dS \tag{6}$$

where   p   = a point in the flow field

     q   = a point on the contour S_B

     $Ge^{-i\omega t}$ = the complex potential generated by a pulsating source of unit strength placed at q

     Q   = complex strength of the source to be determined

     dS   = an infinitesmially small contour length of S_B

The expression, Equation (6), which satisfies the conditions a, b, c, and e identically and the kinematic boundary condition, Equation (5), furnishes an integral equation for the unknown strength Q(q) on S_B, i.e.,

$$\underset{\sim}{n} \cdot \nabla\phi^{(m)} = \underset{\sim}{n} \cdot R_e \left(\nabla \int_{S_B} Q^{(m)}(q) G(p,q) e^{-i\omega t} dS \right) = v_n^{(m)} \tag{7}$$

To render the problem numerically tractable, the actual continuous contour is approximated by a series of N straight line segments connecting N + 1 input points (y_i, z_i) where y_i is the half-breadth of the section at depth z_i. A pulsating line source of constant strength Q_i is placed over each line segment, where Q_i varies from segment to segment. Under these assumptions, the continuous integral Equation (7) is reduced to a system of N complex algebraic equations for the complex strengths Q_i.

Once the Q_i are obtained, the pressure $P^{(m)}$ on the hull section contour is found by using the linearized Bernoulli equation

$$P^{(m)}(y,z) = -\rho \frac{\partial \phi^{(m)}}{\partial t} = \rho\omega \, R_e[i\phi^{(m)} e^{-i\omega t}] \tag{8}$$

The added mass and damping forces on the section are then obtained by integrating $P^{(m)}$ over the contour of the section.

The wave-exciting forces on the section are computed as the sum of the Froude-Krilov force and the diffraction force. The Froude-Krilov force is obtained by

6

integrating the pressure contributed by the undisturbed incident wave over the surface of the contour. The diffraction force represents the disturbance due to the presence of the ship hull and is obtained by using the Haskind relation,[4] which expresses the diffraction force in terms of the previously derived velocity potential $\phi^{(m)}$ for forced oscillation.

The overall added mass, damping, and exciting forces on the entire ship hull are then obtained by integrating the computed sectional forces over the length of the ship.

The SMP program follows the above procedure to calculate the added mass and damping coefficients for 10 frequencies ω ranging between 0.2 and 2.0 rad/sec. Then, by spline fitting the values at these 10 frequencies, the coefficients are calculated for a total of 30 frequencies. For each frequency, the wave exciting forces are calculated for 13 heading angles, evenly spaced at 15 deg segments from head seas ($\beta=0$ deg) to following seas ($\beta=180$ deg). The resulting hydrodynamic coefficients are then written onto the file COFFIL which can then be input into the motion part of SMP, described later in this section.

POTENTIAL FORCE CALCULATIONS: MOTIONSO

The theory used by MOTIONSO to calculate the added mass and damping coefficients is also an linearized theory. It is similar to the above theory for SMP, with the principal difference that the conditions (a) to (e) are generalized to three dimensions. That is, interaction between ship sections is now accounted for and the boundary-value problem has to be solved for the entire ship. As a result of this generalization, the formulation given in Equations (1) through (8) is modified as follows.

1. The potential for force oscillation $\phi^{(m)}$, Equation (1), can be calculated for all six values of m, instead of only four, as in the case of SMP.

2. The Laplace equation, Equation (2), must now be satisfied three-dimensionally

$$\nabla^2 \phi^{(m)} = \phi_{xx}^{(m)} + \phi_{yy}^{(m)} + \phi_{zz}^{(m)} = 0 \tag{9}$$

3. The term S_B, appearing in Equations (5), (6), and (7), now represents the submerged surface of the entire ship instead of a sectional contour.

7

4. The term $Q(q) \ G(p,q)e^{-i\omega t}$, appearing in Equations (6) and (7) now represents a three-dimensional pulsating source, with strength Q, instead of a two-dimensional source.

5. In order to render the integral Equation (7) numerically tractable, the entire ship hull is now divided into N panels, instead of series of sections represented by line segments. A pulsating three-dimensional source of constant strength Q_i is then placed over each panel, where Q_i varies from panel to panel.

There is also a significant difference in the way the two programs calculate the wave exciting force. Instead of using the Haskind relation to calculate the diffraction force, MOTIONSO directly calculates the diffraction potential Φ_D from the following boundary condition on S_B

$$\frac{\partial(\Phi_w + \Phi_D)}{\partial n} = 0 \qquad (10)$$

where Φ_w is the known potential of the incoming wave and S_B is the surface of the ship hull. Once Φ_D is obtained, the pressure on the ship hull is obtained by using an equation similar to Equation (8)

$$\frac{P}{\rho} = - \frac{\partial(\Phi_w + \Phi_D)}{\partial t} = \omega \ Re[i(\Phi_w + \Phi_D)] \qquad (11)$$

The exciting force is then obtained by integrating the above values of P over the surface of the ship hull.

It must be emphasized that the above differences are given only for the case of zero speed. In the case of forward speed, there are additional significant differences. These will be discussed in a sequel report dealing with the more general forward speed case.

Program MOTIONSO uses the above procedure to calculate the potential forces (inviscid forces) for a given frequency ω. In the present work, potential forces were calculated for five frequencies ranging between 0.25 and 1.0 for each panel representation of a ship hull. The computer time and cost are dependent upon the number of panels used to represent the ship hull. On the TI ASC computer at the Naval Research Laboratory, central processor time for a given frequency ranges from

8

35 sec for the 71-panel representation of CVA-59 to 90 sec for the 104-panel representation of FRIESLAND. Corresponding computer costs range from approximately $50 to $125 for each frequency.* It should be noted that MOTIONSO was not specifically programmed to calculate the zero speed case. Instead, it was programmed as a special case of the more general calculation for forward speed. A program** has been developed specifically for the zero speed case, with substantially reduced computer cost. For comparison purposes, SMP requires typically 300 seconds of central processor time on the CDC 6600 computer, currently used at the Center, to calculate the potential forces for 10 frequencies at a given speed. The cost is typically $30 for all 10 frequencies.

MOTION CALCULATIONS: SMP

The motion calculation part of SMP solves the following linear coupled differential equation in the frequency domain for the six modes of motion of the ship

$$\sum_{k=1}^{6} [(M_{jk}+A_{jk})\ddot{\eta}_k+B_{jk}\dot{\eta}_k+C_{jk}\eta_k] = F_j \, e^{-i\omega t} \qquad j=1 \text{ throug}^\iota 6 \quad (12)$$

where η_k = ship motions

M_{jk} = components of the generalized mass matrix

A_{jk} = added mass coefficients

B_{jk} = damping coefficients

C_{jk} = hydrostatic restoring coefficients

F_j = complex amplitudes of exciting forces

The numbering convention for the ship motions is shown in Figure 1.

The motion part of SMP calculates the values of M_{jk} and C_{jk} using the input geometry of the ship and appendages. It also calculates lift, in the case of forward speed, and viscous roll damping coefficients, for the appendages. The motion part of

---

*Using block time priority, which is the least expensive, the above cost range for MOTIONSO is reduced to approximately $20 to $50 on the Center's CDC 6600 computer. However, the memory capability of the computer restricts the present version of the program to only 80 ship panels.

**Unpublished program by Chang. The program uses a doublet distribution instead of a source distribution and evaluates the potential by using Bessel functions.

SMP accepts as input the potential force coefficients A_{jk}, B_{jk}, and F_j. In the computation of motion, these force coefficients were calculated by MOTIONSO as an input to the motion calculation part of SMP and the results are compared with those obtained entirely by SMP.

The program assumes that the ship is symmetrical about the vertical x-z plane (lateral symmetry). This then reduces the set of 6 Equations (12) to 2 sets of 3 equations, one set for the vertical modes of motion: surge, heave, and pitch (j=1,3, 5) and one set for the lateral modes of motion: sway, roll, and yaw (j=2,4,6). The previously mentioned lift and viscous roll damping forces affect only the lateral motions. Thus, the vertical motions are determined solely by the mass, potential, and hydrostatic forces.

At the discretion of the user, SMP can provide printouts giving large variety of motions, loads, and pressures. For example, the program can furnish the response amplitude operators as input for computing motions in an irregular sea. It can also calculate relative motions at arbitrary points on the ship hull. The principal interests in the present work are the response amplitude operators (RAO) defined as the following function of frequency ω and angle β

$$RAO_j(\omega,\beta) = \left(\frac{|\eta_j|}{A_w}\right)^2 \qquad \text{for } j = 1,2,\ldots,6 \qquad (13)$$

where A_w is the wave amplitude. Since SMP prints the angular motions in units of degrees, the RAO's are related to the dimensionless transfer functions $H(\omega,\beta)$ by

$$RAO_j = \begin{cases} |H_j|^2 & \text{for } j = 1,2,3 \\[2em] |H_j|^2 \left(\frac{360}{\lambda}\right)^2 & \text{for } j = 4,5,6 \end{cases} \qquad (14)$$

where $\lambda = \dfrac{2\pi g}{\omega^2}$ is the wavelength.

10

DESCRIPTION OF SHIP HULLS

CHOICE OF SHIP HULLS

The choice of ship hulls was based on two principal considerations. First, it was important that the chosen hulls have available experimental data to validate the theoretical predictions. Second, it was desired to choose ship hulls which would cover a relatively wide range of geometrical characteristics in order to make a comprehensive evaluation of the theoretical predictions.

Based on the above considerations, four ship hulls were finally chosen for the present evaluation: the DE-1006 destroyer, the FRIESLAND frigate, the S7-175 container ship, and the CVA-59 carrier. Experiments have been conducted at the Center in which all six motions of models of the DE-1006 and CVA-59 ships have been measured for two speeds and a series of heading angles. The data have been analyzed but have not yet been published. The S7-175 was of special interest since it was the subject of a comprehensive world-wide evaluation of existing ship motion programs sponsored by the 15th ITTC Seakeeping Committee.[6] The evaluation was conducted for a given ship speed for all six motions for a series of heading angles. Smith[7] has measured the heave and pitch motions of a model of the FRIESLAND for a series of speeds at a heading angle β of 0 deg (head seas). While there is the disadvantage in this case that lateral motions were not measured, measurements were made of the added mass, damping, and exciting forces in the vertical plane. These data furnish a direct evaluation of the potential force coefficients calculated by SMP and MOTIONSO. The description of the motion prediction part of SMP shows that a number of other forces, in addition to the potential forces, were included in the calculations of horizontal modes of motion. Thus, the motion measurements furnish only an indirect validation of the potential force calculations.

An unfortunate aspect of the previous data is that they were all obtained at forward speed. Thus, they are largely not applicable to the present initial evaluation for zero speed. Only the case of the experiment conducted at 5 knots for the CVA-59 is included in the present work. In this case, it was felt that the Froude number (F_n) of 0.05 was close enough to the zero speed case, and the shifts in encounter frequency ω_e from wave frequency ω would be small enough, to consider it as a zero speed case, where F_n and ω_e are defined by

$$F_n = \frac{U}{\sqrt{gL}} \tag{15}$$

11

and

$$\omega_e = \omega \left(1 + \frac{\omega U}{g} \cos \beta\right) \tag{16}$$

where U = velocity of the ship

L = length of the ship

β = wave heading angle

The remaining experimental data will be considered in a sequel report dealing with the forward speed case.

GEOMETRICAL CHARACTERISTICS OF HULL AND APPENDAGES

Table 1 gives a brief summary of the geometrical characteristics of the four hulls. The table shows the length L, displaced weight W, block coefficient C_B, draft-to-beam ratio D/B, transom stern width-to-beam ratio TW/B, and the presence or absence of a bulbous bow. Table 1 shows that there is a relatively large range in each of the above characteristics

      (a)   308 ft (93.9 m) $\leq$ L $\leq$ 990 (301.7 m)

      (b)   1,873 long tons $\leq$ W $\leq$ 75,954 long tons

      (c)   0.51 $\leq$ C_B $\leq$ 0.60

      (d)   0.28 $\leq$ D/B $\leq$ 0.37

      (e)   0. $\leq$ TW/B $\leq$ 0.84

      (f)   No bulbous bow to a large bulbous bow

Tables 2, 3, 4, and 5, respectively, give more detailed descriptions of the hull and appendage characteristics of the DE-1006, FRIESLAND, S7-175, and CVA-59. Figures 2, 3, 4, and 5 show corresponding sectional contours of the above ships at the longitudinal stations shown in Table 6, which gives the SMP point representation of the hull shapes. In these figures, the right side of the figure shows the sections for the aft half.

Tables 3 and 4 show that the same set of appendages was used for the DE-1006 and the FRIESLAND. This was due to the fact that the appendage characteristics for the FRIESLAND, a Dutch frigate, could not be readily obtained. For convenience, the appendage data for the DE-1006 which is the closest in overall size of the other three ships considered in this report, were also used for the FRIESLAND. Tables 2

12

and 3 show that the DE-1006 is 15 percent shorter and has 35 percent less displace-
ment than the FRIESLAND. However, it should be noted that SMP assumes that the
appendages affect only the lateral motions, for which no experimental data are
available in the case of the FRIESLAND.

COMPUTER MODELING OF SHIP HULLS

Programs SMP and MOTIONSO approximate the actual continuous hull surface by a
series of discrete points which are connected to form linear segments or quadri-
lateral panels, respectively. Tables 6 and 7 show the point distribution for each
of the four chosen ships used by SMP and MOTIONSO, respectively. The table shows
that both programs model the hull by describing the shape of the vertical cross
sections at a series of longitudinal x-stations. For a given cross section, the
input points on the girth are chosen so as to give the most accurate linear-segment
representation of the section. Usually, this leads to segments of approximately
equal lengths. As examples of point spacing, the crosses in Figures 2 through 5
represent the points read into SMP to represent each cross section. The solid lines
represent the spline fit curves through the input points. The numbering of the
longitudinal stations follows the convention used by SMP. The length of the ship is
divided into 20 equally spaced stations, with station 0 at the forward perpendicular
and station 20 at the aft perpendicular. For the case of MOTIONSO, Table 7 also
shows that FRIESLAND and CVA-59 were each modeled by two different point distribu-
tions. This was done to investigate the effect of number and distribution of points
on the results calculated by MOTIONSO.

Tables 6 and 7 show that, for a given ship hull, SMP uses a point distribution
which is 50 to 100 percent more dense than the corresponding distribution used by
MOTIONSO. This is due to the higher overall computer cost of MOTIONSO and its
dependence on number of panels. Recall that the calculation of the potential forces
for ten frequencies using SMP is approximately $30 on the Center's CDC 6600 computer
while the corresponding cost for one frequency using MOTIONSO ranges from $50 to
$125 on the TI ASC computer at the Naval Research Laboratory.

PRESENTATION OF RESULTS

Figures 6 through 9 show the potential force and motion coefficients for values
of the dimensionless frequency σ between 0 and 4, where σ is related to ω by

$$\sigma = \omega \sqrt{\frac{L}{g}} \qquad (17)$$

Figures 6 and 8 show the potential forces as the dimensionless added mass, damping, and wave exciting force coefficients: a_{ij}, b_{ij}, and f_j defined in terms of the dimensional quantities A_{ij}, B_{ij}, and F_j by

$$a_{ij} = \frac{A_{ij}}{\rho V}$$

$$\text{for } i,j = 1,2,3 \qquad (18a)$$

$$b_{ij} = \frac{B_{ij}}{\left(\rho V \sqrt{\frac{g}{L}}\right)}$$

$$a_{ij} = \frac{A_{ij}}{\rho V L}$$

$$\text{for } \begin{matrix} i = 1,2,3 \\ j = 4,5,6 \end{matrix} \qquad (18b)$$

$$b_{ij} = \frac{B_{ij}}{\left(\rho V L \sqrt{\frac{g}{L}}\right)}$$

$$a_{ij} = \frac{A_{ij}}{\rho V L^2}$$

$$\text{for } i,j = 4,5,6 \qquad (18c)$$

$$b_{ij} = \frac{B_{ij}}{\left(\rho V L^2 \sqrt{\frac{g}{L}}\right)}$$

$$f_j = \frac{F_j}{\left(A_w \rho V \frac{g}{L}\right)} \qquad \text{for } j = 1,2,3 \qquad (18d)$$

$$f_j = \frac{F_j}{(\rho V g A_w)} \qquad \text{for } j = 4,5,6 \qquad (18e)$$

where ρ is the fluid density and V is the displaced volume.

14

Figures 7 and 9 show the motions in terms of the RAO's, defined in Equation (13). In addition to the calculated motions, Figures 7 and 9 also show experimental data for the CVA-59. The measurements were originally given in terms of the transfer function $H(\omega,\beta)$, but were converted to RAO's by using the relations given in Equation (14).

Figure 6 shows the potential force coefficients in the vertical plane $(j=1,3,5)$ calculated by SMP and MOTIONSO for the ship representations shown in Tables 6 and 7, respectively. Figure 7 shows the motion coefficients in the vertical plane, calculated by the motion prediction part of SMP, resulting from the forces shown in Figure 6. Figures 8 and 9, respectively, show corresponding results for the calculated potential force and motion coefficients in the lateral plane $(j=2,4,6)$. In addition, Figures 7 and 9 show measured motions for the CVA-59. As mentioned previously, experimental data for the remaining hulls were obtained at speeds which are too high to approximate the zero speed case.

Although the exciting forces and motions were calculated for a series of heading angles β ranging from 0 to 180 deg, Figures 6-7 and 8-9, respectively, show results for $\beta = 0$ (head seas) and $\beta = 90$ (beam seas). This was done largely to minimize the already large number of plots. In addition, results at other heading angles may be viewed to some extent as a combination of the above two headings.

DISCUSSION OF RESULTS

The data shown in Figures 6 through 9 are compared and discussed in three principal ways. First, the potential force and resultant motion coefficients predicted by MOTIONSO for the different panel representations of the FRIESLAND, S7-175, and CVA-59 are compared. This comparison furnishes insight into the effect of location and density of panels on the results calculated by MOTIONSO. Second, the results predicted by MOTIONSO and SMP are compared with each other for all four ship hulls. Finally, in the case of CVA-59, the motions predicted by both programs are compared with measured data.

In the above paragraph as well as in the remainder of this chapter, the phrase "motions predicted by MOTIONSO" is often used, either explicitly or implicitly. Recalling that MOTIONSO calculates only potential forces, the above phrase should be interpreted as an abbreviated way of stating "motions predicted by the motion calculation part of SMP using the potential force calculated by MOTIONSO."

15

MOTIONSO RESULTS FOR DIFFERENT PANEL REPRESENTATIONS

Table 7 shows that MOTIONSO calculations were made for 78-panel and 104-panel representations of FRIESLAND, 71-panel and 103-panel representations of CVA-59, and 78-panel and 82-panel representations of S7-175. For the first two ships, the same x-stations were used for the sparser and denser panel representations. In the case of FRIESLAND, the 78-panel representation has two less panels at each x-station than the 104-panel representation. In the case of CVA-59, the 71-panel representation has three less panels per station over the forward two-thirds of the ship. Over the aft third, the difference in number of panels decreases to zero as the stern is approached. In the case of the S7-175, the 82-panel representation is identical to the 78-panel representation except for the addition of four panels to model the bulbous bow.

For the vertical modes, Figures 6 and 7 show the striking result that the large majority of the force and motion coefficients for the different panel representations agree to within one to two percent for each ship. The largest differences, approximately five percent, occur for the coefficients A_{31} and B_{31}, which are assumed to be identically zero by SMP. This striking agreement suggests that the calculated results for the vertical modes could have been obtained with comparable accuracy for even more sparse panel representations.

Figures 8 and 9 show that, in the case of the lateral modes, the calculated force and motion coefficients for both panel representations of the FRIESLAND again agree to within two percent, for most cases. Again, the largest differences usually do not exceed five percent.

However, the situation is quite different in the case of the lateral force coefficients for CVA-59 and S7-175. Here, there are almost always differences of at least five percent at the two highest values of σ for which calculations were made using MOTIONSO. The largest differences, on the order of 50 percent, occur for the force coefficients involving the yaw mode ($j=6$). The large discrepancy appears to be due to the failure of the sparser panel representation to properly model the bulbous bow (see Figures 4 and 5). In the case of yaw, errors in the bow region are magnified by the large moment arm from the center of gravity and result in a large discrepancy in yaw coefficients.

In the case of motions, Figure 9 shows that there is agreement to within two percent for sway ($j=2$) and roll ($j=4$). There are differences on the order of 30

percent in the case of yaw ($j=6$). However, these differences are not significant since the yaw motions are at least one order of magnitude smaller than the pitch and roll motions. On the whole, the discrepancy between motions is less than the discrepancies between the force coefficients. The smaller discrepancy in the motions is not surprising since the motions are calculated by using potential forces as well as a constant set of hydrostatic, inertia, and roll damping forces, which do not differ for the different panel representations.

It is also of interest to note the following two trends in the case of S7-175 and CVA-59. First, with the single exception of the roll moment coefficient F_4, the effect of denser modeling of the CVA-59 bulbous bow is to reduce the magnitude of the lateral force coefficients calculated by MOTIONSO. Second, in most cases where a large discrepancy exists, the calculated results for the dense panel representation tend to be in better agreement with SMP results. (This trend is particularly evident in the case of CVA-59.) Taken together, these trends indicate that the principal effect of more careful modeling of the bulbous bow is to provide a finer distribution of the coefficients in the end region so that their contribution to the moment about the center of gravity is represented more accurately. The better agreement of MOTIONSO with SMP when MOTIONSO panel density is increased may stem from the fact that SMP has smaller strips in the bow.

COMPARISON OF SMP AND MOTIONSO RESULTS

The numerical results obtained from MOTIONSO have been compared with the corresponding results of strip theory. Some general trends observed in the comparison are presented in the following sections.

Vertical Modes

Figure 6 shows the added mass and damping coefficients A_{ij} and B_{ij} in the vertical plane. With the exception of A_{31}, B_{31}, A_{51}, B_{51}, and B_{53}, there tends to be poor agreement at the lower values of σ and better agreement at the higher values of σ. Typically, the difference is 50 percent at lower values of σ but the percentage decreases to 10 to 20 percent at the higher values of σ. Program MOTIONSO usually predicts values of A_{ij} which are higher than those predicted by SMP, while the reverse is true for B_{ij}. The above trend in the differences conforms to the fact

that the strip theory is more valid in high frequency regions. In the case of A_{31}, B_{31}, A_{51}, and B_{51}, which involve the coupling of surge with heave and pitch, SMP predicts identically zero values, i.e., no coupling between these modes. In the case of B_{53}, the agreement is poor at all frequencies for all four ships. The difference is typically 30 percent. The agreement is even worse for B_{53}, at lower frequencies.

In the case of the exciting force coefficients F_j in the vertical plane, Figure 6 shows that the agreement is usually within one percent for the case of head seas, $\beta = 0$ deg. This suggests that the Froude-Krilov component, which is calculated in a similar way by both programs, dominates the diffraction component.

Figure 7 shows that, with the exception of the two lowest frequencies in the case of surge, the motions usually agree within one or two percent. The reasons for this behavior can be seen by considering the set of differential Equations (12) for the motion as well as the previously observed trend for the added mass, damping, and wave exciting forces. In the case of heave (j=3) and pitch (j=5) the hydrostatic restoring forces tend to dominate the frequency-dependent added mass and damping forces at the lower frequencies. Thus, the motion predictions are still in good agreement despite the large differences in the added mass and damping forces at low frequencies. Since the surge mode has no hydrostatic restoring forces, the differences in the added mass and damping forces at the lower frequencies lead to differences of 20 to 50 percent in the motions. In the case of CVA-59, it is shown later that the MOTIONSO results are in better agreement with experimental values than the SMP results.

In addition to the prediction of ship motion in six degrees of freedom, the prediction of the local flow field would be equally important for ship designers. One such example is the calculation of the relative wave motion around a ship bow. This information provides a guide for the selection of the necessary free board. The applicability of a numerical scheme to such computations should be established individually, and should not be judged from verification of the overall ship motion predictions. This is more important at the low frequencies where the hydrodynamic forces predicted from the strip theory and the three-dimensional computation do not agree well.

Lateral Modes

Figure 8 gives a comparison of the potential forces for the lateral motion modes. It shows that general agreement between the results of MOTIONSO and strip

18

theory is fairly good. Nevertheless, significant discrepancies appear for some of the ship hulls in the yaw mode. That is, except for the 104-panel representation of CVA-59, the differences in the added mass and damping coefficients involving yaw (j=6) can often exceed 20 percent, while the differences in the coefficients involving only roll and sway are within 10 percent. It is also noted that, in the lateral modes, the discrepancies between the damping coefficients tend to be noticeably smaller than the corresponding differences in the added mass coefficients; the differences do not increase with decreasing frequencies. This result has been known, and indicates the possible successful application of strip theory to the computation of the lateral motions of a ship at low frequencies.

The calculated wave-exciting forces for beam seas are shown in Figures 8m, 8n, and 8p. The agreement between predictions of SMP and MOTIONSO wave-exciting forces is generally better than the agreement in their corresponding motion coefficients, A_{ij} and B_{ij}. The agreement is within 20 percent and improves with decreasing frequency. Again, of the four ship hulls, the 78-panel representation of S7-175 generally exhibits the poorest agreement. Also, due to the previously mentioned effect of geometric modeling of the ends of the ship, the yaw exciting force exhibits larger differences than the sway or roll exciting forces.

Figure 9 shows that the calculated sway and roll motions for all ships, as well as the yaw motion for the 104-panel representation of CVA-59, usually agree within one or two percent. The calculated yaw motions for the remaining three ships exhibit differences which tend to increase with frequency, reaching values of perhaps 30 percent at the higher frequencies. However, as mentioned previously, these differences should not be viewed as being significant due to the much smaller magnitude of the yaw motions. As in the case of the vertical modes, the agreement in the motions is somewhat better than the corresponding agreement in the potential force coefficients. In this case, the addition of the inertia, hydrostatic restoring, and viscous roll damping forces tends to lessen the importance of the added mass and damping coefficients appearing in Equation (12) for the motions.

COMPARISON OF CALCULATED AND MEASURED MOTIONS

In addition to the calculated motions, Figures 7 and 9 show measured motions for the CVA-59 in the vertical and lateral planes, respectively. Before the comparison of the calculations and the experimental results, a few remarks on the

19

experimental results should be made. The data were not taken at zero speed, but at Froude number 0.05 corresponding to a full-scale speed of 5 knots. It also should be noted that the data were originally presented as transfer functions H. Equation (14) was used to convert the transfer functions to RAO's to conform to the output format of the motion prediction part of SMP. Equation (14) shows that the RAO's are proportional to the squares of the transfer functions. Thus, the results given in RAO's amplify the scatter in the experimental data as well as the discrepancy between the experimental and the predicted results. Also, in the case of the angular motions ($j=4,5,6$), since RAO's are obtained by dividing the transfer functions by the wavelength, RAO's tend to amplify the experimental inaccuracy at the higher frequencies (shorter wavelengths) relative to those at the lower frequencies (longer wavelengths).

Figures 7 and 9 show that, with the exception of the surge motions, the motions calculated by SMP and MOTIONSO (for the 103-panel representation of CVA-59) are in excellent agreement with experimental data.

In the case of surge, the experimental data are in better agreement with the MOTIONSO results. At the lowest frequency for which motions were calculated by MOTIONSO, the experimental result is approximately 20 percent higher than the MOTIONSO result and 50 percent higher than the SMP result. However, the large scatter in the experimental data in the low frequency range should be noted. As frequency increases, the calculated results decrease faster than the measured data. In the case of heave, the calculated results agree to within a few percent with the measured data, except for one data point at the lowest frequency where the difference is approximately 30 percent.

The pitch, sway, and yaw motions all exhibit resonance behavior. The largest differences usually occur at the resonance peaks. In the cases of pitch, roll, and yaw, the measured peaks are less than the peaks calculated by SMP and MOTIONSO by approximately 50 percent. It should be noted that resonance occurs over a narrow frequency band and that there is a dense distribution of calculated points near resonance. Thus, it is likely that there could be better agreement between the above differences if additional measured data points were available around the resonance peak.

Away from resonance, there appears to be a small frequency shift in pitch. The sway motion shows differences on the order of 15 percent. However, much of this difference is due to the large scatter in the experimental data. The roll and yaw motions show relatively good agreement away from resonance.

It should be noted that the accuracy of the calculated motions depends not only upon the accuracy of the potential force coefficients but also upon the accuracy of the viscous roll damping model. Some discrepancies could have been caused by the damping introduced by the five knot speed at which the experimental data was obtained and the zero speed of computed results where damping is zero.

SUMMARY

For the zero speed case considered in this report, the principal difference between SMP and MOTIONSO is that SMP uses a strip theory while MOTIONSO uses a three-dimensional approach. Another difference is that SMP uses the Haskind relation to calculate the diffraction force while MOTIONSO uses a more direct calculation. Program SMP typically uses 150 to 200 points to represent the ship hull while MOTIONSO typically uses 90 to 120 points (70 to 100 panels). The SMP requires approximately $30 to calculate the added mass, damping, and exciting forces for 10 frequencies using the CDC 6600 computer at the Center. The MOTIONSO requires $50 to $125 to calculate the above forces for one frequency using the TI ASC computer at the Naval Research Laboratory.

This report has presented potential force and motion coefficients calculated by SMP and MOTIONSO for four ship hulls at values of the dimensionless frequency σ between 0 and 4. In the case of the vertical modes, MOTIONSO calculates force and motion coefficients for the FRIESLAND, S7-175, and CVA-59 which usually agree to within two percent for different panel representations of the same ship hull. This suggests that accurate coefficients for these modes may be calculated for panel representations which are sparser than those considered in the present report. In the case of FRIESLAND, the agreement continues to be good for the lateral modes. However, in the case of S7-175 and CVA-59, calculated results involving yaw (j=6) for different panel representations differ by up to 50 percent. The difference may be due to the inaccurate modeling of the bulbous bow of the S7-175 and CVA-59 by the sparser panel representations. Force coefficients for the denser panel representations are usually lower than corresponding values for the sparser panel representations, and tend to be closer to values calculated by SMP.

In the case of the vertical modes, SMP and MOTIONSO predict added mass and damping coefficients which typically differ by 50 percent at the lower frequencies and 10 percent at the higher frequencies. The exciting forces for the case of head

seas usually agree to within one percent. This suggests that the diffraction effect computed by either method does not significantly affect the total exciting forces.
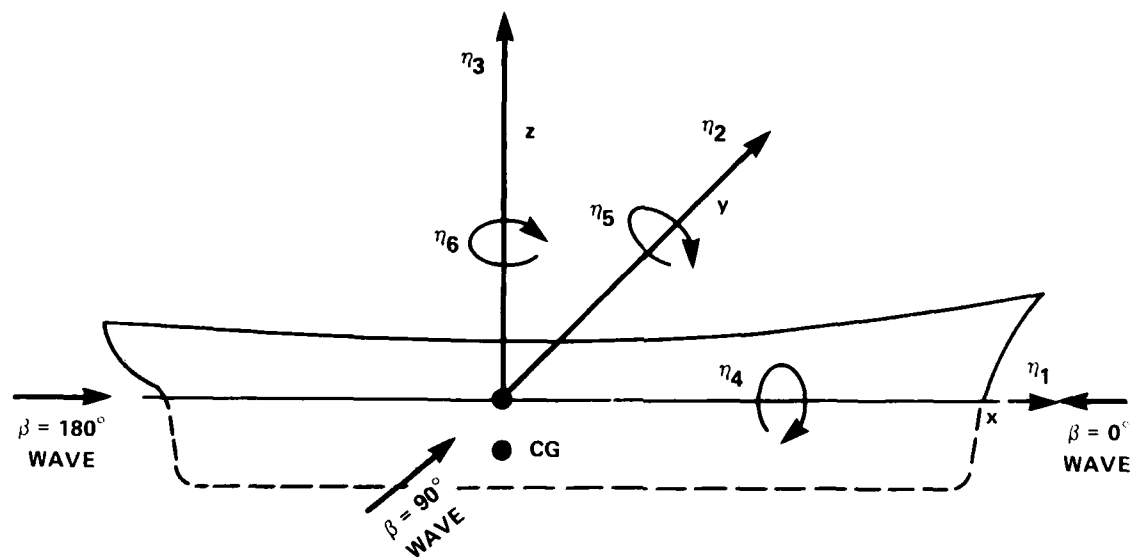
The agreement in the force coefficients predicted by SMP and MOTIONSO for the lateral modes does not show any well-defined dependence on frequency, but is, instead, more dependent upon the ship hull. The best agreement in the force coefficients occurs for the 103-panel representation of CVA-59, for which the differences are usually less than 10 percent. The worst disagreement occurs for the sparser panel representations of CVA-59 and S7-175, respectively, 71- and 78-panels, for which differences range as high as 60 percent. Both hulls have a bulbous bow. The differences in the added mass and damping coefficients tend to be smaller (usually less than 10 percent) for the modes involving only sway and roll than the modes involving yaw (often exceeding 20 percent). Also, for a given coupling mode (fixed values of i and j), the difference in the damping coefficient tends to be smaller than the corresponding difference in the added mass coefficient. The exciting force coefficients, with the largest differences of 20 percent, usually occur at the higher frequencies.

Due to the presence of an additional set of constant inertia, restoring, and viscous roll damping forces in the equations of motion, SMP and MOTIONSO predict motions which tend to be in better agreement than corresponding results for the potential forces. The calculated motions for heave, pitch, sway, and roll usually agree to within five percent. The calculated surge motions differ by 20 o 50 percent at the lower frequencies, but agree well at the higher frequencies. The calculated yaw motions, which are much smaller than the other angular motions, show differences up to 30 percent.

The agreement between the calculated and measured motions for CVA-59 depends upon frequency and the particular mode. In the case of surge, where the SMP and MOTIONSO predictions do not agree, the measured motions are approximately 20 percent higher than the MOTIONSO results and 50 percent higher than the SMP results. The agreement is good in the case of heave, except at the lowest frequencies where the difference is approximately 30 percent. In the case of pitch, sway, roll, and yaw, the calculated motions qualitatively exhibit the same behavior as the measured motions in the resonance region. Away from resonance, the differences for these modes are typically 20 percent.

22

ACKNOWLEDGMENTS

23

Figure 1 – Definition of Coordinate System and Ship Motions Used in SMP

η_1 = SURGE η_3 = HEAVE η_5 = PITCH

η_2 = SWAY η_4 = ROLL η_6 = YAW

24

YFWD STATION SPACING = 15.40 FEET
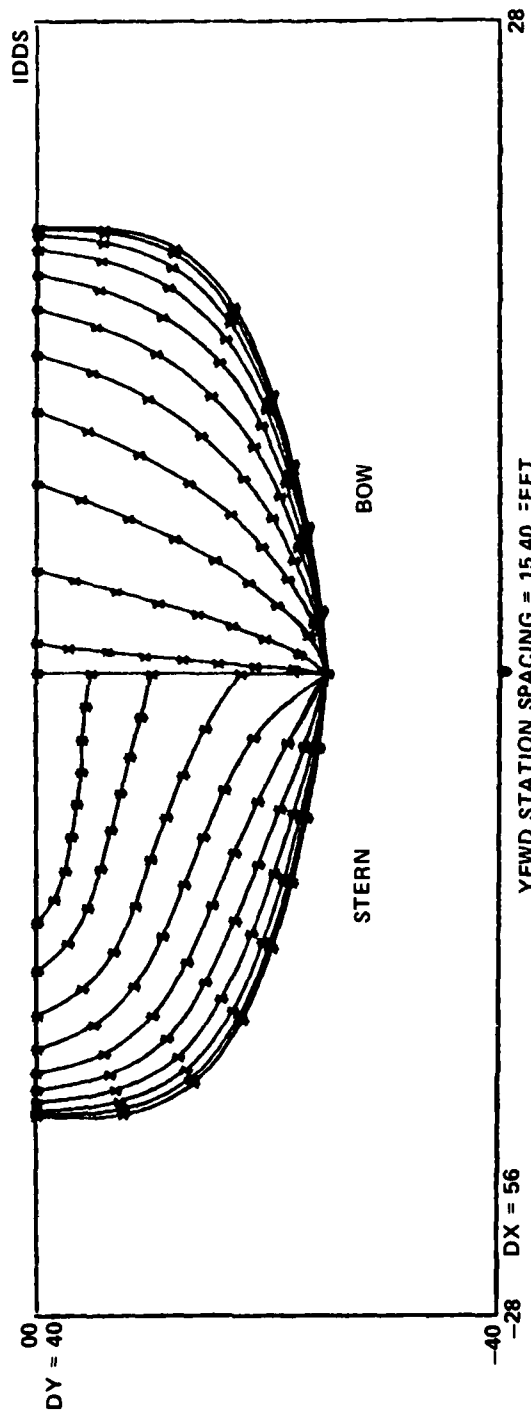
Figure 2 – Section Contours for DE-1006
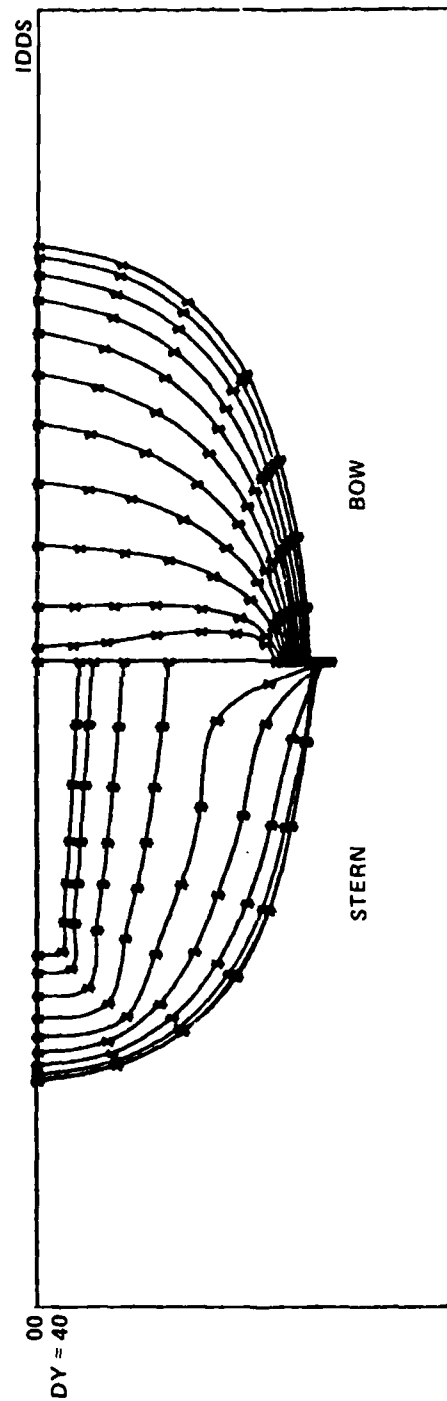
Figure 3 – Section Contours for FRIESLAND

25

IDDS

DY = 90
00

STERN

BOW
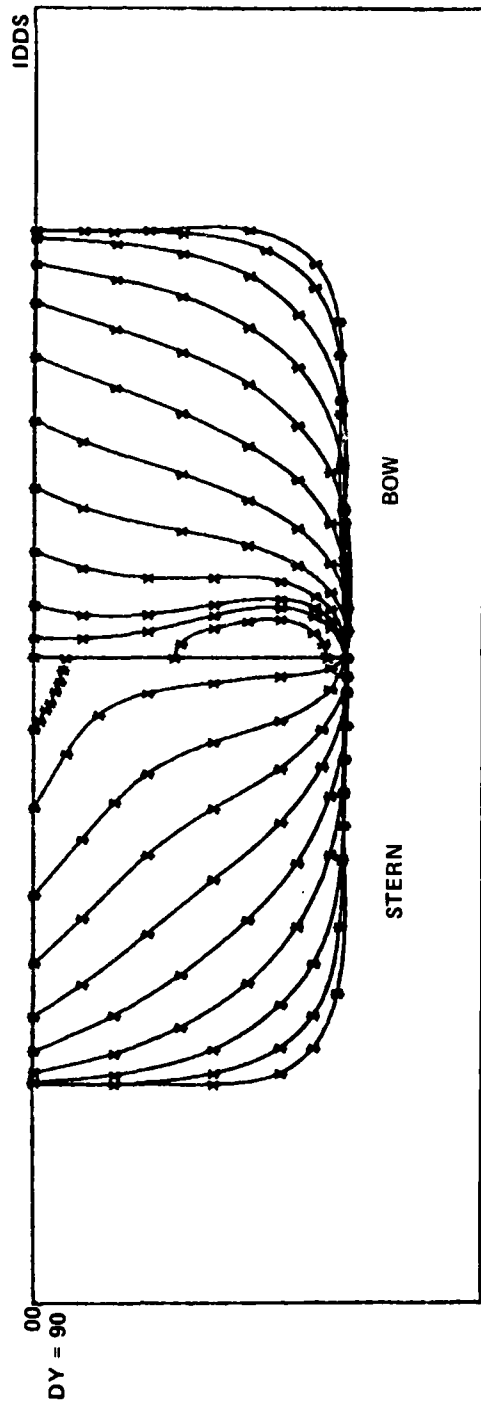
Figure 4 - Section Contours for S7-175

STERN

BOW

63

-63 DX = 126

-90

YFWD STATION SPACING = 28.71 FEET
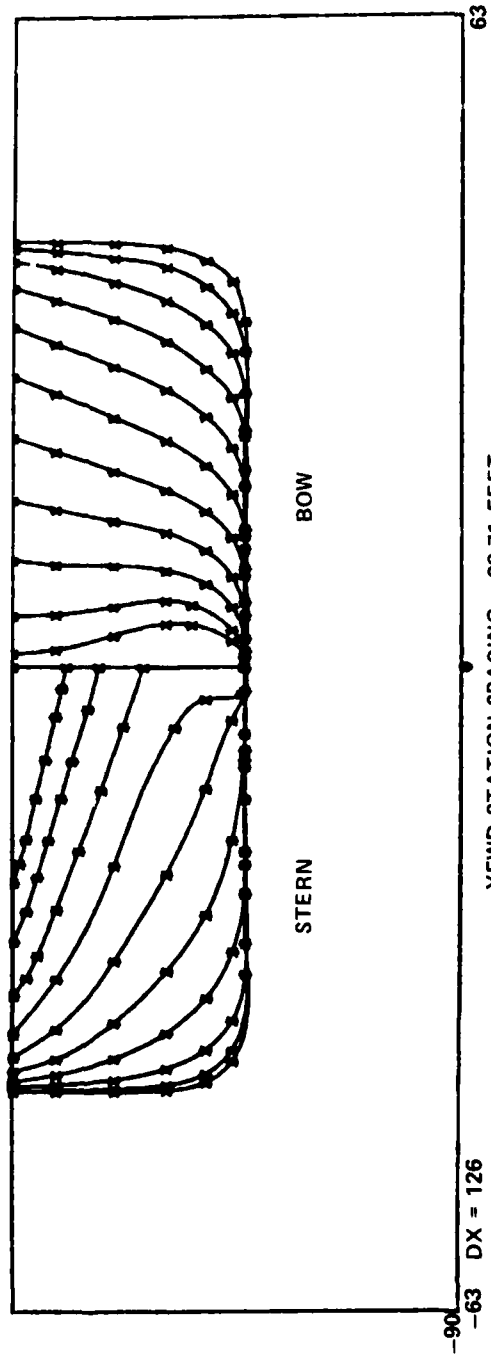
Figure 5 - Section Contours for CVA-59

26

Figure 6 - Potential Force Coefficients for Vertical Plane (j=1,3,5)

- ● SMP
- ○ MOTIONSO (SPARSER PANEL REPRESENTATION)
- ☐ MOTIONSO (DENSER PANEL REPRESENTATION)
- △ EXPERIMENT

DE = 1006, $\sigma = w \sqrt{\frac{L}{g}}$

FRIESLAND, $\sigma = w \sqrt{\frac{L}{g}}$

S7-175, $\sigma = w \sqrt{\frac{L}{g}}$

CVA-59, $\sigma = w \sqrt{\frac{L}{g}}$
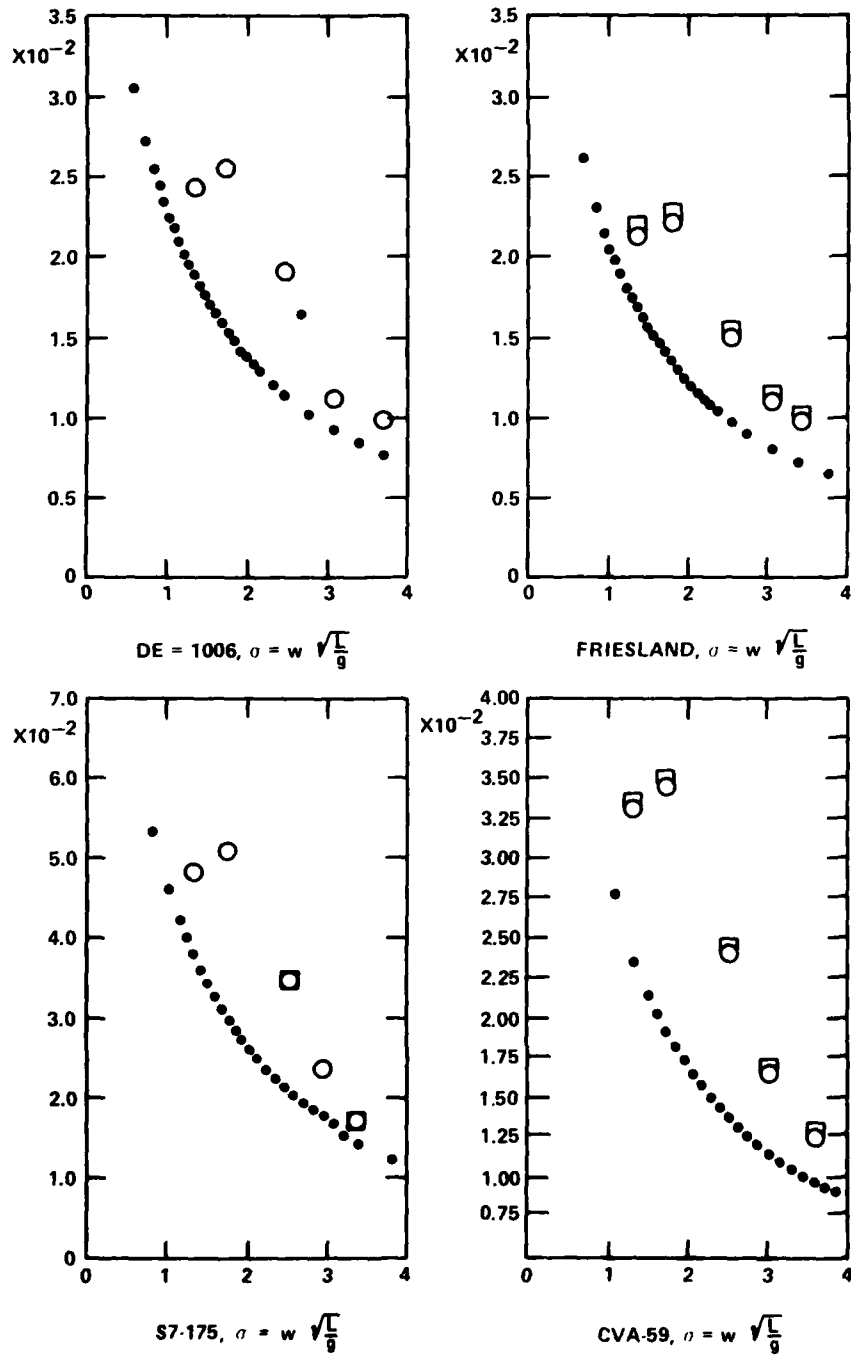
Figure 6a - Surge Added Mass Coefficient A_{11}

27
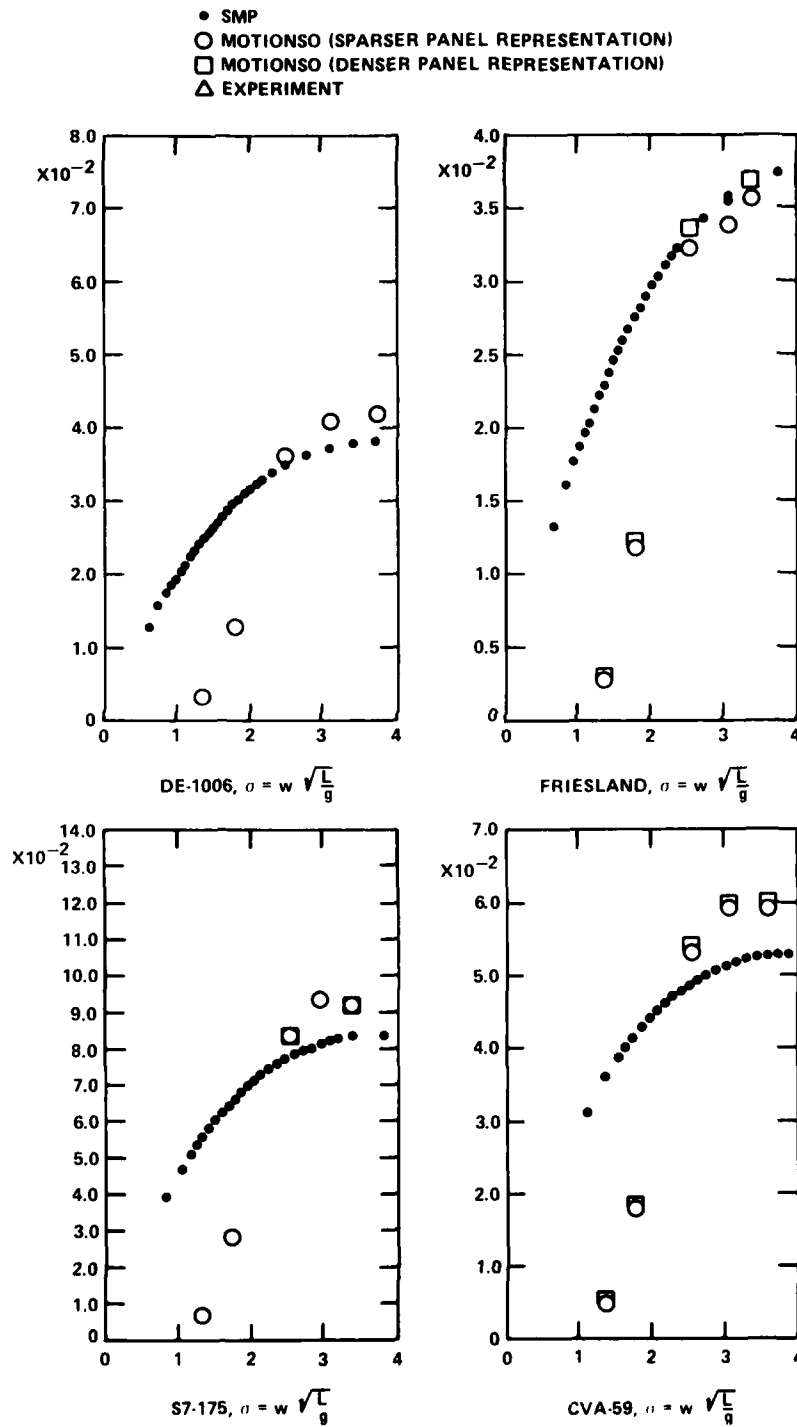
Figure 6 - (Continued)

Figure 6b - Surge Damping Coefficient B_{11}

Figure 6 - (Continued)

- • SMP
- ○ MOTIONSO (SPARSER PANEL REPRESENTATION)
- □ MOTIONSO (DENSER PANEL REPRESENTATION)
- △ EXPERIMENT

DE-1006, $\sigma = w \sqrt{\frac{L}{g}}$

FRIESLAND, $\sigma = w \sqrt{\frac{L}{g}}$

S7-175, $\sigma = w \sqrt{\frac{L}{g}}$

CVA-59, $\sigma = w \sqrt{\frac{L}{g}}$

Figure 6c - Heave-Surge Added Mass Coefficient A_{31}

29

Figure 6 – (Continued)

● SMP
○ MOTIONSO (SPARSER PANEL REPRESENTATION)
□ MOTIONSO (DENSER PANEL REPRESENTATION)
△ EXPERIMENT

DE-1006, $\sigma = w \sqrt{\dfrac{L}{g}}$

FRIESLAND, $\sigma = w \sqrt{\dfrac{L}{g}}$

S7-175, $\sigma = w \sqrt{\dfrac{L}{g}}$

CVA-59, $\sigma = w \sqrt{\dfrac{L}{g}}$
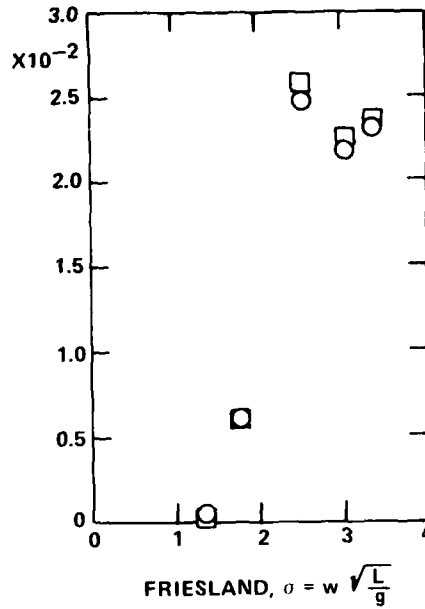
Figure 6d – Heave-Surge Damping Coefficient B_{31}

30

Figure 6 - (Continued)

● SMP
○ MOTIONSO (SPARSER PANEL REPRESENTATION)
□ MOTIONSO (DENSER PANEL REPRESENTATION)
△ EXPERIMENT

DE-1006, $\sigma = w \sqrt{\frac{L}{g}}$

FRIESLAND, $\sigma = w \sqrt{\frac{L}{g}}$

S7-175, $\sigma = w \sqrt{\frac{L}{g}}$

CVA-59, $\sigma = w \sqrt{\frac{L}{g}}$
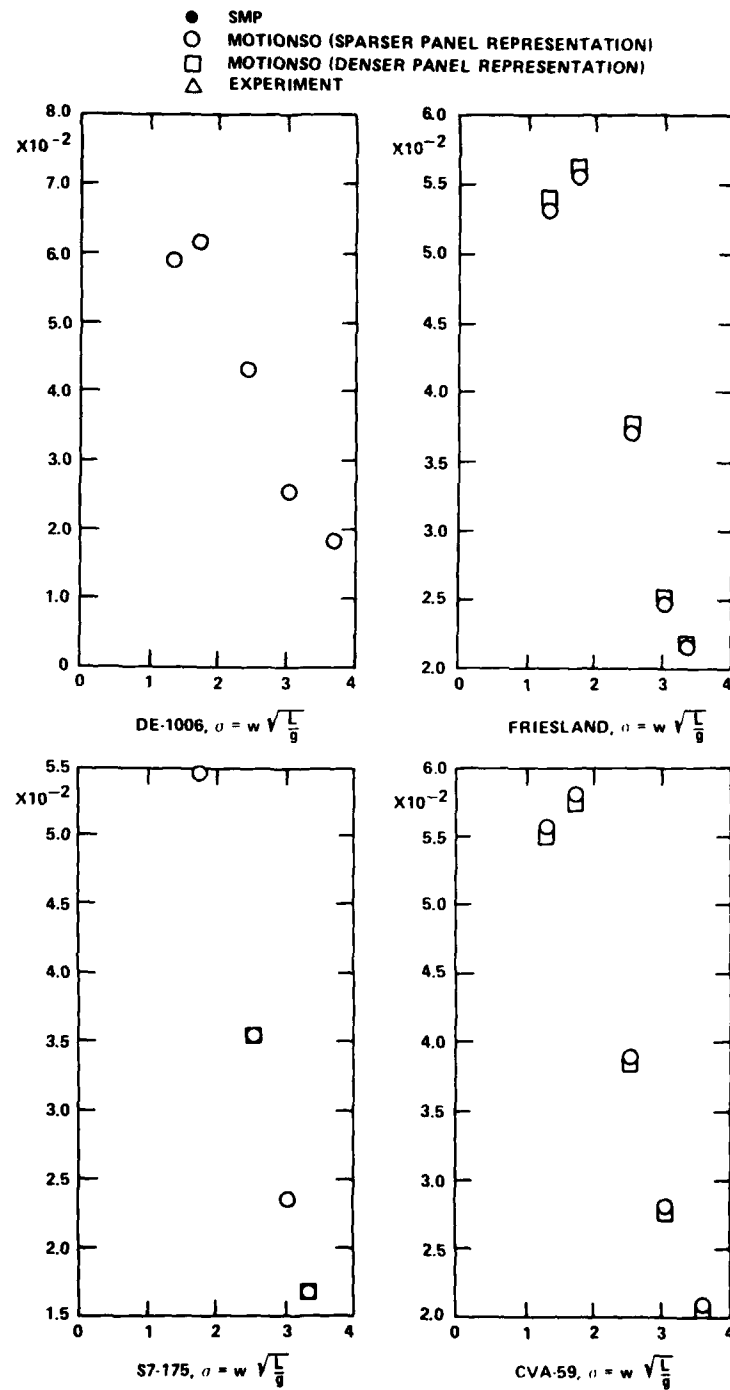
Figure 6e - Pitch-Surge Added Mass Coefficient A_{51}

31
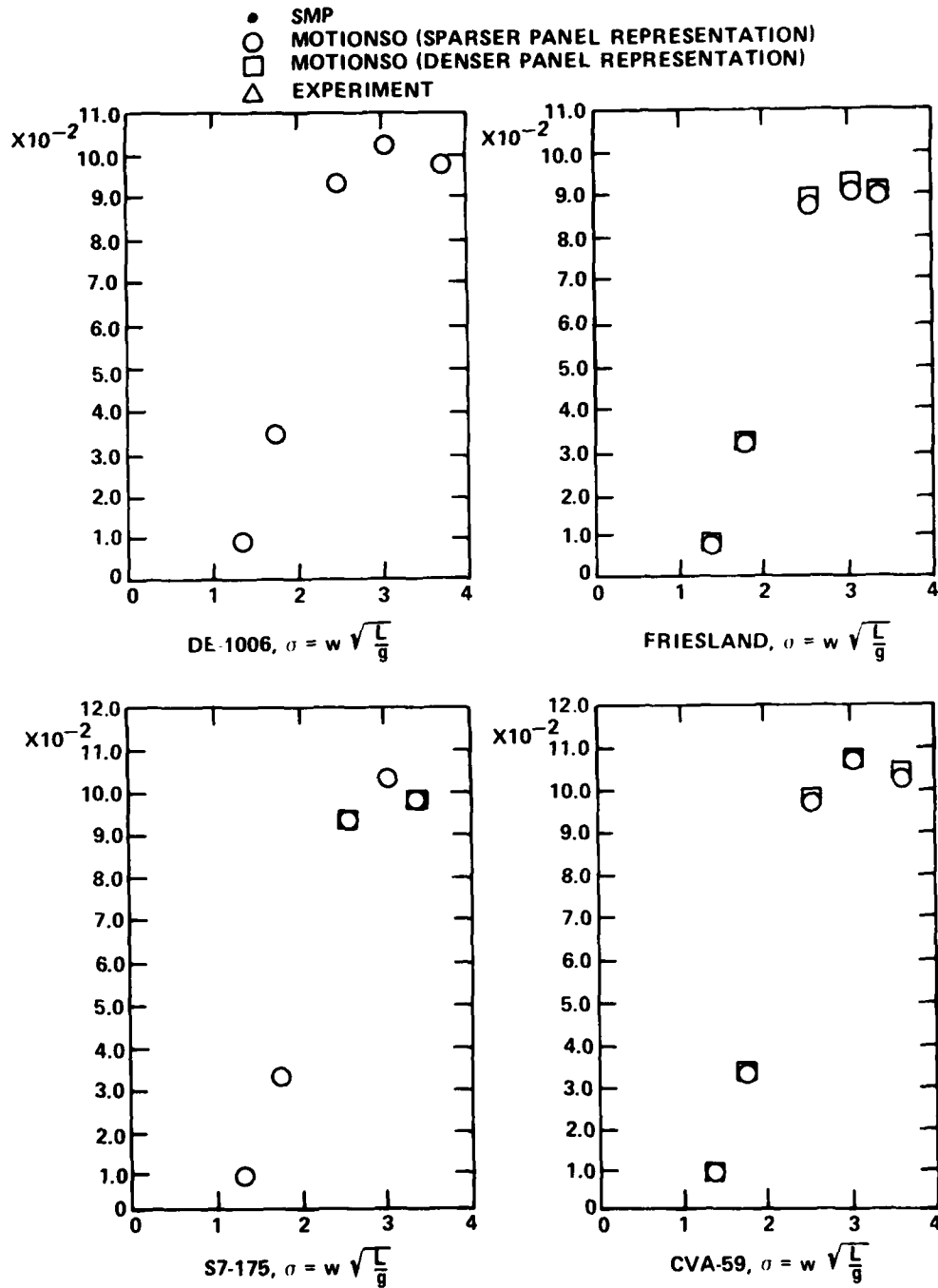
Figure 6 - (Continued)

Figure 6f - Pitch-Surge Damping Coefficient B_{51}

32
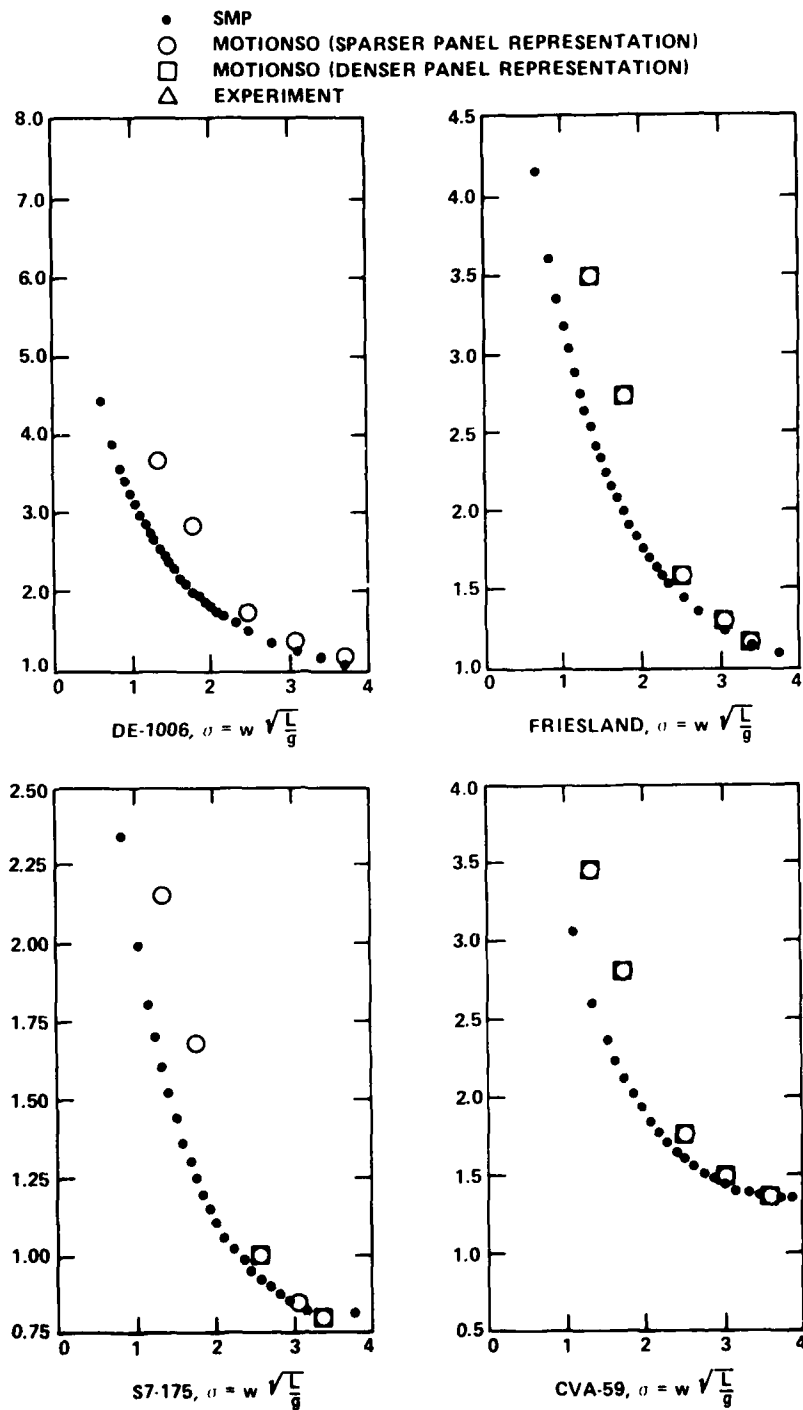
Figure 6 - (Continued)

Figure 6g - Heave Added Mass Coefficient A_{33}

33

Figure 6 - (Continued)

● SMP
○ MOTIONSO (SPARSER PANEL REPRESENTATION)
□ MOTIONSO (DENSER PANEL REPRESENTATION)
△ EXPERIMENT

DE-1006, $\sigma = w \sqrt{\frac{L}{g}}$

FRIESLAND, $\sigma = w \sqrt{\frac{L}{g}}$

S7-175, $\sigma = w \sqrt{\frac{L}{g}}$

CVA-59, $\sigma = w \sqrt{\frac{L}{g}}$
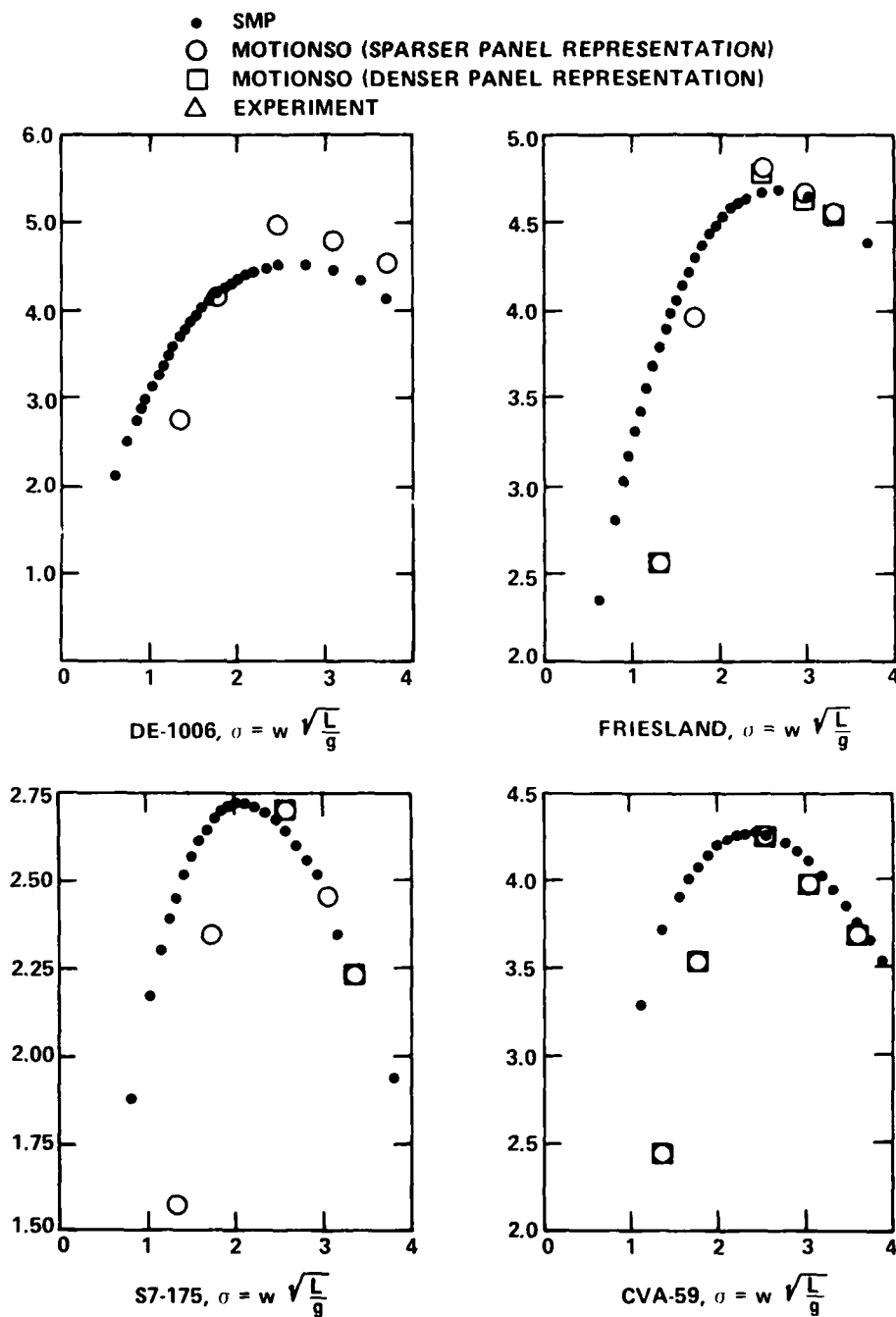
Figure 6h - Heave Damping Coefficient B_{33}

34
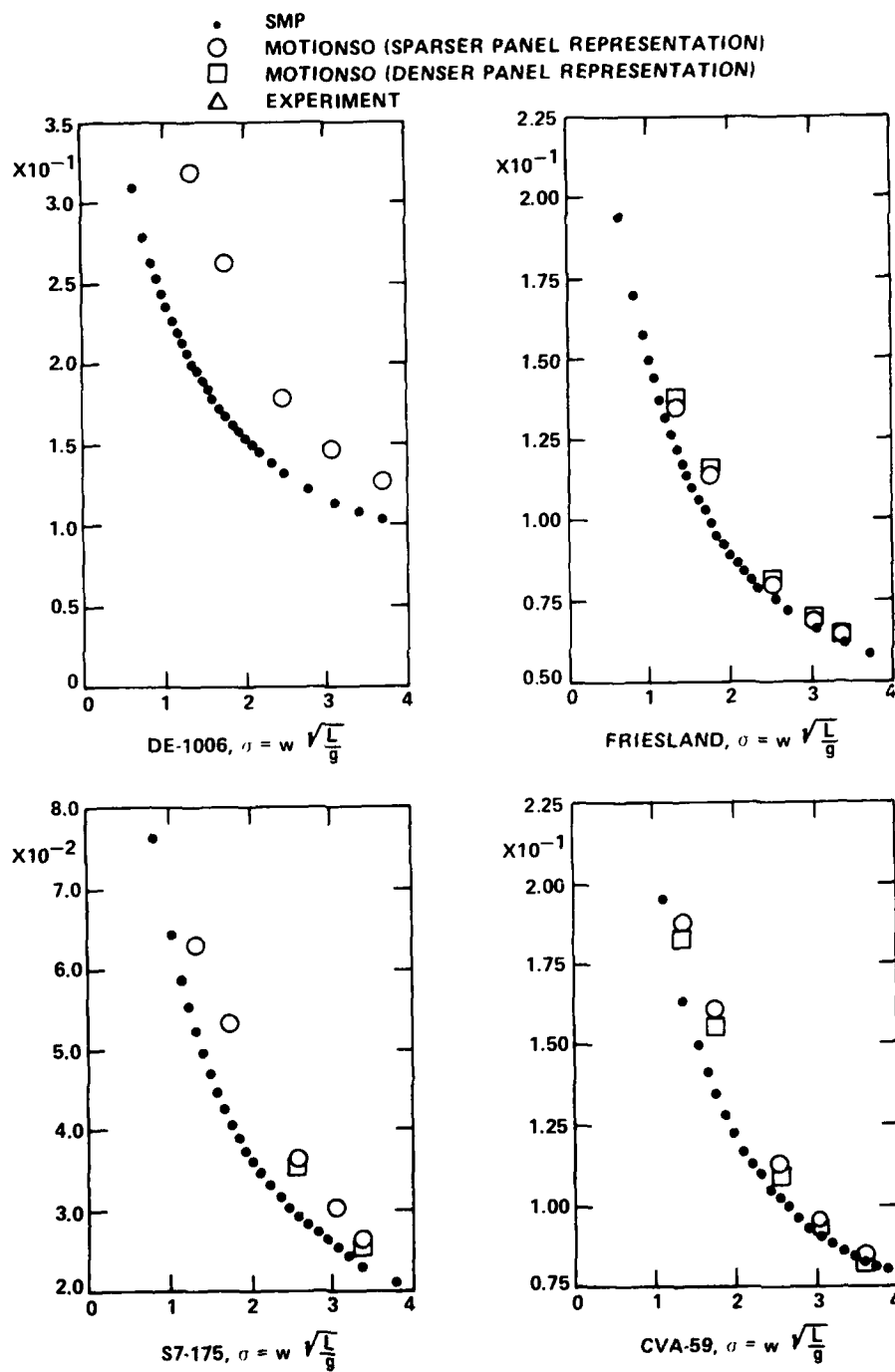
Figure 6 - (Continued)

Figure 6i - Pitch-Heave Added Mass Coefficient A_{53}

Figure 6 - (Continued)
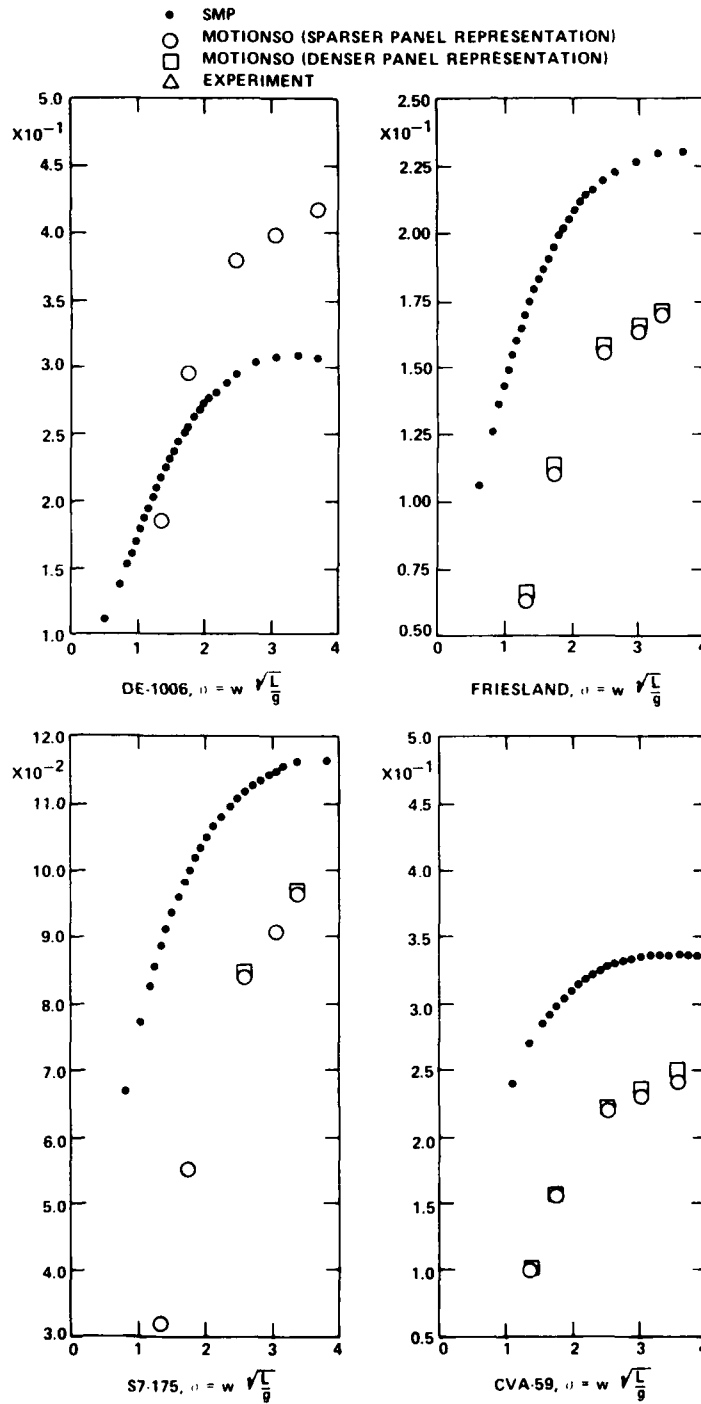
Figure 6j - Pitch-Heave Damping Coefficient B_{53}

36
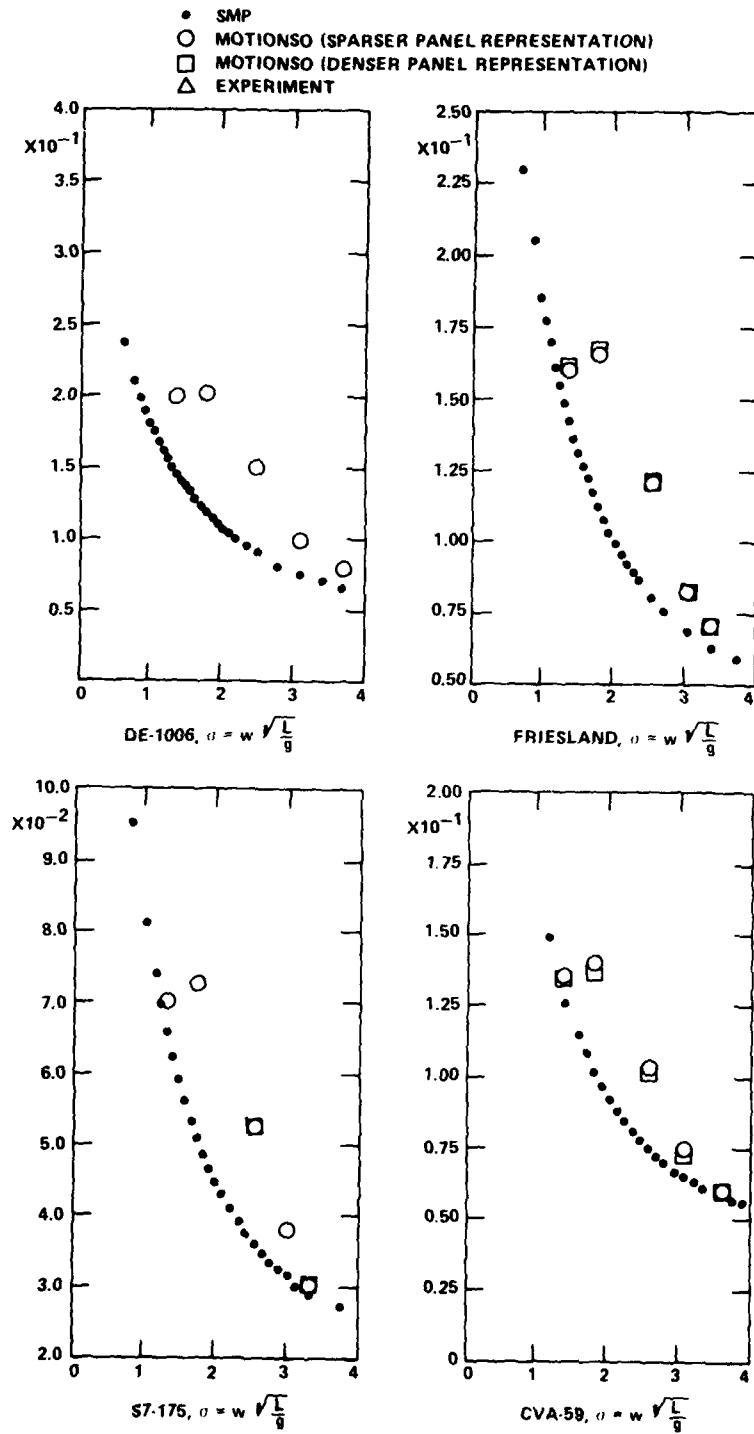
Figure 6 - (Continued)

Figure 6k - Pitch Added Mass Coefficient A_{55}

Figure 6 – (Continued)

● SMP
○ MOTIONSO (SPARSER PANEL REPRESENTATION)
☐ MOTIONSO (DENSER PANEL REPRESENTATION)
△ EXPERIMENT

DE-1006, $\sigma = w \sqrt{\frac{L}{g}}$

FRIESLAND, $\sigma = w \sqrt{\frac{L}{g}}$

S7-175, $\sigma = w \sqrt{\frac{L}{g}}$

CVA-59, $\sigma = w \sqrt{\frac{L}{g}}$
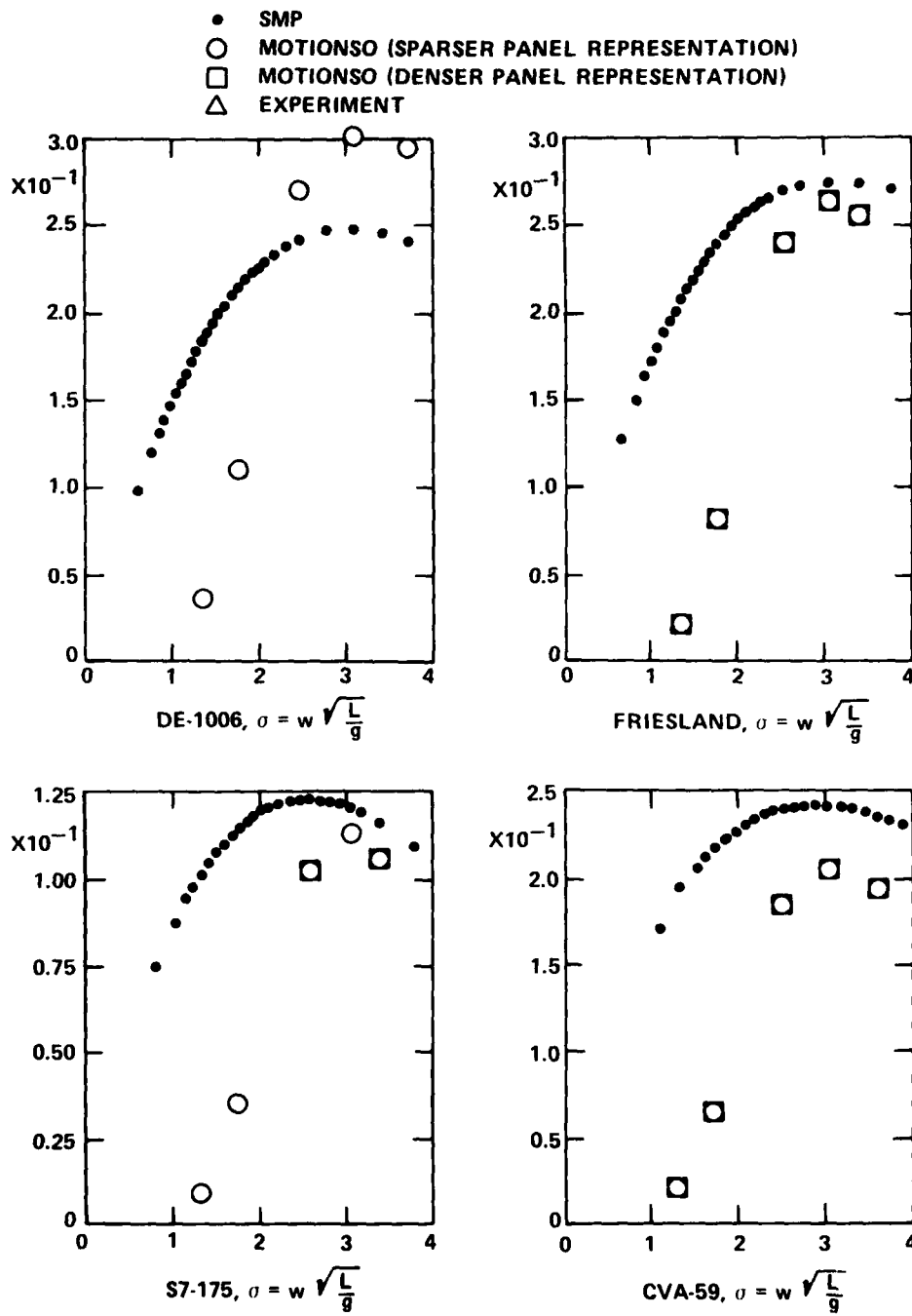
Figure 61 – Pitch Damping Coefficient B_{55}

Figure 6 - (Continued)
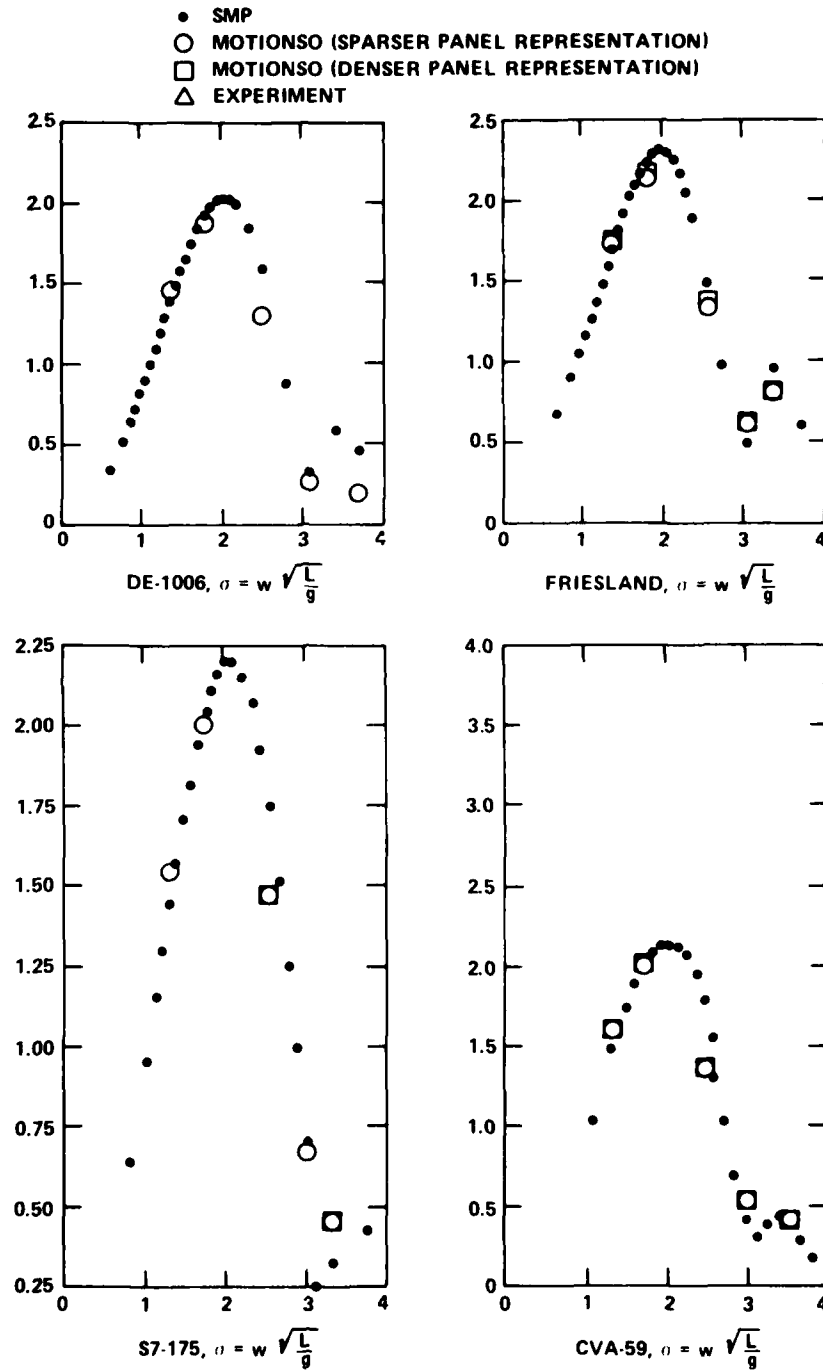
Figure 6m - Surge Exciting Force Coefficient F_1 for $\beta = 0$ Degree

39

Figure 6 - (Continued)

- ● SMP
- ○ MOTIONSO (SPARSER PANEL REPRESENTATION)
- □ MOTIONSO (DENSER PANEL REPRESENTATION)
- △ EXPERIMENT

DE-1006, $\sigma = w \sqrt{\frac{L}{g}}$

FRIESLAND, $\sigma = w \sqrt{\frac{L}{g}}$

S7-175, $\sigma = w \sqrt{\frac{L}{g}}$

CVA-59, $\sigma = w \sqrt{\frac{L}{g}}$

Figure 6n - Heave Exciting Force Coefficient F_3 for $\beta = 0$ Degree

Figure 6 - (Continued)

● SMP
○ MOTIONSO (SPARSER PANEL REPRESENTATION)
□ MOTIONSO (DENSER PANEL REPRESENTATION)
△ EXPERIMENT

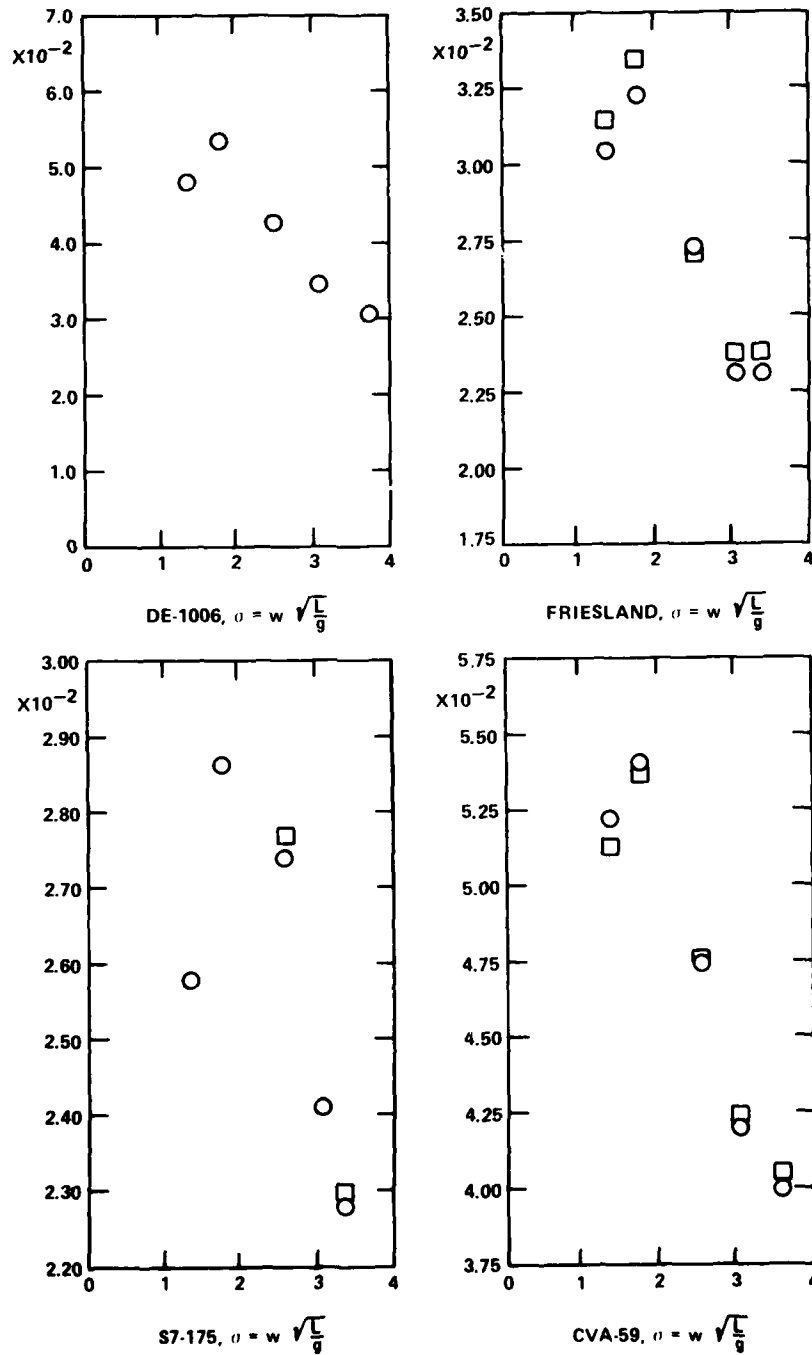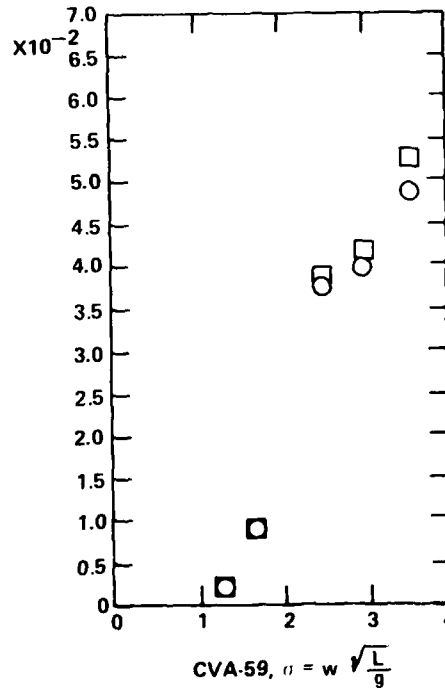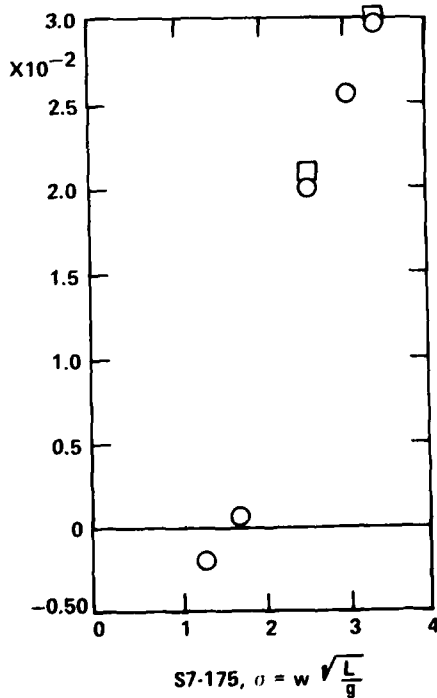DE-1006, $\sigma = w \sqrt{\frac{L}{g}}$

FRIESLAND, $\sigma = w \sqrt{\frac{L}{g}}$

S7-175, $\sigma = w \sqrt{\frac{L}{g}}$

CVA-59, $\sigma = w \sqrt{\frac{L}{g}}$

Figure 6p - Pitch Exciting Force Coefficient F_5 for $\beta = 0$ Degree

41

Figure 7 – Motion Coefficients for Vertical Plane for $\beta = 0$ Degree
(j=1,3,5)

- SMP
○ MOTIONSO (SPARSER PANEL REPRESENTATION)
☐ MOTIONSO (DENSER PANEL REPRESENTATION)
△ EXPERIMENT

DE-1006, $\sigma = w \sqrt{\frac{L}{g}}$

FRIESLAND, $\sigma = w \sqrt{\frac{L}{g}}$

S7-175, $\sigma = w \sqrt{\frac{L}{g}}$

CVA-59, $\sigma = w \sqrt{\frac{L}{g}}$
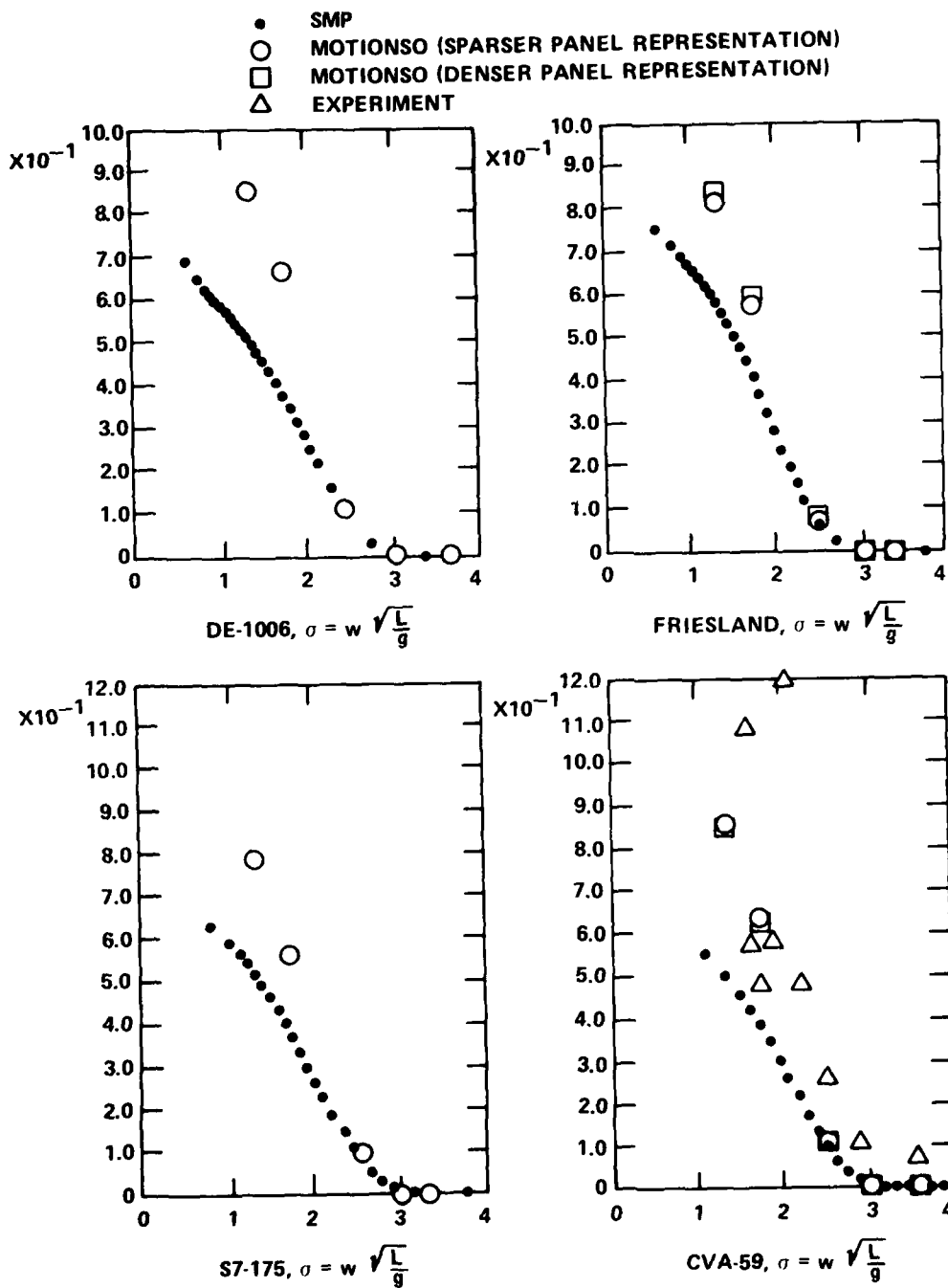
Figure 7a – Surge Response Amplitude Operator RAO_1 for $\beta = 0$ Degree

● SMP
○ MOTIONSO (SPARSER PANEL REPRESENTATION)
□ MOTIONSO (DENSER PANEL REPRESENTATION)
△ EXPERIMENT

DE-1006, $\sigma = w \sqrt{\frac{L}{g}}$

FRIESLAND, $\sigma = w \sqrt{\frac{L}{g}}$

S7-175, $\sigma = w \sqrt{\frac{L}{g}}$

CVA-59, $\sigma = w \sqrt{\frac{L}{g}}$
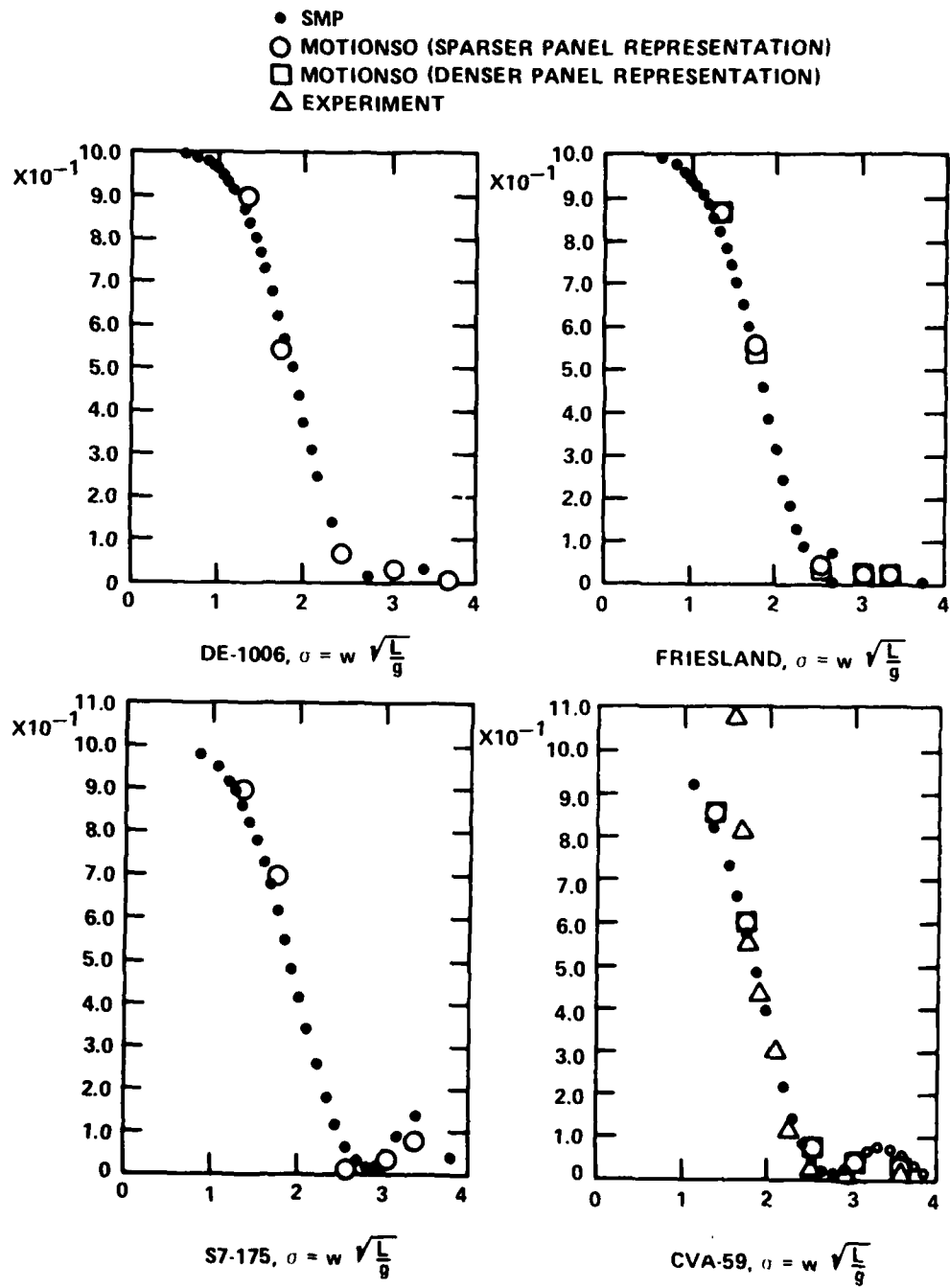
Figure 7b - Heave Response Amplitude Operator RAO_3 for β = 0 Degree

● SMP
○ MOTIONSO (SPARSER PANEL REPRESENTATION)
□ MOTIONSO (DENSER PANEL REPRESENTATION)
△ EXPERIMENT

DE-1006, $\sigma = w \sqrt{\frac{L}{g}}$
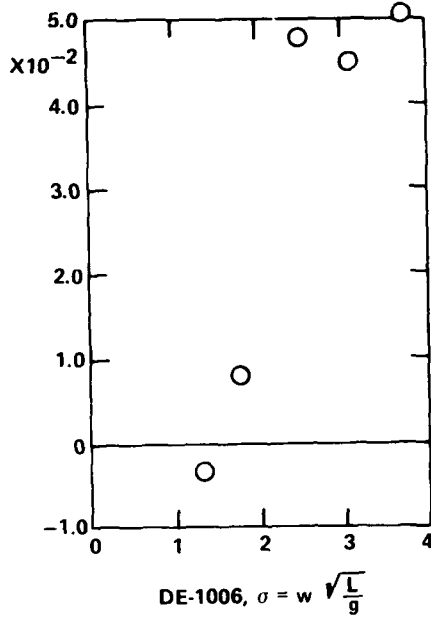
FRIESLAND, $\sigma = w \sqrt{\frac{L}{g}}$

S7-175, $\sigma = w \sqrt{\frac{L}{g}}$

CVA-59, $\sigma = w \sqrt{\frac{L}{g}}$
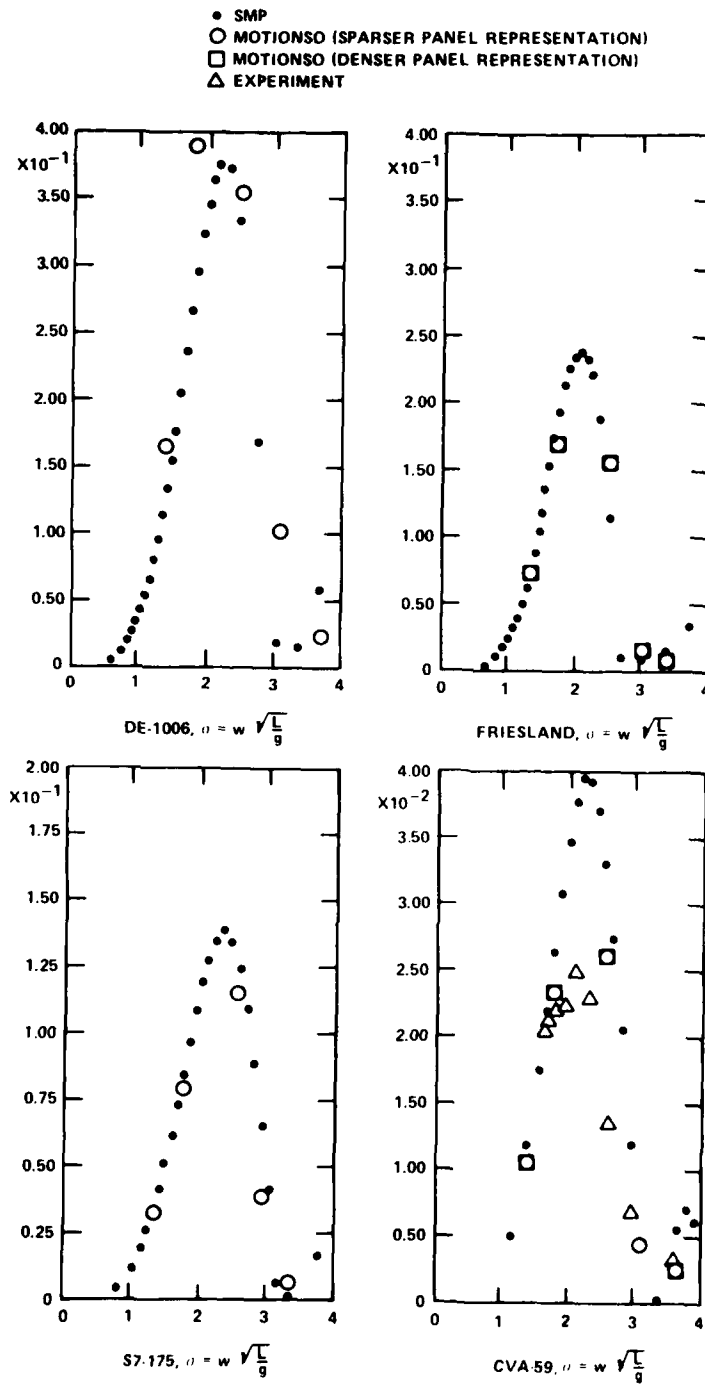
Figure 7c - Pitch Response Amplitude Operator RAO_5 for $\mu = 0$ Degree

44

Figure 8 - Potential Force Coefficients for Lateral Plane (j=2,4,6)

- ● SMP
- ○ MOTIONSO (SPARSER PANEL REPRESENTATION)
- □ MOTIONSO (DENSER PANEL REPRESENTATION)
- △ EXPERIMENT

DE-1006, $\sigma = w \sqrt{\frac{L}{g}}$

FRIESLAND, $\sigma = w \sqrt{\frac{L}{g}}$

S7-175, $\sigma = w \sqrt{\frac{L}{g}}$

CVA-59, $\sigma = w \sqrt{\frac{L}{g}}$
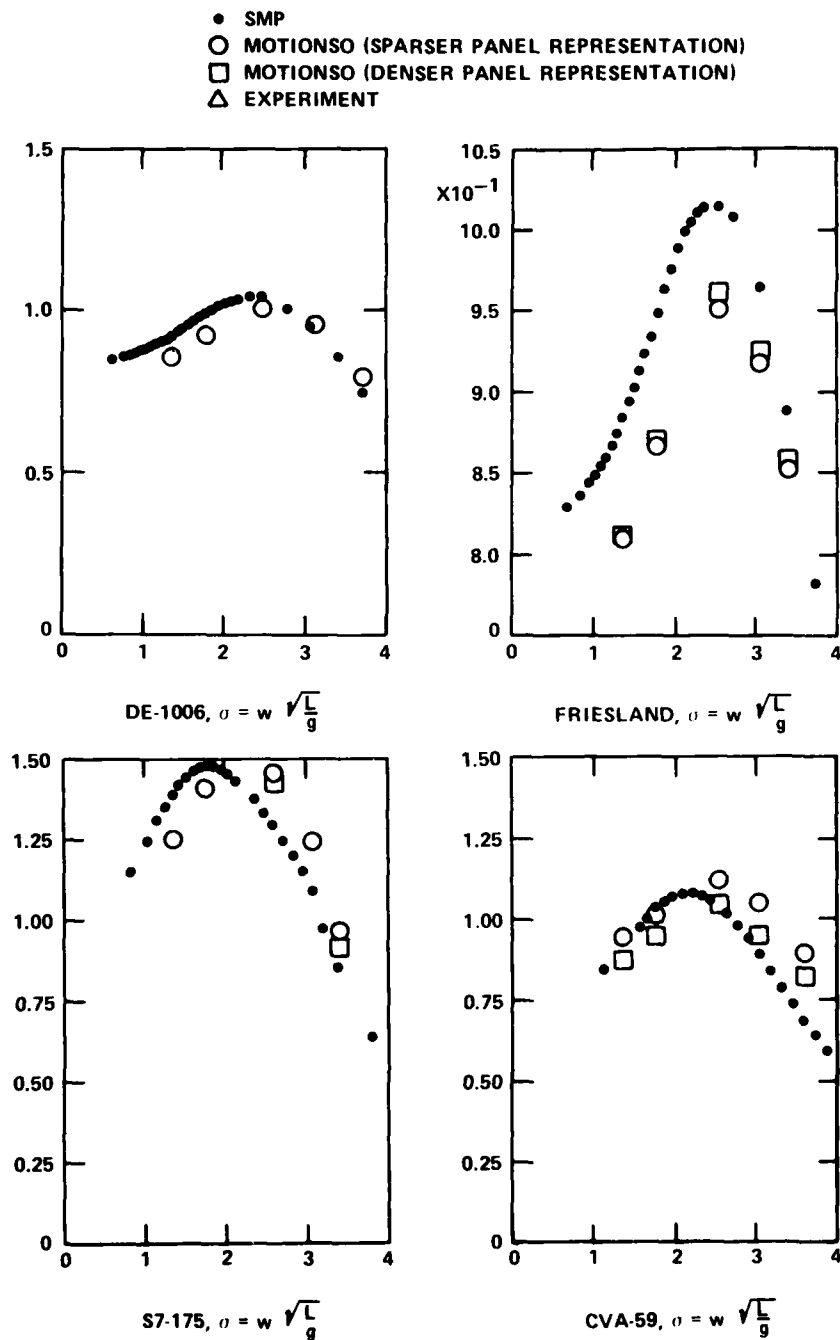
Figure 8a - Sway Added Mass Coefficient A_{22}

45

Figure 8 – (Continued)

● SMP
○ MOTIONSO (SPARSER PANEL REPRESENTATION)
□ MOTIONSO (DENSER PANEL REPRESENTATION)
△ EXPERIMENT

DE-1006, $\sigma = w \sqrt{\dfrac{L}{g}}$

FRIESLAND, $\sigma = w \sqrt{\dfrac{L}{g}}$

S7-175, $\sigma = w \sqrt{\dfrac{L}{g}}$

CVA-59, $\sigma = w \sqrt{\dfrac{L}{g}}$
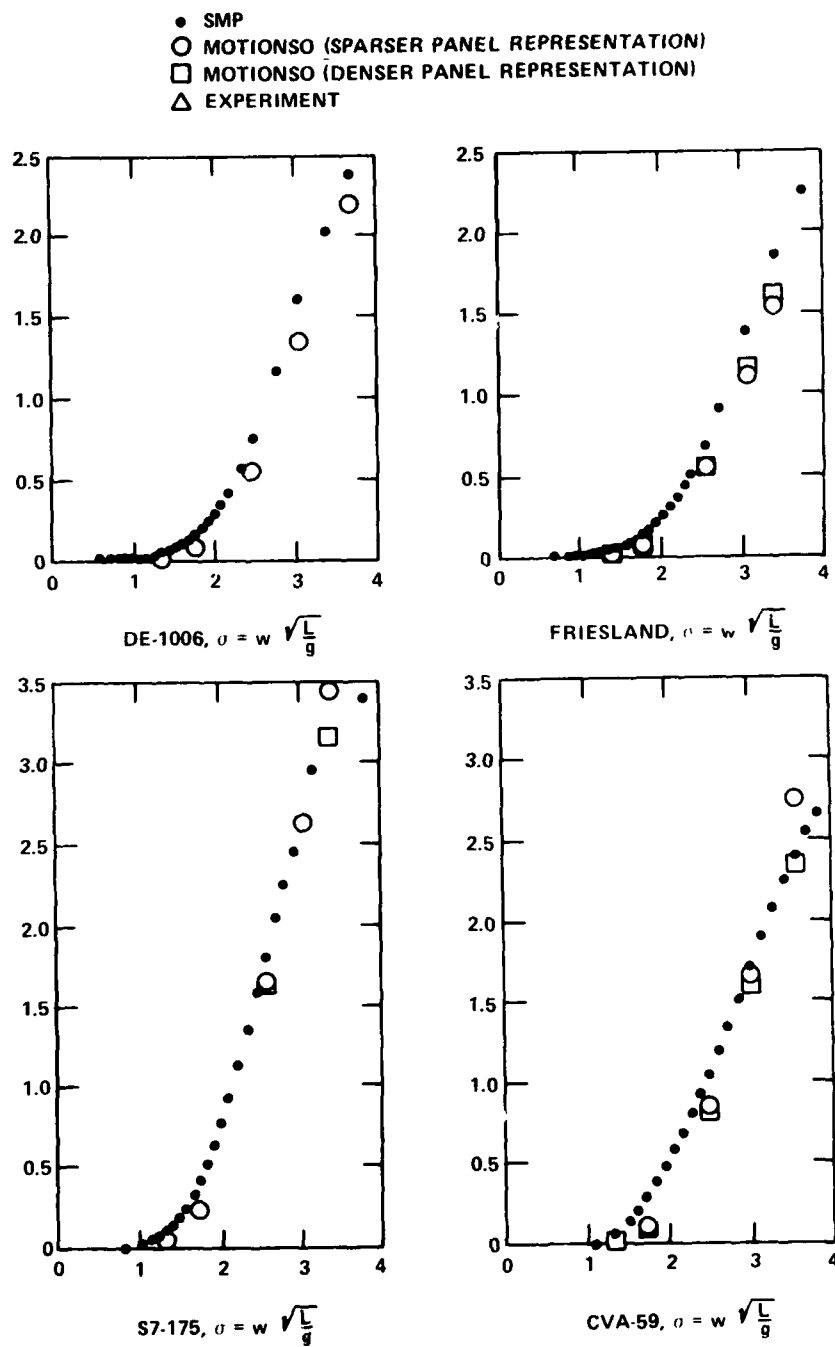
Figure 8b – Sway Damping Coefficient B_{22}

Figure 8 - (Continued)

- ● SMP
- ○ MOTIONSO (SPARSER PANEL REPRESENTATION)
- □ MOTIONSO (DENSER PANEL REPRESENTATION)
- △ EXPERIMENT

DE-1006, $\sigma = w \sqrt{\frac{L}{g}}$

FRIESLAND, $\sigma = w \sqrt{\frac{L}{g}}$

S7-175, $\sigma = w \sqrt{\frac{L}{g}}$

CVA-59, $\sigma = w \sqrt{\frac{L}{g}}$

Figure 8c - Roll-Sway Added Mass Coefficient A_{42}

Figure 8 - (Continued)

● SMP
○ MOTIONSO (SPARSER PANEL REPRESENTATION)
□ MOTIONSO (DENSER PANEL REPRESENTATION)
△ EXPERIMENT

DE-1006, $\sigma = w \sqrt{\frac{L}{g}}$

FRIESLAND, $\sigma = w \sqrt{\frac{L}{g}}$

S7-175, $\sigma = w \sqrt{\frac{L}{g}}$

CVA-59, $\sigma = w \sqrt{\frac{L}{g}}$
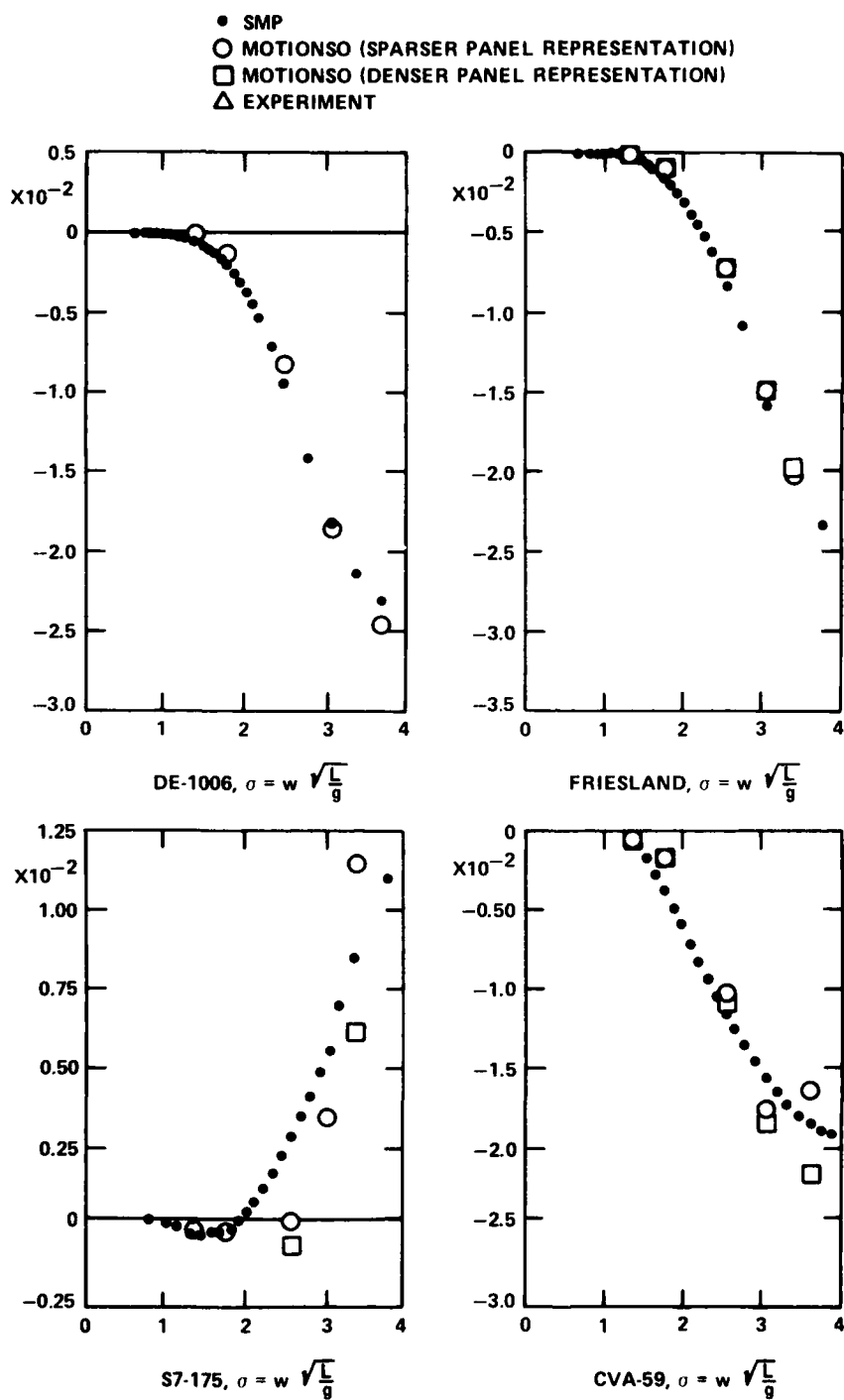
Figure 8d - Roll-Sway Damping Coefficient B_{42}

48

Figure 8 - (Continued)

● SMP
○ MOTIONSO (SPARSER PANEL REPRESENTATION)
□ MOTIONSO (DENSER PANEL REPRESENTATION)
△ EXPERIMENT

DE-1006, $\sigma = w \sqrt{\frac{L}{g}}$

FRIESLAND, $\sigma = w \sqrt{\frac{L}{g}}$

S7-175, $\sigma = w \sqrt{\frac{L}{g}}$

CVA-59, $\sigma = w \sqrt{\frac{L}{g}}$
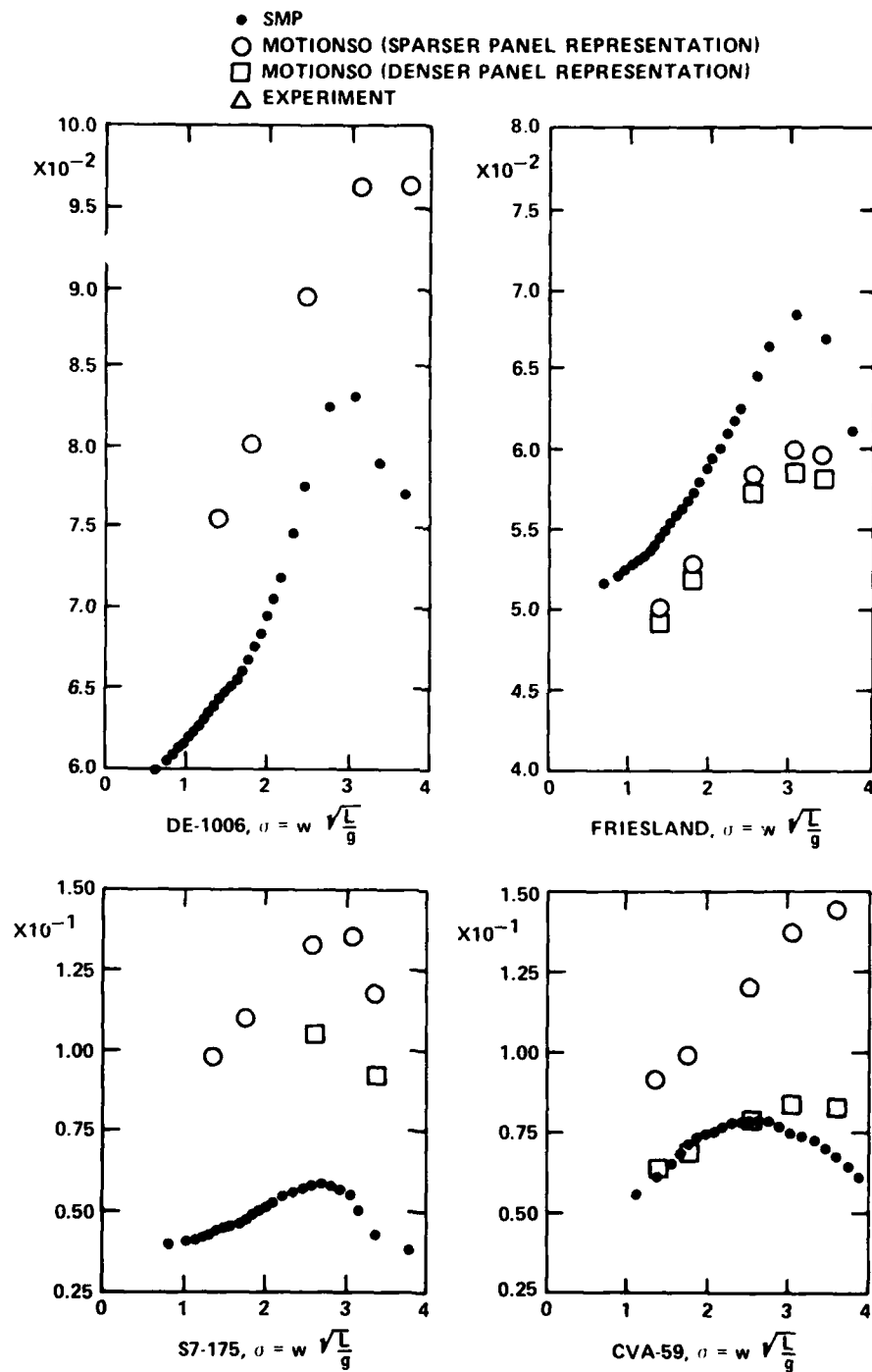
Figure 8e - Yaw-Sway Added Mass Coefficient A_{62}

Figure 8 - (Continued)

●   SMP
○   MOTIONSO (SPARSER PANEL REPRESENTATION)
□   MOTIONSO (DENSER PANEL REPRESENTATION)
△   EXPERIMENT
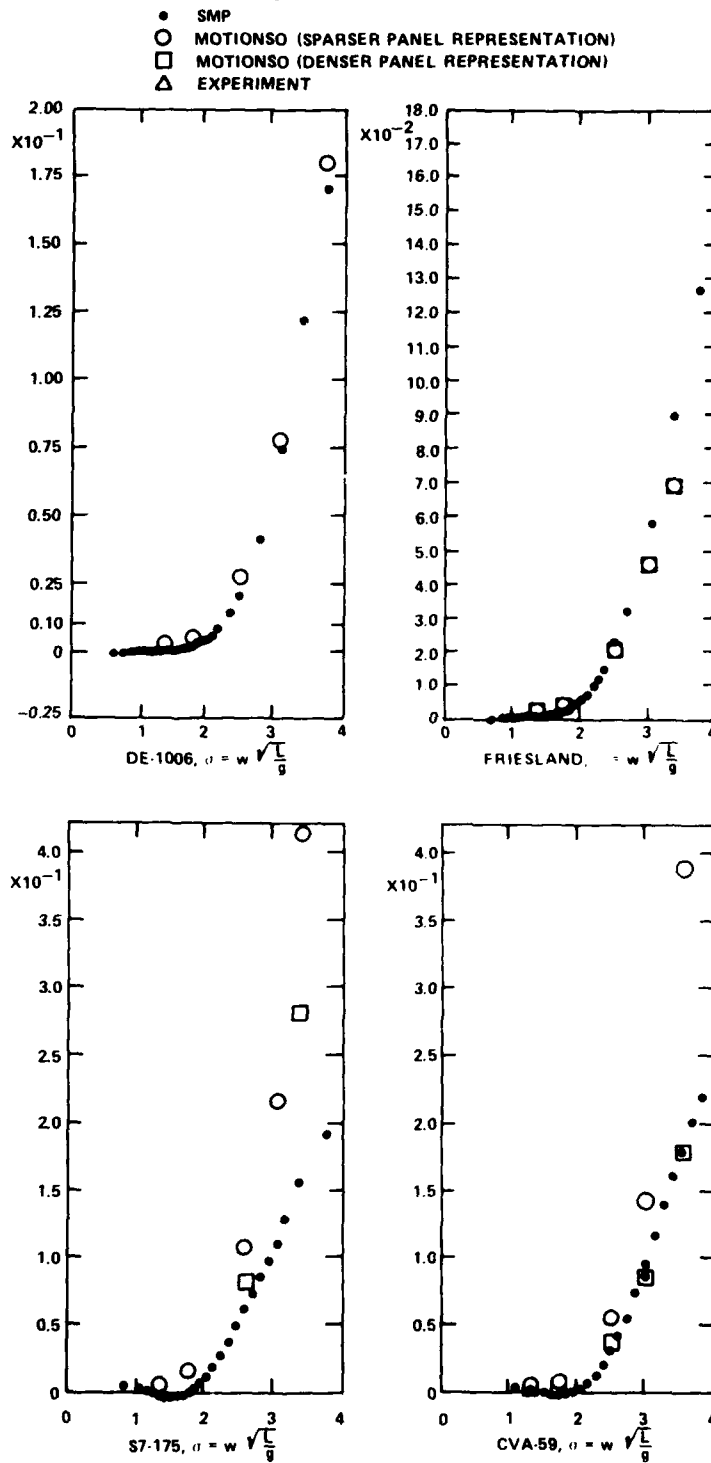
Figure 8f - Yaw-Sway Damping Coefficient B_{62}

50

Figure 8 - (Continued)

- SMP
○ MOTIONSO (SPARSER PANEL REPRESENTATION)
□ MOTIONSO (DENSER PANEL REPRESENTATION)
△ EXPERIMENT
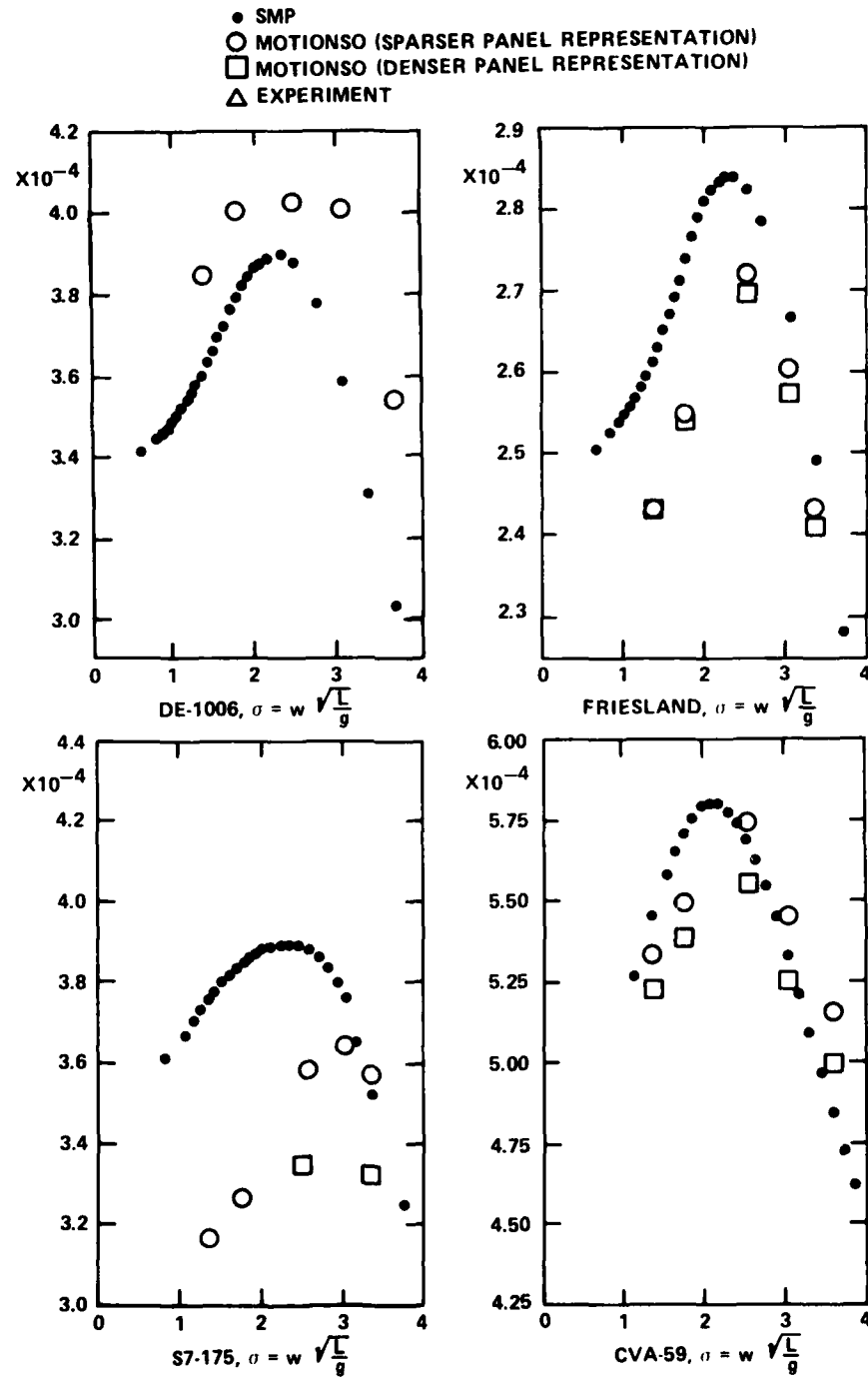
Figure 8g - Roll Added Mass Coefficient A_{44}

Figure 8 - (Continued)

● SMP
○ MOTIONSO (SPARSER PANEL REPRESENTATION)
□ MOTIONSO (DENSER PANEL REPRESENTATION)
△ EXPERIMENT

DE-1006, $\sigma = w \sqrt{\frac{L}{g}}$

FRIESLAND, $\sigma = w \sqrt{\frac{L}{g}}$

S7-175, $\sigma = w \sqrt{\frac{L}{g}}$

CVA-59, $\sigma = w \sqrt{\frac{L}{g}}$
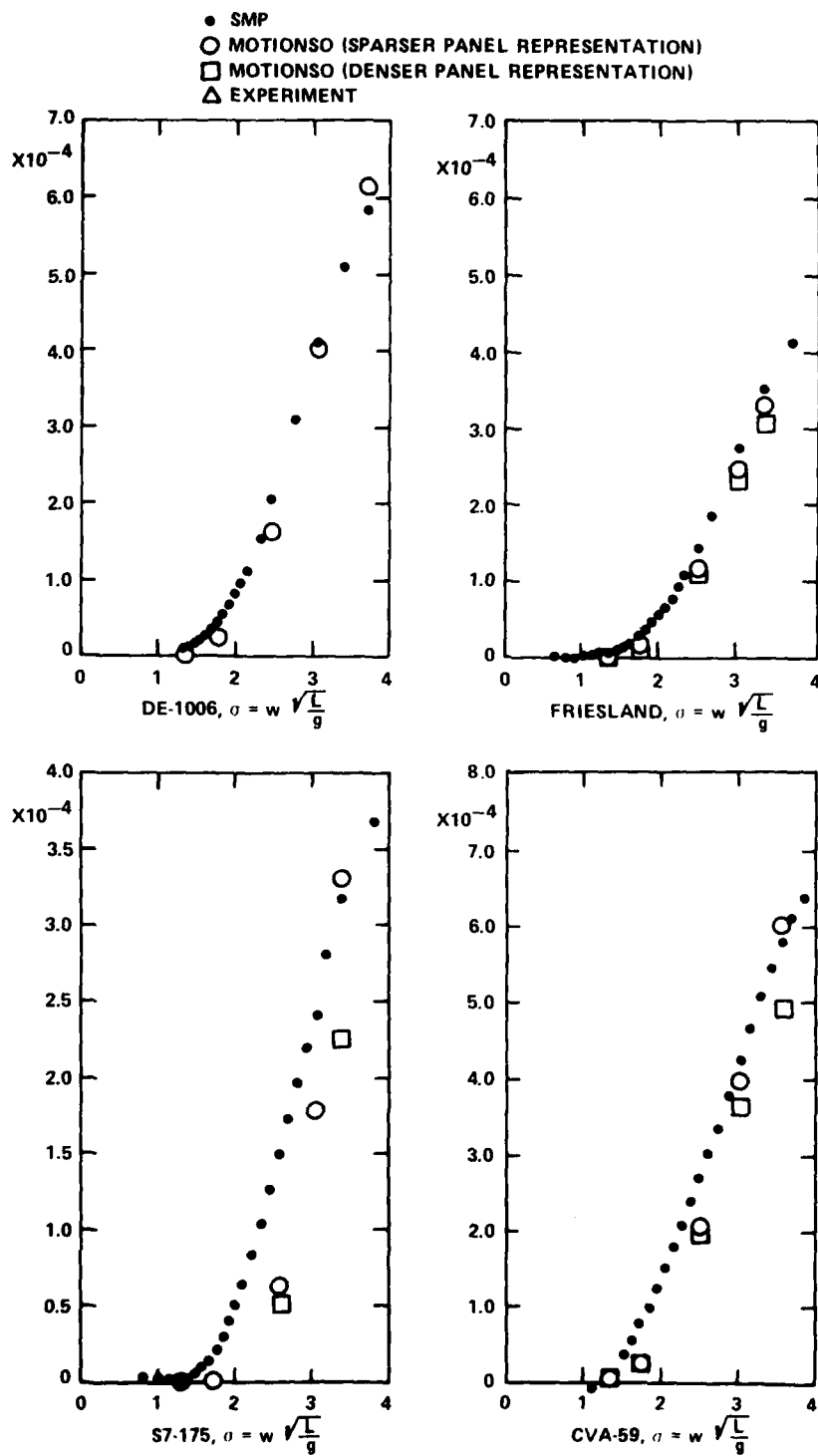
Figure 8h - Roll Damping Coefficient B_{44}

Figure 8 - (Continued)

- ● SMP
- ○ MOTIONSO (SPARSER PANEL REPRESENTATION)
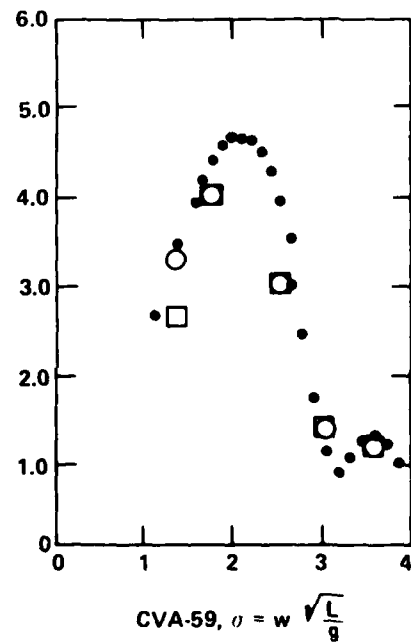- □ MOTIONSO (DENSER PANEL REPRESENTATION)
- △ EXPERIMENT

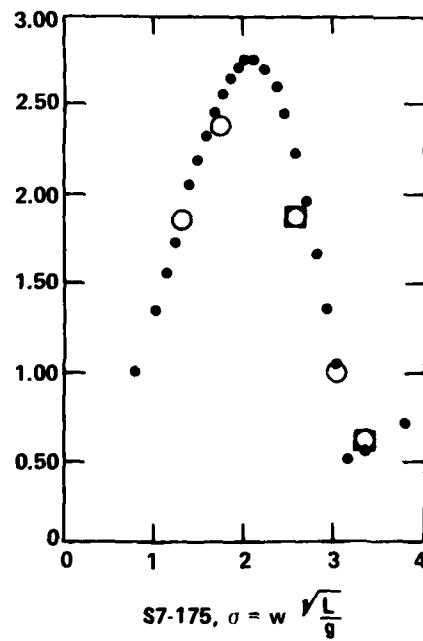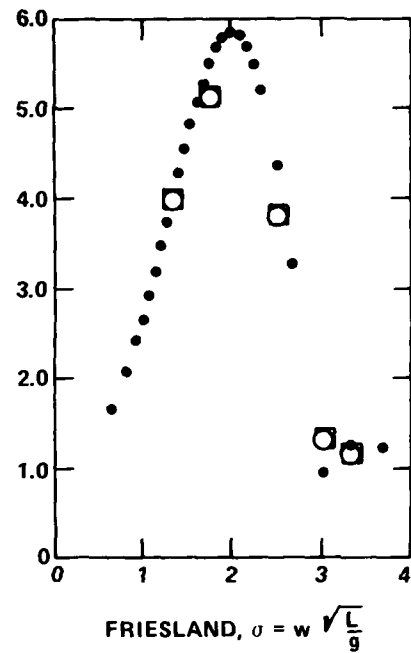DE-1006, $\sigma = w \sqrt{\frac{L}{g}}$

FRIESLAND, $\sigma = w \sqrt{\frac{L}{g}}$

S7-175, $\sigma = w \sqrt{\frac{L}{g}}$

CVA-59, $\sigma = w \sqrt{\frac{L}{g}}$
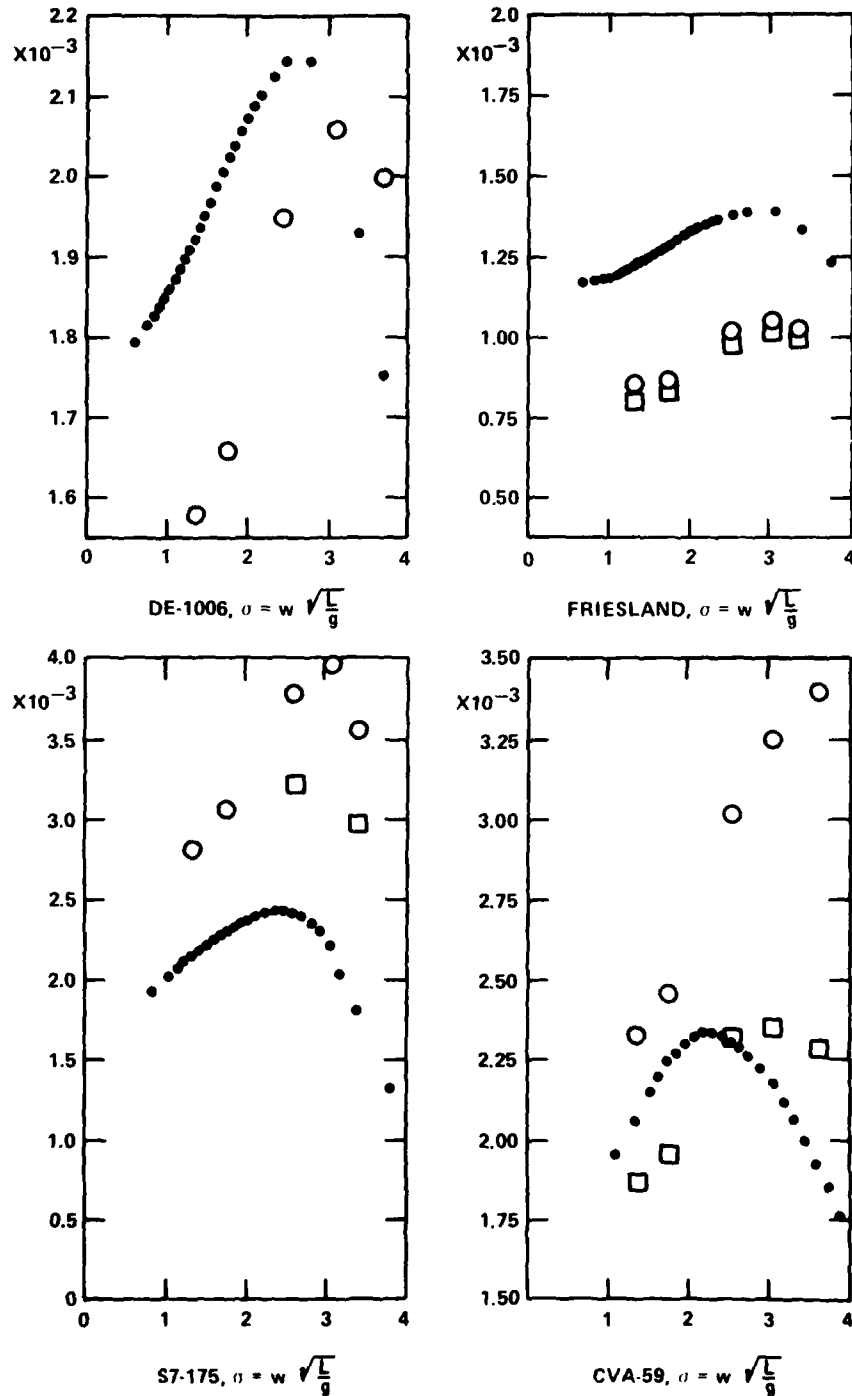
Figure 8i - Yaw-Roll Added Mass Coefficient A_{64}

53
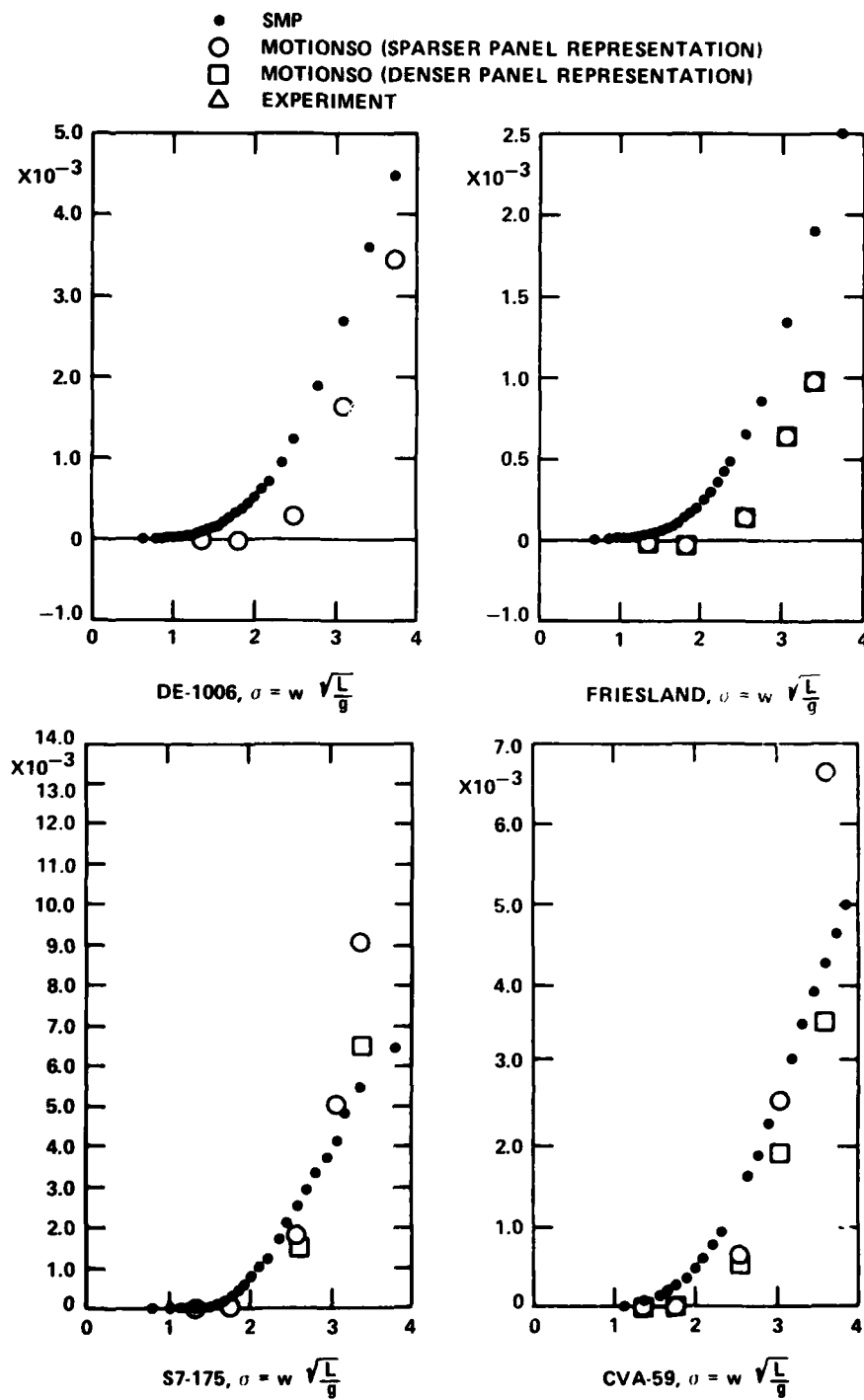
Figure 8 - (Continued)

Figure 8j - Yaw-Roll Damping Coefficient B_{64}

Figure 8 – (Continued)

- ● SMP
- ○ MOTIONSO (SPARSER PANEL REPRESENTATION)
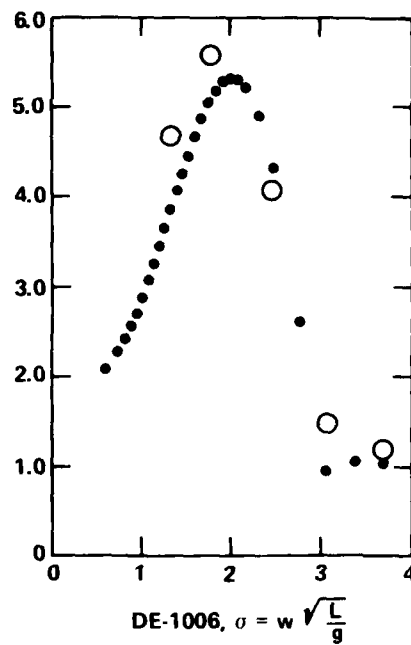- □ MOTIONSO (DENSER PANEL REPRESENTATION)
- △ EXPERIMENT

DE-1006, $\sigma = w \sqrt{\frac{L}{g}}$

FRIESLAND, $\sigma = w \sqrt{\frac{L}{g}}$

S7-175, $\sigma = w \sqrt{\frac{L}{g}}$

CVA-59, $\sigma = w \sqrt{\frac{L}{g}}$
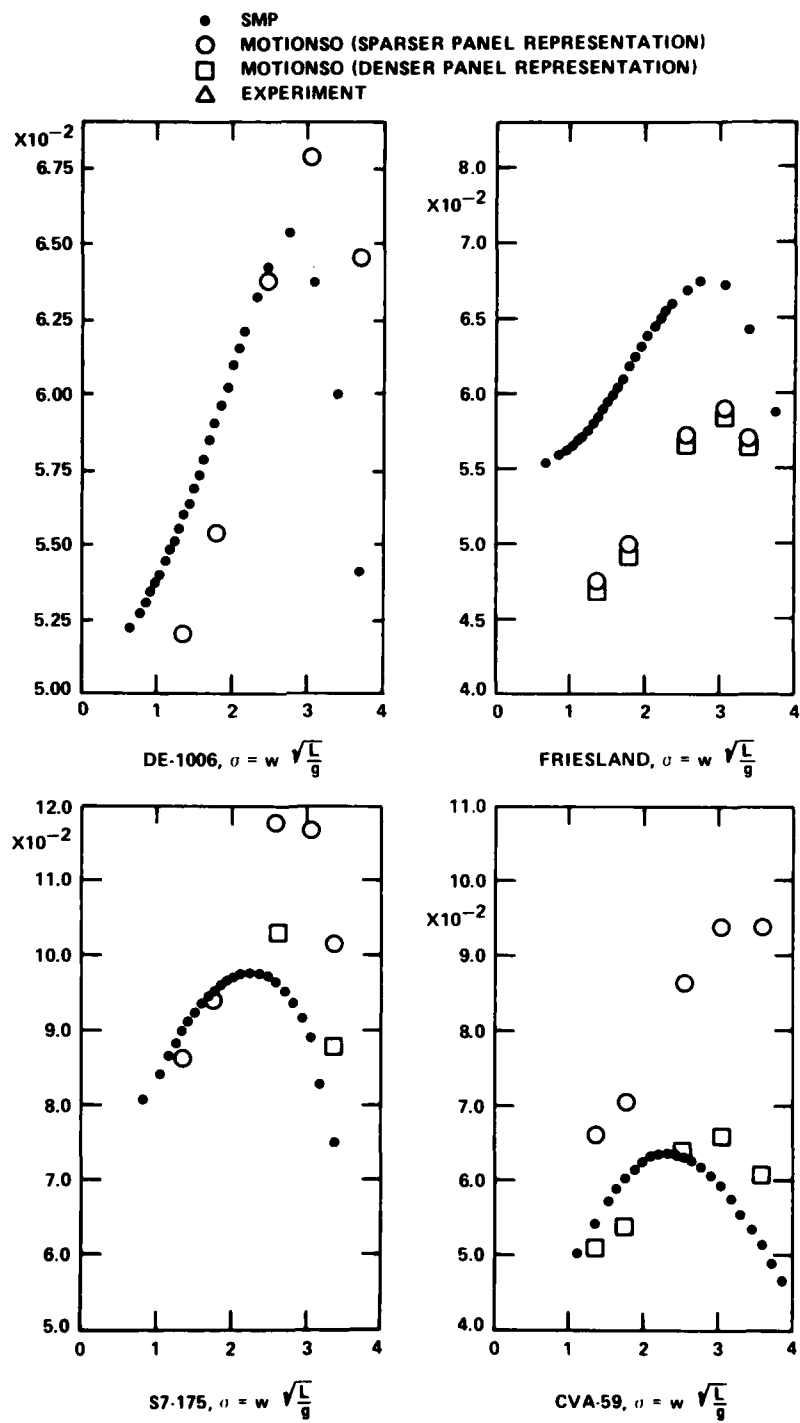
Figure 8k – Yaw Added Mass Coefficient A_{66}

Figure 8 - (Continued)

- ● SMP
- ○ MOTIONSO (SPARSER PANEL REPRESENTATION)
- □ MOTIONSO (DENSER PANEL REPRESENTATION)
- △ EXPERIMENT

DE-1006, $\sigma = w \sqrt{\frac{L}{g}}$

FRIESLAND, $\sigma = w \sqrt{\frac{L}{g}}$

S7-175, $\sigma = w \sqrt{\frac{L}{g}}$

CVA-59, $\sigma = w \sqrt{\frac{L}{g}}$
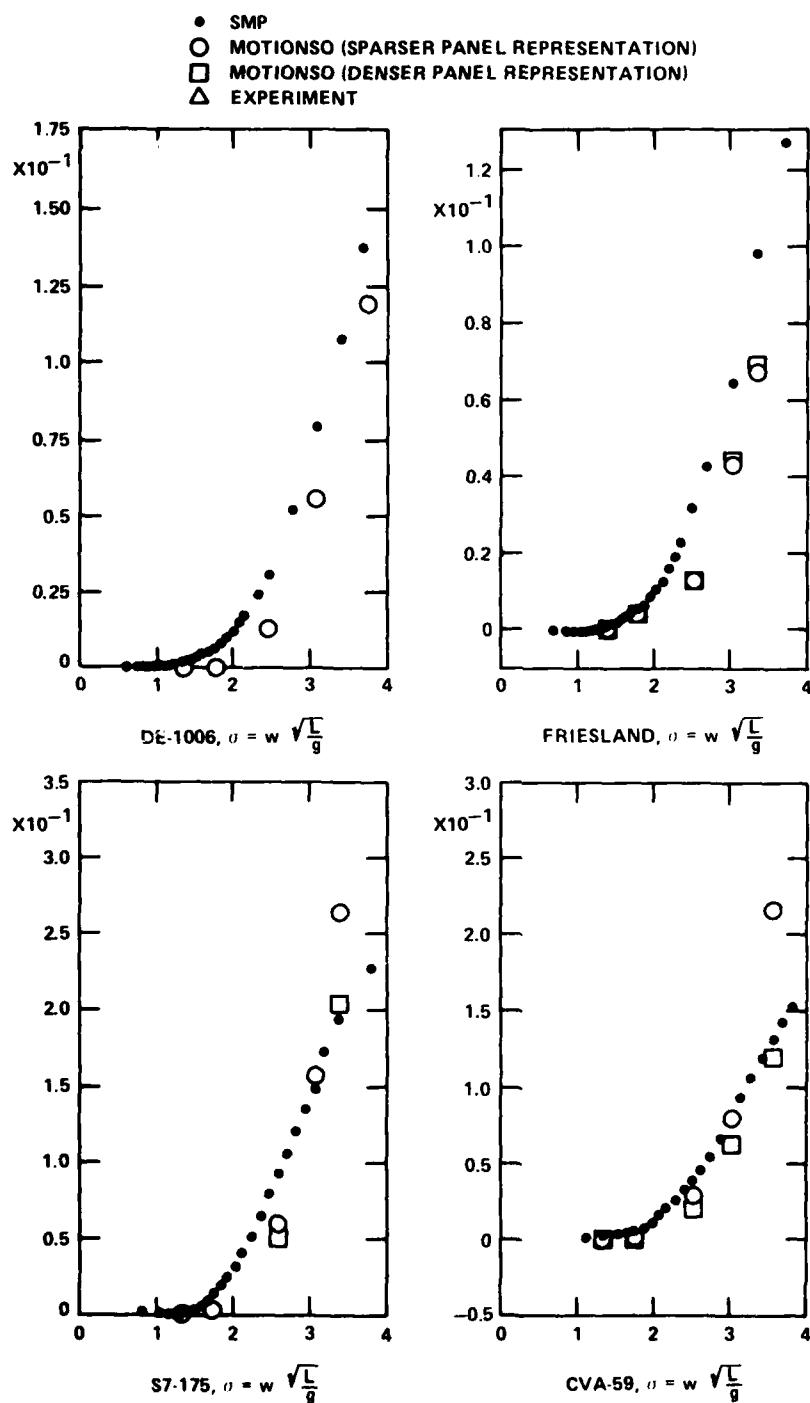
Figure 81 - Yaw Damping Coefficient B_{66}

56
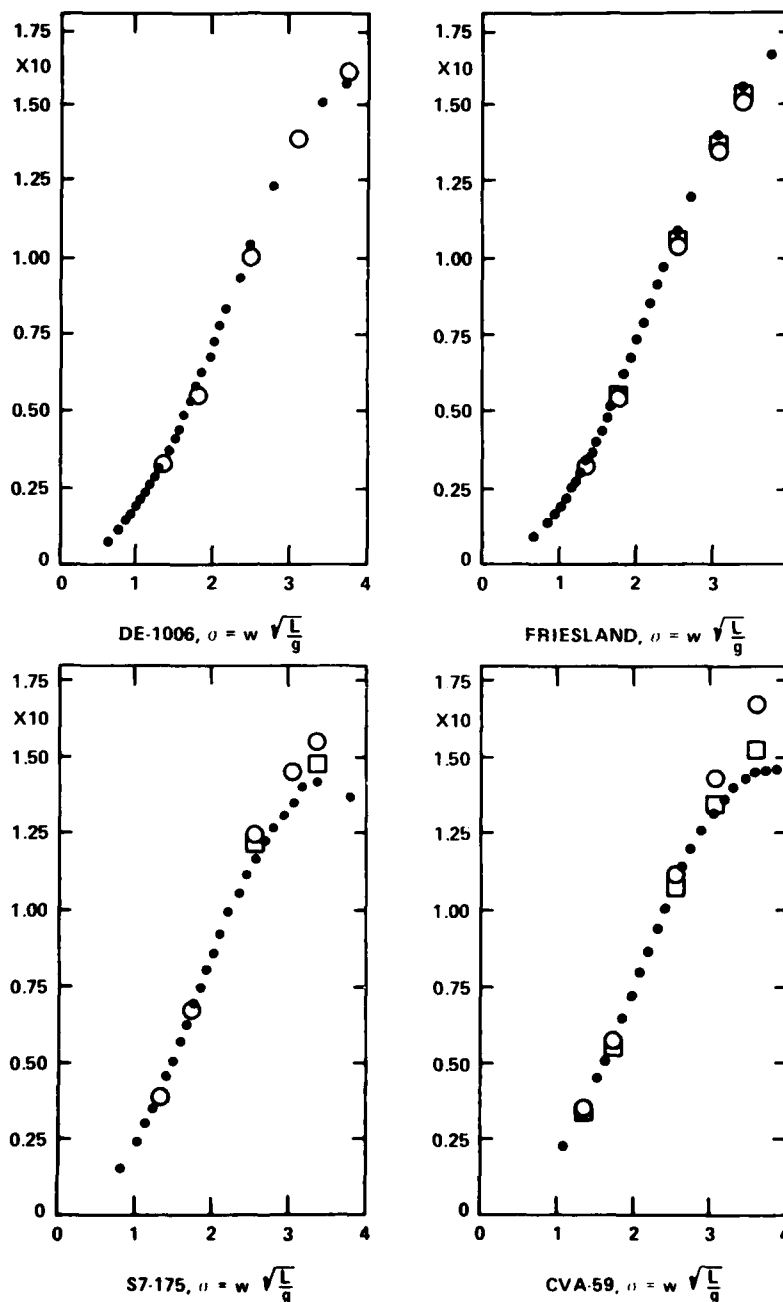
Figure 8 – (Continued)

Figure 8m – Sway Exciting Force Coefficient F_2 for β = 90 Degrees

57

Figure 8 - (Continued)

● SMP
○ MOTIONSO (SPARSER PANEL REPRESENTATION)
□ MOTIONSO (DENSER PANEL REPRESENTATION)
△ EXPERIMENT

DE-1006, $\sigma = w \sqrt{\frac{L}{g}}$

FRIESLAND, $\sigma = w \sqrt{\frac{L}{g}}$

S7-175, $\sigma = w \sqrt{\frac{L}{g}}$

CVA-59, $\sigma = w \sqrt{\frac{L}{g}}$
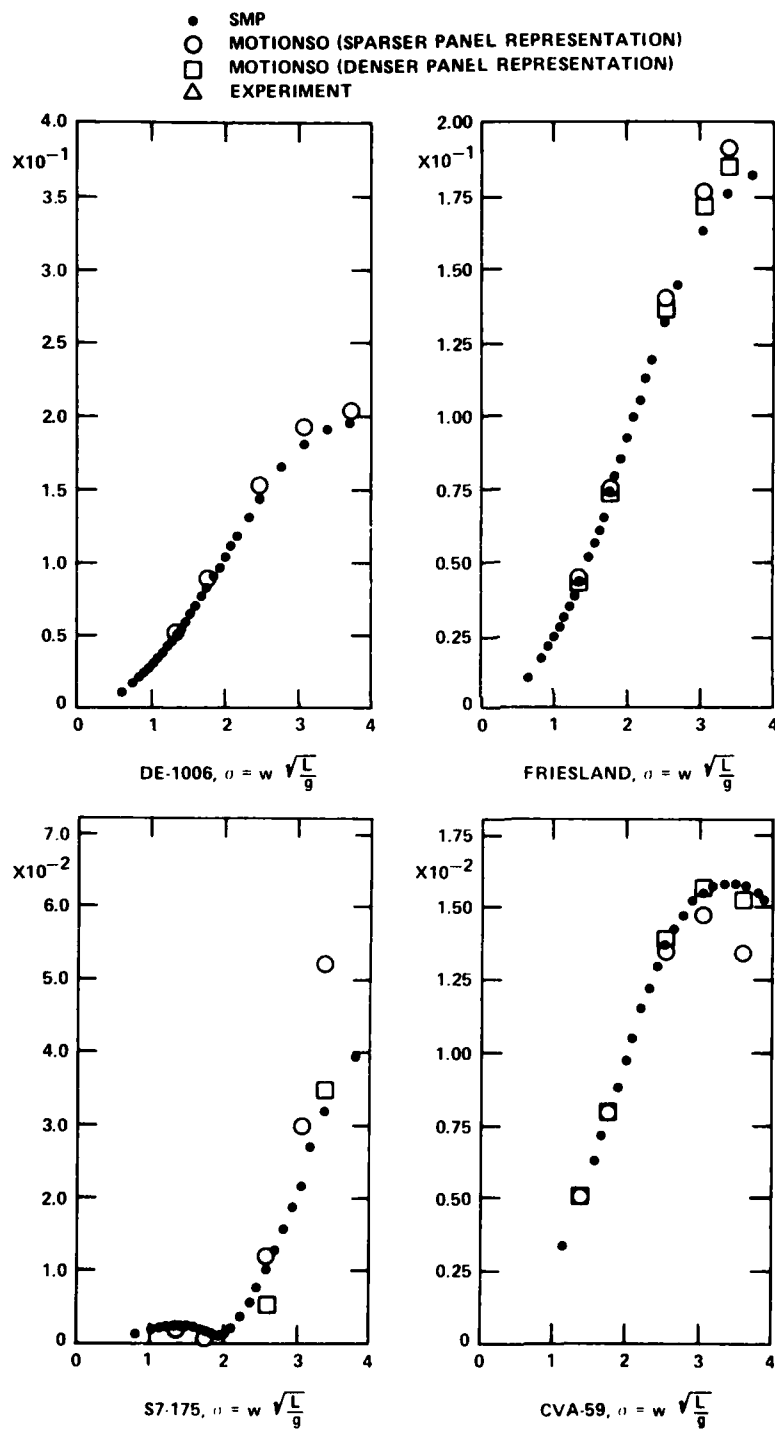
Figure 8n - Roll Exciting Force Coefficient F_4 for β = 90 Degrees

58
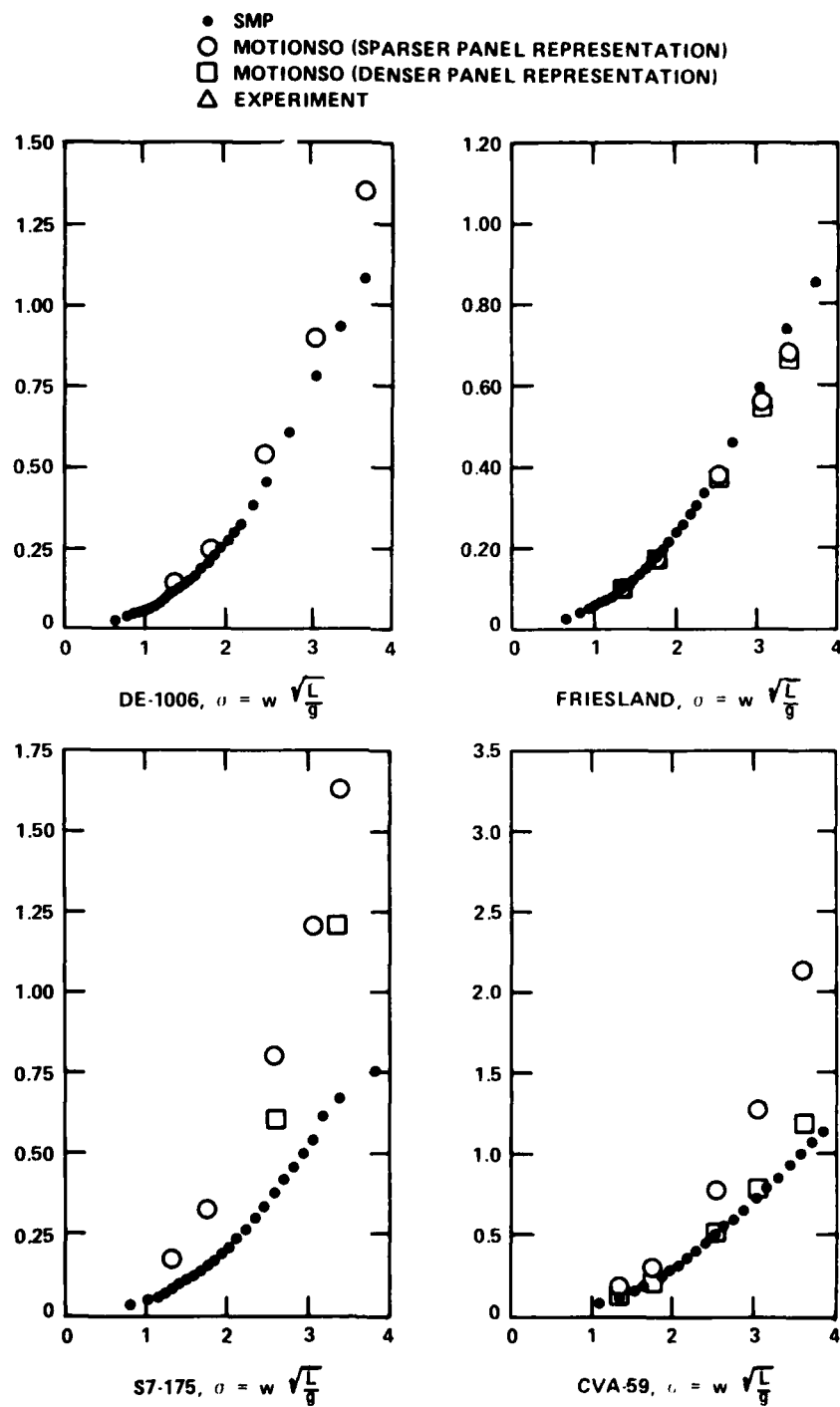
Figure 8 – (Continued)

Figure 8p – Yaw Exciting Force Coefficient F_6 for β = 90 Degrees

59

Figure 9 – Motion Coefficients for Lateral Plane for β = 90 Degrees (j=2,4,6)
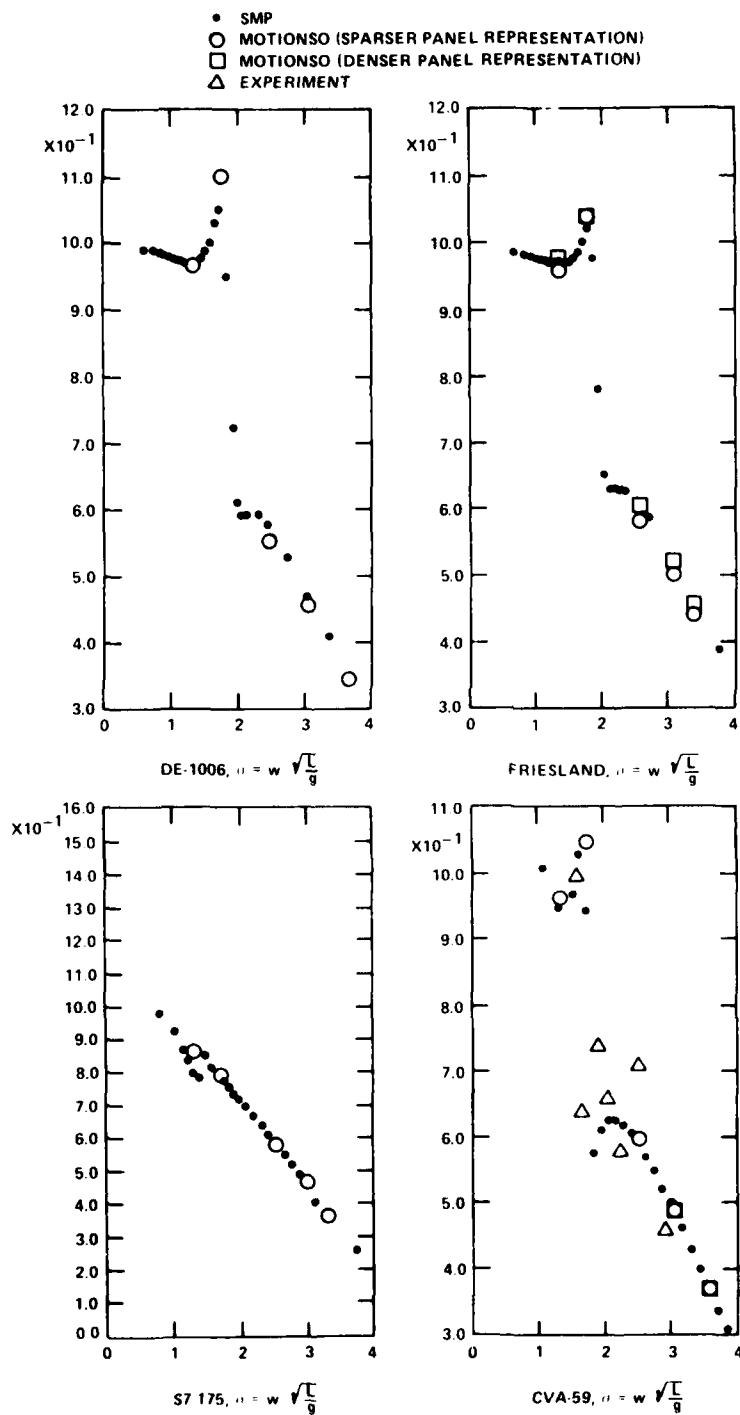
Figure 9a – Sway Response Amplitude Operator RAO_2 for β = 90 Degrees

60

Figure 9 – (Continued)

- • SMP
- O MOTIONSO (SPARSER PANEL REPRESENTATION)
- □ MOTIONSO (DENSER PANEL REPRESENTATION)
- △ EXPERIMENT

DE-1006, $\sigma = w \sqrt{\frac{L}{g}}$

FRIESLAND, $\sigma = w \sqrt{\frac{L}{g}}$

S7-175, $\sigma = w \sqrt{\frac{L}{g}}$

CVA-59, $\sigma = w \sqrt{\frac{L}{g}}$
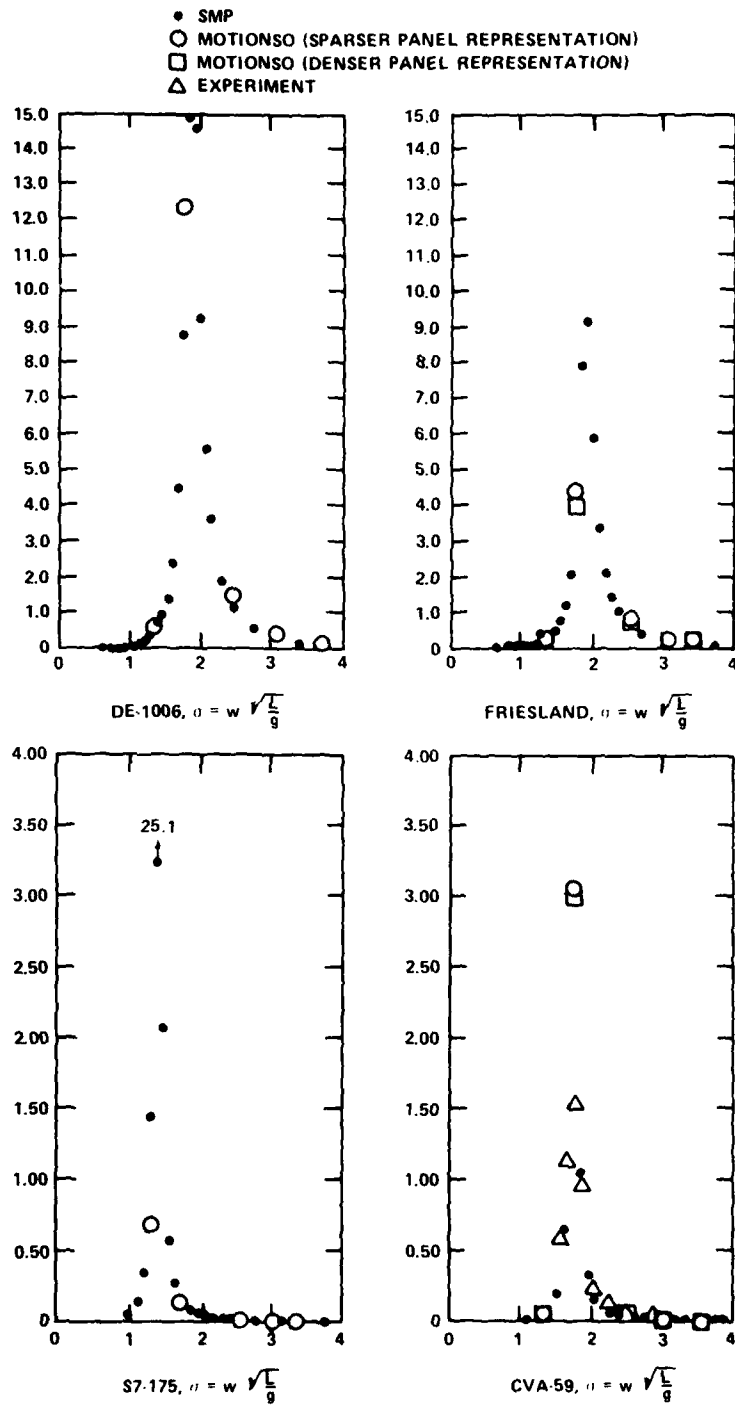
Figure 9b – Roll Response Amplitude Operator RAO_4 for $\beta = 90$ Degrees

61

Figure 9 - (Continued)

- • SMP
- O MOTIONSO (SPARSER PANEL REPRESENTATION)
- □ MOTIONSO (DENSER PANEL REPRESENTATION)
- △ EXPERIMENT

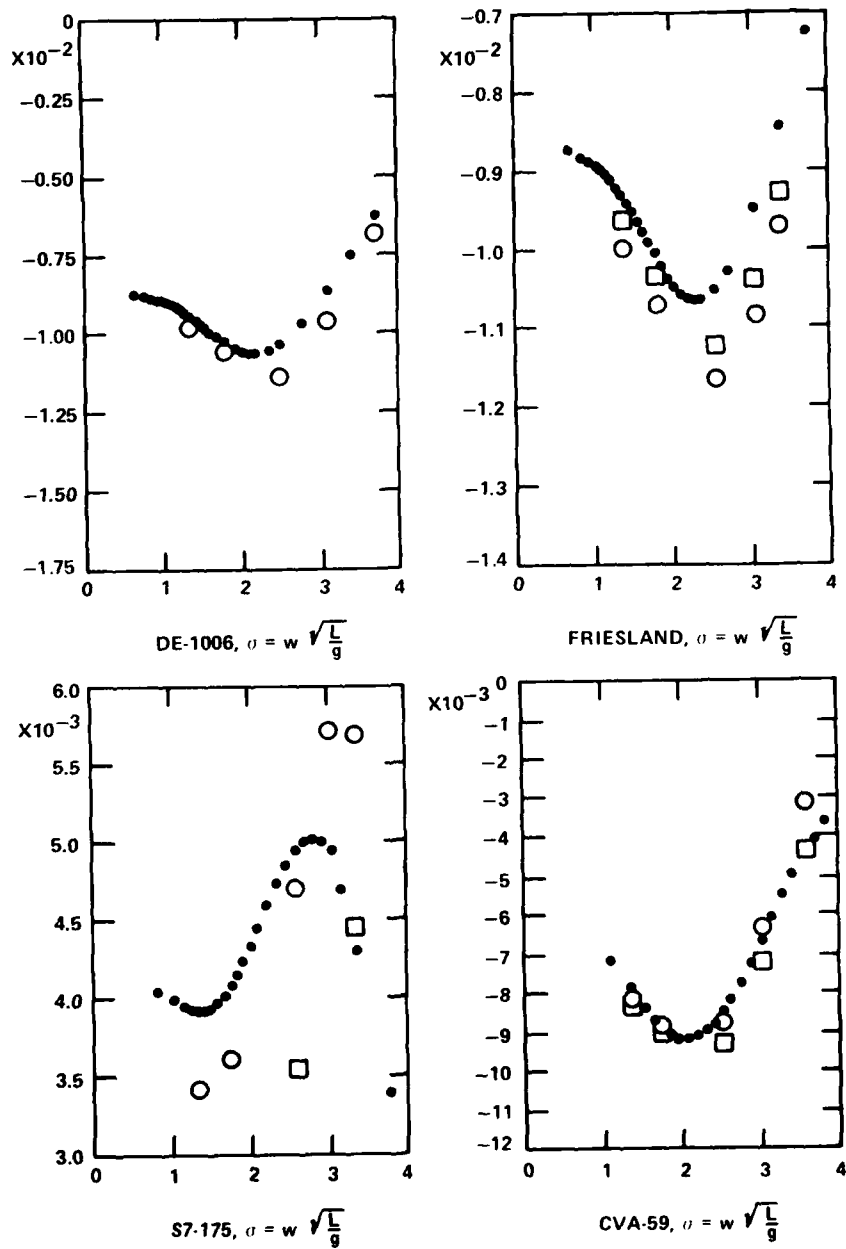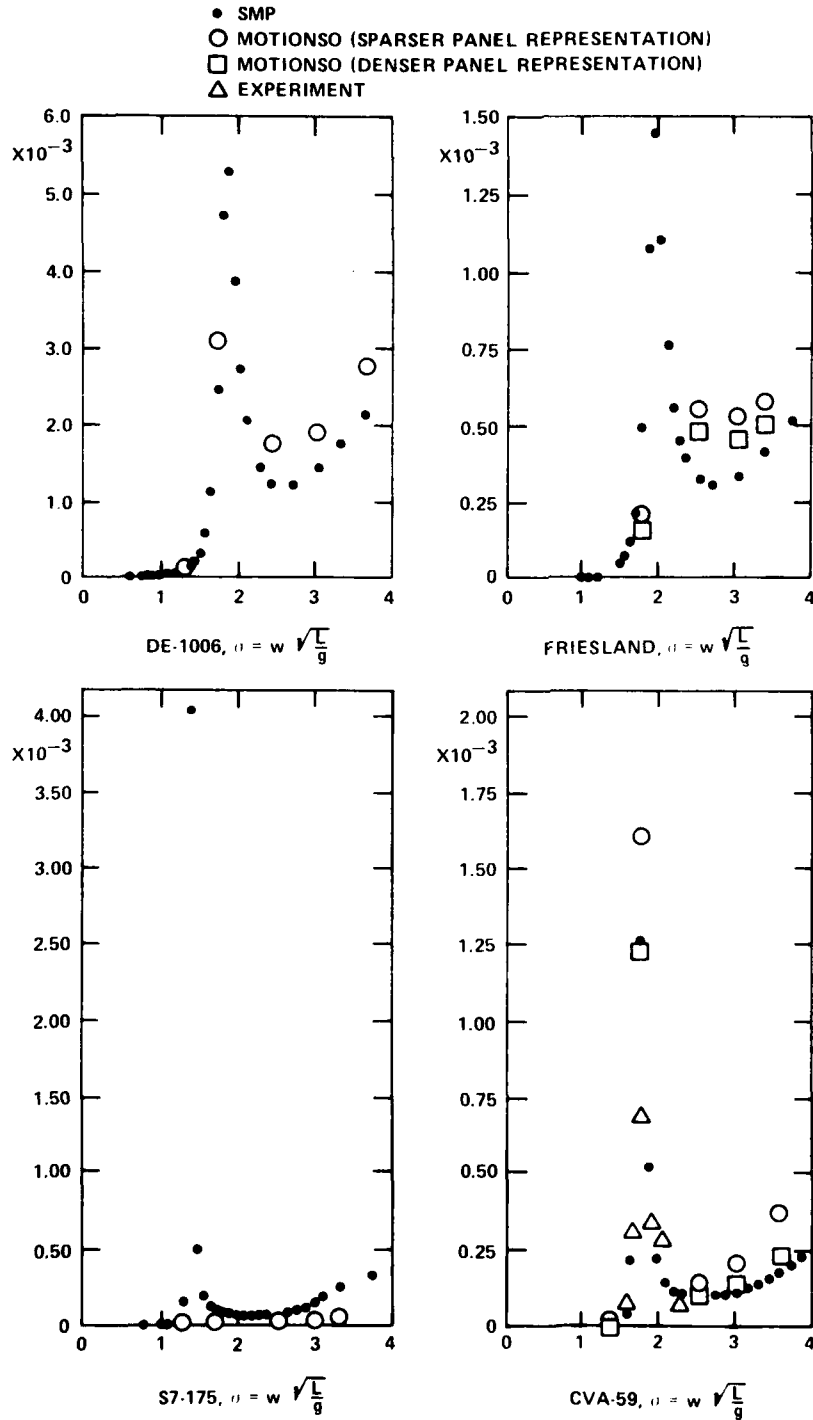Figure 9c - Yaw Response Amplitude Operator RAO_6 for $\mu = 90$ Degrees

62

TABLE 1 – SUMMARY OF GEOMETRICAL CHARACTERISTICS
OF THE FOUR CHOSEN HULLS

Identification of Ship Hull	L (ft)	W (long ton)	CB	D/B	TW/B	Bulbous Bow
DE-1006	308.0	1,873	0.51	0.33	0.71	Yes
FRIESLAND	368.8	2,837	0.56	0.33	0.84	No
S7-175	574.2	23,779	0.57	0.37	0.00	Yes (Large)
CVA-59	990.0	75,954	0.60	0.28	0.51	Yes

TABLE 2 - CHARACTERISTICS OF HULL AND APPENDAGES FOR DE-1006

DE-1006 KG3, BK1 VALIDATION

TABLE OF SHIP PARTICULARS

SHIP CHARACTERISTICS -

SHIP LENGTH (LPP)	308.00 FEET	LENGTH/BEAM	8.570
BEAM AT MIDSHIPS	35.94 FEET	BEAM/DRAFT	2.995
DRAFT AT MIDSHIPS	12.06 FEET	DRAFT/BEAM	0.334
DISPLACEMENT (S.W.)	1873 L. TONS	DISPL/(.01LPP)**3	64.103
DESIGN SHIP SPEED	27.00 KNOTS	FROUDE NUMBER	0.458

VERTICAL LOCATIONS -

C. OF GRAVITY (VCG)*	3.59 FEET	VCG/BEAM	0.100
C. OF GRAVITY (KG)**	15.63 FEET	KG/BEAM	0.435
METACENTRIC HT. (GM)	2.26 FEET	GM/BEAM	0.063
METACENTER (KM)**	17.89 FEET	KM/BEAM	0.498
C. OF BUOYANCY (KB)**	7.38 FEET	KB/BEAM	0.205

LONGITUDINAL LOCATIONS*** -

C. OF GRAVITY (LCG)	159.25 FEET	LCG/LENGTH	0.517
C. OF BUOYANCY (LCB)	159.25 FEET	LCB/LENGTH	0.517
C. OF FLOTATION (LCF)	174.75 FEET	LCF/LENGTH	0.567

MOTION CHARACTERISTICS -

ROLL GYRADIUS	12.54 FEET	RG/BEAM	0.349
PITCH GYRADIUS	77.00 FEET	PG/LPP	0.250
YAW GYRADIUS	77.00 FEET	YG/LPP	0.250
ESTIMATED ROLL PERIOD	10.33 SECONDS	ROLL FREQ (RADIANS)	0.608

COMPUTED AREAS -

WATERPLANE	8469 SQ. FEET	AWP/(LPP*BEAM)	0.765
WETTED SURFACE (HULL)	12036 SQ. FEET	WS/(2LD+2BD+LB)	0.623

HULL COEFFICIENTS -

BLOCK (CB)	0.51
SECTION (CX)	0.83
PRISMATIC (CP)	0.61

---

*WATERLINE REFERENCE.

**KEEL REFERENCE.

***F.P. REFERENCE.

TABLE 2 (Continued)

DE-1006 KG3, BK1 VALIDATION

TABLE OF SHIP APPENDAGE PARTICULARS

BILGE KEEL CHARACTERISTICS -

BILGE KEEL LENGTH (SET NO. 1)	91.17 FEET
BILGE KEEL WIDTH (SET NO. 1)	1.55 FEET
TOTAL WETTED SURFACE AREA (B.K. SET NO. 1)	565 SQ. FEET

SKEG CHARACTERISTICS -

SKEG LENGTH ALONG KEEL (SET NO. 1)	46.05 FEET
SKEG HEIGHT (SET NO. 1)	7.50 FEET
TOTAL WETTED SURFACE AREA (SKEG SET NO. 1)	345 SQ. FEET

RUDDER CHARACTERISTICS -

RUDDER ROOT CHORD LENGTH (SET NO. 1)	11.09 FEET
RUDDER TIP CHORD LENGTH (SET NO. 1)	8.47 FEET
RUDDER MEAN SPAN (SET NO. 1)	12.45 FEET
TOTAL WETTED SURFACE AREA (RUDDER SET NO. 1)	486 SQ. FEET

PROPELLER SHAFT BRACKETS CHARACTERISTICS -

OUTSIDE BRACKET ROOT CHORD LENGTH (SET NO. 1)	2.77 FEET
OUTSIDE BRACKET MEAN SPAN (SET NO. 1)	8.94 FEET
BRACKET TIP CHORD LENGTH (SET NO. 1)	2.77 FEET
TOTAL WETTED SURFACE AREA (BRACKET SET NO. 1)	99 SQ. FEET

NOTE:

IF A "SET" REPRESENTS A PAIR OF APPENDAGES (E.G., BILGE KEELS), THEN THE WETTED SURFACE IS COMPUTED FOR THE TOTAL AREA OF BOTH APPENDAGES.

TABLE 3 - CHARACTERISTICS OF HULL AND APPENDAGES FOR FRIESLAND

FRIESLAND SEPT 1980

TABLE OF SHIP PARTICULARS

SHIP CHARACTERISTICS -

SHIP LENGTH (LPP)	368.80 FEET	LENGTH/BEAM	9.579
BEAM AT MIDSHIPS	38.50 FEET	BEAM/DRAFT	3.008
DRAFT AT MIDSHIPS	12.80 FEET	DRAFT/BEAM	0.332
DISPLACEMENT (S.W.)	2837 L. TONS	DISPL/(.01LPP)**3	56.563
DESIGN SHIP SPEED	9.70 KNOTS	FROUDE NUMBER	0.150

VERTICAL LOCATIONS -

C. OF GRAVITY (VCG)*	3.60 FEET	VCG/BEAM	0.094
C. OF GRAVITY (KG)**	16.40 FEET	KG/BEAM	0.426
METACENTRIC HT. (GM)	2.19 FEET	GM/BEAM	0.057
METACENTER (KM)**	18.59 FEET	KM/BEAM	0.483
C. OF BUOYANCY (KB)**	7.71 FEET	KB/BEAM	0.200

LONGITUDINAL LOCATIONS*** -

C. OF GRAVITY (LCG)	187.99 FEET	LCG/LENGTH	0.510
C. OF BUOYANCY (LCB)	187.99 FEET	LCB/LENGTH	0.510
C. OF FLOTATION (LCF)	199.53 FEET	LCF/LENGTH	0.541

MOTION CHARACTERISTICS -

ROLL GYRADIUS	13.48 FEET	RG/BEAM	0.350
PITCH GYRADIUS	95.52 FEET	PG/LPP	0.259
YAW GYRADIUS	92.20 FEET	YG/LPP	0.250
ESTIMATED ROLL PERIOD	11.26 SECONDS	ROLL FREQ (RADIANS)	0.558

COMPUTED AREAS -

WATERPLANE	11356 SQ. FEET	AWP/(LPP*BEAM)	0.800
WETTED SURFACE (HULL)	15882 SQ. FEET	WS/(2LD+2BD+LB)	0.645

HULL COEFFICIENTS -

BLOCK (CB)	0.56
SECTION (CX)	0.83
PRISMATIC (CP)	0.68

---

*WATERLINE REFERENCE.

**KEEL REFERENCE.

***F.P. REFERENCE.

TABLE 3 (Continued)

FRIESLAND   SEPT 1980

TABLE OF SHIP APPENDAGE PARTICULARS

BILGE KEEL CHARACTERISTICS -

BILGE KEEL LENGTH (SET NO. 1)	109.16 FEET
BILGE KEEL WIDTH (SET NO. 1)	1.55 FEET
TOTAL WETTED SURFACE AREA (B.K. SET NO. 1)	676 SQ. FEET

SKEG CHARACTERISTICS -

SKEG LENGTH ALONG KEEL (SET NO. 1)	55.14 FEET
SKEG HEIGHT (SET NO. 1)	7.50 FEET
TOTAL WETTED SURFACE AREA (SKEG SET NO. 1)	413 SQ. FEET

RUDDER CHARACTERISTICS -
RUDDER ROOT CHORD LENGTH (SET NO. 1)	13.28 FEET
RUDDER TIP CHORD LENGTH (SET NO. 1)	10.14 FEET
RUDDER MEAN SPAN (SET NO. 1)	12.45 FEET
TOTAL WETTED SURFACE AREA (RUDDER SET NO. 1)	583 SQ. FEET

PROPELLER SHAFT BRACKETS CHARACTERISTICS -

OUTSIDE BRACKET ROOT CHORD LENGTH (SET NO. 1)	3.32 FEET
OUTSIDE BRACKET MEAN SPAN (SET NO. 1)	8.94 FEET
BRACKET TIP CHORD LENGTH (SET NO. 1)	3.32 FEET
TOTAL WETTED SURFACE AREA (BRACKET SET NO. 1)	118 SQ. FEET

NOTE:

IF A "SET" REPRESENTS A PAIR OF APPENDAGES (E.G., BILGE KEELS),
THEN THE WETTED SURFACE IS COMPUTED FOR THE TOTAL AREA OF BOTH
APPENDAGES.

TABLE 4 - CHARACTERISTICS OF HULL AND APPENDAGES FOR S7-175

S7-175 CONTAINER SHIP   OCT 1976

TABLE OF SHIP PARTICULARS

SHIP CHARACTERISTICS -

SHIP LENGTH (LPP)	574.15 FEET	LENGTH/BEAM	6.890
BEAM AT MIDSHIPS	83.33 FEET	BEAM/DRAFT	2.673
DRAFT AT MIDSHIPS	31.17 FEET	DRAFT/BEAM	0.374
DISPLACEMENT (S.W.)	23779 L. TONS	DISPL/(.01LPP)**3	125.638
DESIGN SHIP SPEED	11.00 KNOTS	FROUDE NUMBER	0.137

VERTICAL LOCATIONS -

C. OF GRAVITY (VCG)*	0.07 FEET	VCG/BEAM	0.001
C. OF GRAVITY (KG)**	31.24 FEET	KG/BEAM	0.375
METACENTRIC HT. (GM)	3.27 FEET	GM/BEAM	0.039
METACENTER (KM)**	34.51 FEET	KM/BEAM	0.414
C. OF BUOYANCY (KB)**	17.03 FEET	KB/BEAM	0.204

LONGITUDINAL LOCATIONS*** -

C. OF GRAVITY (LCG)	295.35 FEET	LCG/LENGTH	0.514
C. OF BUOYANCY (LCB)	295.35 FEET	LCB/LENGTH	0.514
C. OF FLOTATION (LCF)	309.27 FEET	LCF/LENGTH	0.539

MOTION CHARACTERISTICS -

ROLL GYRADIUS	27.17 FEET	RG/BEAM	0.326
PITCH GYRADIUS	137.80 FEET	PG/LPP	0.240
YAW GYRADIUS	137.80 FEET	YG/LPP	0.240
ESTIMATED ROLL PERIOD	18.61 SECONDS	ROLL FREQ (RADIANS)	0.338

COMPUTED AREAS -

WATERPLANE	34008 SQ. FEET	AWP/(LPP*BEAM)	0.711
WETTED SURFACE (HULL)	57663 SQ. FEET	WS/(2LD+2BD+LB)	0.649

HULL COEFFICIENTS -

BLOCK (CB)	0.57
SECTION (CX)	0.97
PRISMATIC (CP)	0.59

---

*WATERLINE REFERENCE.

**KEEL REFERENCE.

***F.P. REFERENCE.

TABLE 4 (Continued)

S7-175 CONTAINER SHIP   OCT 1976

TABLE OF SHIP APPENDAGE PARTICULARS

BILGE KEEL CHARACTERISTICS -

BILGE KEEL LENGTH (SET NO. 1)   143.54 FEET
BILGE KEEL WIDTH (SET NO. 1)   1.48 FEET
TOTAL WETTED SURFACE AREA (B.K. SET NO. 1)   849 SQ. FEET

   NOTE:

IF A "SET" REPRESENTS A PAIR OF APPENDAGES (E.G., BILGE KEELS),
THEN THE WETTED SURFACE IS COMPUTED FOR THE TOTAL AREA OF BOTH
APPENDAGES.

TABLE 5 - CHARACTERISTICS OF HULL AND APPENDAGES FOR CVA-59

CVA-59 V=0,25 KNOTS

TABLE OF SHIP PARTICULARS

SHIP CHARACTERISTICS -

SHIP LENGTH (LPP)	990.00	FEET	LENGTH/BEAM	7.657
BEAM AT MIDSHIPS	129.30	FEET	BEAM/DRAFT	3.612
DRAFT AT MIDSHIPS	35.80	FEET	DRAFT/BEAM	0.277
DISPLACEMENT (S.W.)	75954	L. TONS	DISPL/(.01LPP)**3	78.279
DESIGN SHIP SPEED	25.00	KNOTS	FROUDE NUMBER	0.237

VERTICAL LOCATIONS -

C. OF GRAVITY (VCG)*	8.92	FEET	VCG/BEAM	0.069
C. OF GRAVITY (KG)**	44.72	FEET	KG/BEAM	0.346
METACENTRIC HT. (GM)	12.38	FEET	GM/BEAM	0.096
METACENTER (KM)**	57.10	FEET	KM/BEAM	0.442
C. OF BUOYANCY (KB)**	19.48	FEET	KB/BEAM	0.151

LONGITUDINAL LOCATIONS*** -

C. OF GRAVITY (LCG)	512.28	FEET	LCG/LENGTH	0.517
C. OF BUOYANCY (LCB)	512.28	FEET	LCB/LENGTH	0.517
C. OF FLOTATION (LCF)	558.69	FEET	LCF/LENGTH	0.564

MOTION CHARACTERISTICS -

ROLL GYRADIUS	56.25	FEET	RG/BEAM	0.435
PITCH GYRADIUS	248.49	FEET	PG/LPP	0.251
YAW GYRADIUS	248.49	FEET	YG/LPP	0.251
ESTIMATED ROLL PERIOD	19.80	SECONDS	ROLL FREQ (RADIANS)	0.317

COMPUTED AREAS -

WATERPLANE	95741	SQ. FEET	AWP/(LPP*BEAM)	0.748
WETTED SURFACE (HULL)	138732	SQ. FEET	WS/(2LD+2BD+LB)	0.667

HULL COEFFICIENTS -

BLOCK (CB)	0.60
SECTION (CX)	0.99
PRISMATIC (CP)	0.60

---

*WATERLINE REFERENCE.

**KEEL REFERENCE.

***F.P. REFERENCE.

TABLE 5 (Continued)

CVA-59 V=0,25 KNOTS

TABLE OF SHIP APPENDAGE PARTICULARS

BILGE KEEL CHARACTERISTICS -

BILGE KEEL LENGTH (SET NO. 1)	311.85 FEET
BILGE KEEL WIDTH (SET NO. 1)	3.00 FEET
TOTAL WETTED SURFACE AREA (B.K. SET NO. 1)	3742 SQ. FEET

SKEG CHARACTERISTICS -

SKEG LENGTH ALONG KEEL (SET NO. 1)	110.39 FEET
SKEG HEIGHT (SET NO. 1)	13.50 FEET
TOTAL WETTED SURFACE AREA (SKEG SET NO. 1)	1490 SQ. FEET

RUDDER CHARACTERISTICS -

RUDDER ROOT CHORD LENGTH (SET NO. 1)	26.98 FEET
(SET NO. 2)	19.31 FEET
RUDDER TIP CHORD LENGTH (SET NO. 1)	20.29 FEET
(SET NO. 2)	19.31 FEET
RUDDER MEAN SPAN (SET NO. 1)	30.63 FEET
(SET NO. 2)	14.25 FEET
TOTAL WETTED SURFACE AREA (RUDDER SET NO. 1)	2895 SQ. FEET
(RUDDER SET NO. 2)	550 SQ. FEET

NOTE:

IF A "SET" REPRESENTS A PAIR OF APPENDAGES (E.G., BILGE KEELS), THEN THE WETTED SURFACE IS COMPUTED FOR THE TOTAL AREA OF BOTH APPENDAGES.

TABLE 6 - SMP REPRESENTATION OF SHIP HULLS

X-Station	Number of Points																								Total Points
	-1	0	1/4	1	2	3	4	5	6	7	8	9	10	11	12	13	14	15	16	17	18	19	19 3/4	20	
DE-1006	0	0	8	8	8	8	8	8	8	8	8	8	8	8	8	8	8	8	8	8	8	8	8	0	168
FRIESLAND	0	0	9	9	9	9	9	9	9	9	9	9	9	9	9	9	9	9	9	9	9	9	9	0	189
S7-175	8	0	8	8	8	8	8	8	8	8	8	8	8	8	8	8	8	8	8	8	8	8	8	0	176
CVA-59	0	0	8	8	8	8	8	9	10	10	10	10	10	10	10	10	10	8	8	8	8	8	8	0	187

TABLE 7 – MOTIONSO REPRESENTATION OF SHIP HULLS

Number of Points and Panels

DE-1006

																Total
X-Station	0.0	0.5	1.5	3.0	5.0	7.0	9.0	11.0	13.0	15.0	16.0	17.0	18.0	20.0	21.0	
Points	7	7	7	7	7	7	7	7	7	7	7	6	6	6	6	101
Panels	6	6	6	6	6	6	6	6	6	6	6	5	5	5	–	81

FRIESLAND

															Total
X-Station	0.0	0.5	1.5	3.0	5.0	7.0	9.0	11.0	13.0	15.0	17.0	18.5	19.5	20.0	
Points	7	7	7	7	7	7	7	7	7	7	7	7	7	7	98
Panels	6	6	6	6	6	6	6	6	6	6	6	6	6	–	78
Points	9	9	9	9	9	9	9	9	9	9	9	9	9	9	126
Panels	8	8	8	8	8	8	8	8	8	8	8	8	8	–	104

S7-175*

														Total
X-Station	0.0	0.7	2.0	4.0	6.0	8.0	10.0	12.0	14.0	16.0	18.0	19.3	20.0	
Points	7	7	7	8	9	9	9	9	8	8	7	3	3	94
Panels	6	6	7	8	8	8	8	8	7	7	3	2	–	78

CVA-59

															Total
X-Station	0.0	0.75	2.0	3.5	5.0	7.0	9.0	11.0	13.0	15.0	16.5	18.0	19.5	20.0	
Points	4	4	7	8	8	8	8	8	9	5	5	4	4	4	86
Panels	3	4	6	7	7	7	7	7	7	6	4	3	3	–	71
Points	7	7	10	11	11	11	11	11	12	7	7	5	4	4	118
Panels	6	7	9	10	10	10	10	10	10	8	6	4	3	–	103

*The 82-panel representation of S7-175 is obtained by adding five points and four panels at X-Station = 0.1 to model the bulbous bow.

73

REFERENCES

1. Meyers, W.G. et al., "Manual-NSRDC Ship-Motion and Sea-Load Computer Program," NSRDC Report 3376 (Feb 1975).

2. Chang, M.S., "Computations of Three-Dimensional Ship-Motions with Forward Speed," Second International Conference on Numerical Ship Hydrodynamics, pp. 124-135 (Sep 1977).

3. Salvesen, N. et al., "Ship Motions and Sea Loads," Transactions of the Society of Naval Architects and Marine Engineers, Vol. 78, pp. 250-287 (Nov 1970).

4. Frank, W., "Oscillation of Cylinders In or Below the Free Surface of Deep Fluids," DTMB Report 2375 (Oct 1967).

5. Frank, W. and N. Salvesen, "The Frank Close-Fit Ship-Motion Computer Program," NSRDC Report 3289 (Jun 1970).

6. "Report of the Seakeeping Committee," 15th International Towing Tank Conference, The Hague, The Netherlands, pp. 55-114 (Sep 1978).

7. Smith, W.E., "Computation of Pitch and Heave Motions for Arbitrary Ship Forms," International Shipbuilding Progress, Vol. 14, No. 155, pp. 267-290 (Jul 1967).

INITIAL DISTRIBUTION

Copies			CENTER DISTRIBUTION		
1	CHONR/438 Lee		Copies	Code	Name
1	ONR/Boston		1	15	
1	ONR/Chicago		1	1504	
			1	152	
1	ONR/New York		1	154	
1	ONR/Pasadena		1	1542	
			15	1542	Chang
1	ONR/San Francisco		1	156	
1	NRL/Lib		1	1564	
12	NAVSEA		1	1568	
	1 SEA 03D		1	1572	
	1 SEA 0322				
	1 SEA 033		10	5211.1	Reports Distributions
	1 SEA 03512				
	1 SEA 037		1	522.1	Unclassified Library (C)
	1 SEA 312		1	522.2	Unclassified Library (A)
	1 SEA 32				
	1 SEA 321				
	1 SEA 52				
	1 SEA 521				
	1 SEA 524				
	1 SEA 6030B				
1	SNAME/Tech Lib				
12	DTIC				

DTNSRDC ISSUES THREE TYPES OF REPORTS

1. DTNSRDC REPORTS, A FORMAL SERIES, CONTAIN INFORMATION OF PERMANENT TECHNICAL VALUE. THEY CARRY A CONSECUTIVE NUMERICAL IDENTIFICATION REGARDLESS OF THEIR CLASSIFICATION OR THE ORIGINATING DEPARTMENT.

2. DEPARTMENTAL REPORTS, A SEMIFORMAL SERIES, CONTAIN INFORMATION OF A PRELIMINARY, TEMPORARY, OR PROPRIETARY NATURE OR OF LIMITED INTEREST OR SIGNIFICANCE. THEY CARRY A DEPARTMENTAL ALPHANUMERICAL IDENTIFICATION.

3. TECHNICAL MEMORANDA, AN INFORMAL SERIES, CONTAIN TECHNICAL DOCUMENTATION OF LIMITED USE AND INTEREST. THEY ARE PRIMARILY WORKING PAPERS INTENDED FOR INTERNAL USE. THEY CARRY AN IDENTIFYING NUMBER WHICH INDICATES THEIR TYPE AND THE NUMERICAL CODE OF THE ORIGINATING DEPARTMENT. ANY DISTRIBUTION OUTSIDE DTNSRDC MUST BE APPROVED BY THE HEAD OF THE ORIGINATING DEPARTMENT ON A CASE-BY-CASE BASIS.

DA
FILM